U.PORTO
FACULDADE DE CIÊNCIAS
UNIVERSIDADE DO PORTO
INSTITUTO DE CIÊNCIAS BIOMÉDICAS ABEL SALAZAR
UNIVERSIDADE DO PORTO

MANNOSYLATED NANOPARTICLES FOR TARGETED DELIVERY OF AMPHOTERICIN B TOWARDS VISCERAL LEISHMANIASIS

Daniela Filipa dos Santos Barros

Dissertação do Mestrado em Bioquímica

2012

Daniela Filipa dos Santos Barros

Mannosylated nanoparticles for targeted delivery of amphotericin B towards visceral leishmaniasis

Dissertação de Candidatura ao grau de Mestre em Bioquímica da Universidade do Porto

Orientador – Doutora Sofia Antunes Costa Lima
Categoria – Investigadora Doutorada
Afiliação – Instituto de Biologia Molecular e Celular (IBMC)
Co-orientador – Professora Doutora Anabela Cordeiro da Silva
Categoria – Professora Associada com Agregação
Afiliação – Faculdade de Farmácia da Universidade do Porto
Instituto de Biologia Molecular e Celular (IBMC)

2012

U.PORTO

FACULDADE DE CIÊNCIAS
UNIVERSIDADE DO PORTO

INSTITUTO DE CIÊNCIAS BIOMÉDICAS ABEL SALAZAR
UNIVERSIDADE DO PORTO

Todas as correções determinadas pelo júri, e só essas, foram efetuadas.

O Presidente do Júri,

Porto, _____/_____/_____

ACKOWLEDGMENTS

Finished this stage of my academic training, I would like to acknowledge everyone who accompanied me not only during this stage of my life but also in the last years.

First, I would like to thank Professor Anabela Cordeiro da Silva for having received me in her group and also for being an excellent group leader able to instill in each of us the love by science.

To Doctor Sofia Costa Lima, my supervisor, for all the help, availability, support, encouragement and friendship. For all the confidence that she always had in me and in my abilities, thus encouraging me to progress and grow as a future researcher.

I would like to thank also my lab mates of Parasite Disease Group for their friendship and motivation. For the sharing of knowledge and experiences, as well as for the pleasant environment always present in the lab.

Thanks also to D.Rosa for the help and support and for ensure that we have always the necessary tools to develop a good work.

A special thank to Patrícia, my “bench mate”, for her friendship, help, support in times of greater nervousness and for all the funny moments we share.

I also would like to thank Ricardo Vidal for the technical support in DLS and FTIR, Catarina Leitão for all the help she gave me in FACS and Rui Fernandes for the technical support in TEM.

To my friends for their friendship, support and patience. For all the moments of relaxation and fun, ... Essentially, for always being there when I needed it most.

To my parents and sister, to whom I dedicate this thesis, for the unconditional support, patience and love. For being present in all the important moments of my life…for making me the person that I am today.

To Ricardo, whom also I dedicate this thesis, for his support, encouragement, friendship, love, pampering and patience. For all the moments that we shared and that make it all worthwhile.

ABSTRACT

Leishmaniasis is a neglected tropical disease caused by obligate intra-macrophagic protozoa that has a higher incidence in less developed countries and is responsible for high mortality. Since there is no commercially available human vaccine against leishmaniasis the control of this disease is dependent on drug therapy and vector control. However, current therapies are far from satisfactory, especially due to the emergence of resistances, elevated toxicity and increased prevalence of human immunodeficiency virus (HIV)-*Leishmania* co-infections [1-3]. Thus, it is of great importance to develop alternative treatments, like nanotechnology-based drug delivery systems, which may reduce toxicity and side effects of the drugs, and enhance their efficacy.

Active targeting of polymeric nanoparticles to mannose receptor (MR), an endocytic receptor highly expressed on antigen presenting cells (APCs) (macrophages and dendritic cells (DCs)), seems to be a good strategy for targeting and delivery of drugs in the treatment of visceral leishmaniasis (VL). One of the drugs currently used in the treatment of VL is amphotericin B (AmB), however its use have some drawbacks, including the high toxicity, the high costs associated with its use, the limited availability in some areas, difficulties associated with the administration, prolonged duration of therapy and the severe side effects [1, 3-4]. Thus in order to improve AmB efficacy as an antileishmanial drug and reduce its toxicity, the first part of this work aims to develop and characterize a nanoparticulate system targeting MR in APCs, the target cells in VL, being that the strategy chosen involves: (1) the preparation of unloaded mannose-coated poly(lactic-co-glycolic acid) (M-PLGA) nanoparticles by three different techniques physical adsorption (PA), one-step chemical reaction (CR1) and two-step chemical reaction (CR2); (2) use of the developed nanoparticulate system to encapsulate AmB and evaluate their *in vitro* efficacy against *Leishmania* –infected macrophages; (3) assessment of the new targeted-nanoformulations uptake by APCs.

Empty and AmB- loaded PLGA nanoparticles were prepared by the nanoprecipitation method [5] and for the three different techniques (PA, CR1 and CR2) used to prepare empty M-PLGA nanoparticles, PA and CR1 were choose to conjugate mannose with AmB-loaded PLGA nanoparticles.

The AmB-loaded M-PLGA nanoparticles, prepared by PA and CR1, present a mean diameter of 200.2 nm and 190.8 nm, respectively, low PDI (<0.1), anionic surface charge (-14.7 mV and -16.2 mV, respectively) and are spherical in shape. The yield associated with incorporation level of mannose, determined by phenol-sulfuric acid reaction, is around 95% for PA and 98% for CR1. Encapsulation efficiency (E.E.) of 1.8% and 4.1% were obtained for nanoparticles prepared by PA and CR1, respectively, which is low as

compared with non functionalized PLGA nanoparticles (E.E. ≈ 20%). The AmB-loaded M-PLGA nanoparticles, prepared by PA and CR1, exhibited a triphasic release profile. The nanoformulations don't present cytotoxicity against human THP1 differentiated macrophages and bone marrow derived macrophages (BMMϕ). The functionalization of PLGA nanoparticles leads to an improvement of AmB antileishmanial activity, perhaps related with a more efficient uptake. *Ex vivo* studies clearly demonstrate that FITC-loaded M-PLGA nanoparticles present an enhanced uptake by APCs and neutrophils when compared with other splenocytes (e.g. lymphocytes). Thus, the data obtained until now show that mannosylated nanoformulations, in particular the ones prepared by CR1, could have a promising role in the delivery of AmB and consequently in the treatment of VL.

Based on the fact that active targeting of nanoparticles to MR can potentially improve their efficacy in the induction of an immune response [6-8], the second part of this work aims to identify the optimum targeted nanoformulation for efficient delivery to APCs, using PLGA nanoparticles functionalized with three different sugars, mannose (M), mannan (MN) and mannosamine (Ms) and evaluate the extent in which these formulations affect the activation status of the cells, as well as the type of response that they will modulate in APCs, using flow cytometry. Results show that the functionalization of PLGA nanoparticles with ligands that are specifically recognized by MR in APCs, particularly with MN and Ms, improve their immunotherapeutic effect, through the induction of a more efficient activation of macrophages and DCs, evidenced by the enhanced expression of cell surface markers, including CD40, CD80, CD86 and MHC II and by the higher production of pro-inflammatory cytokines interleukin (IL)-4, IL-6, IL-12 and tumor necrosis factor-alpha (TNF-α), which could lead to the development of a robust immune response. Furthermore, fluorescence microscopy results show that, although non-functionalized and M-, MN- and Ms- functionalized PLGA nanoparticles are all efficiently internalized by macrophages, their distribution pattern is different, being that in the case of MN- and Ms-PLGA nanoparticles the presence of green dots in the cytoplasm suggests that the uptake of these nanoparticles occurs by an endocytic pathway. The obtained results strongly suggest that functionalization of PLGA nanoparticles with MN and Ms are a promising strategy to target MR in APCs and to promote the development of a robust immune response, as a result of the more efficient activation of macrophages and DCs.

RESUMO

A leishmaniose é uma doença tropical negligenciada causada por protozoários intracelulares obrigatórios, com uma maior incidência em países em desenvolvimento, onde é responsável por uma elevada mortalidade. Uma vez que não existe, até à data, uma vacina disponível para a prevenção e o tratamento da leishmaniose em humanos, o controlo desta doença está dependente da terapêutica farmacológica e do controlo do vector. Contudo, as terapias atualmente disponíveis não são satisfatórias, principalmente devido ao aparecimento de resistências, elevada toxicidade e número crescente de casos de co-infecção HIV-*Leishmania* [1-3]. Assim, o desenvolvimento de tratamentos alternativos, como por exemplo sistemas de veiculação de fármacos, que permitam reduzir a toxicidade e os efeitos secundários dos fármacos, e aumentar a sua eficácia, assume uma grande importância.

O direcionamento de nanopartículas poliméricas para o recetor da manose, um recetor endocítico expresso em elevado número nas células apresentadoras de antigénios (macrófagos e células dendríticas), representa uma estratégia promissora para aumentar a eficiência de fármacos no tratamento da leishmaniose visceral. A anfotericina B é um dos fármacos atualmente utilizados no tratamento da leishmaniose visceral, contudo a sua utilização tem algumas desvantagens, como a elevada toxicidade, os elevados custos, a reduzida disponibilidade deste fármaco em algumas áreas, as dificuldades associadas à sua administração, a duração prolongada do tratamento e os efeitos secundários indesejáveis [1, 3-4]. Assim, no sentido de aumentar a eficácia da anfotericina B no tratamento da leishmaniose visceral e reduzir a sua toxicidade, a primeira parte deste trabalho tem como objectivo desenvolver e caracterizar uma nanoformulação direcionada para o recetor da manose expresso nas células apresentadoras de antigénios. Estas são células alvo na leishmaniose visceral, sendo que a estratégia escolhida envolve: (1) preparação de nanopartículas revestidas com manose usando três técnicas diferentes, adsorção física, reação química em um passo e reacção química em dois passos; (2) utilização da nanoformulação desenvolvida para encapsular a anfotericina B e avaliação *in vitro* da sua atividade anti-parasitária; (3) avaliação da internalização das nanoformulação desenvolvidas pelas células apresentadoras de antigénios.

As nanopartículas de poly(lactic-co-glycolic acid) (PLGA) vazias e contendo anfotericina B foram preparadas por nanoprecipitação e das três técnicas utilizadas para preparar as nanopartículas de manose-PLGA vazias, a adsorção física e a reação química em um passo foram as escolhidas para revestir com manose as nanopartículas de PLGA contendo anfotericina B.

As nanopartículas de manose-PLGA contendo anfotericina B preparadas por adsorção física e a reação química em um passo, apresentaram diâmetros médios de 200,2 e 190,8 nm, respectivamente, baixos índices de polidispersão (<0,1), carga superficial negativa (-14,7 mV e -16,2 mV, respectivamente) e uma forma esférica. O nível de incorporação da manose foi determinado pela reação do fenol-ácido sulfúrico, tendo-se obtido rendimentos de 95% para as nanopartículas preparadas por adsorção física e 98% para as preparadas por reação química em um só passo. Eficiências de encapsulação da anfotericina B de 1,8% e 4,1% foram obtidas para as nanopartículas preparadas por adsorção física e reação química em um passo, respectivamente, valores baixos quando comparados com os obtidos para as nanoparticulas de PLGA não revestidas com manose (Eficiência de encapsulação≈20%). A anfotericina B encapsulada nas nanopartículas de manose-PLGA preparadas por adsorção física e por reação química em um só passo apresentaram um padrão de libertação de fármaco trifásico. As nanoformulações desenvolvidas não apresentam toxicidade para macrófagos diferenciados de monócitos THP-1 e para macrófagos derivados da medula óssea de ratinho. O revestimento das nanopartículas de PLGA favorece a actividade antileishmania da anfotericina B, o que provavelmente está relacionado com a internalização mais eficiente destas nanopartículas. Estudos *ex vivo* demonstraram que as nanopartículas de manose-PLGA contendo fluoresceína são preferencialmente internalizadas pelas células apresentadoras de antigénios e neutrófilos, em comparação com outras células (*p.e*. linfócitos). Assim, os resultados obtidos até agora demonstram que as nanoformulações manosiladas, em particular as preparadas por reação química em um passo, poderão ter um papel promissor na veiculação da anfotericina B e, consequentemente, no tratamento da leishmaniose visceral.

O revestimento das nanopartículas com ligandos que são especificamente reconhecidos pelo recetor da manose parece favorecer um desenvolvimento mais eficaz da resposta imunológica [6-8]. Assim, o objetivo da segunda parte deste trabalho consiste em utilizar nanopartículas de PLGA revestidas com três açúcares diferentes, manose (M), mannan (MN) e manosamina (Ms), para identificar o açúcar que influencia a modulação/ativação das células apresentadoras de antigénios (macrófagos e células dendríticas). Os resultados demonstraram que o revestimento das nanopartículas de PLGA com diferentes ligandos, em particular com MN e Ms, favorecem o seu efeito imunoterapêutico, uma vez que estimulam uma activação mais eficiente dos macrófagos e das células dendríticas, o que é evidenciado pelo aumento na expressão de marcadores de superfície celular, incluindo CD40, CD80, CD86 e MHCII e pela elevada produção de citocinas pro-inflamatórias (IL-4, IL-6, IL-12 e TNF-α), o que pode favorecer o desenvolvimento de uma resposta imunológica intensa. Os resultados de microscopia

de fluorescência demonstraram que, apesar de todas as nanopartículas, revestidas ou não com M, MN e Ms serem eficientemente internalizadas pelos macrófagos, a sua distribuição intracelular é diferente, sendo que, no caso das nanopartículas de MN- e Ms-PLGA a presença de vesículas no citoplasma sugere que a internalização destas nanopartículas ocorre por via endocítica. Os resultados obtidos sugerem que o revestimento das nanopartículas de PLGA com MN e Ms constituí uma estratégia promissora para direcionar estas nanoformulações para as células apresentadoras de antigénios e promover o desenvolvimento de uma resposta imunológica mais eficiente.

TABLE OF CONTENTS

INDEX OF FIGURES

INDEX OF TABLES

ABBREVIATIONS

AFM	Atomic force microscopy
AmB	Amphotericin B
APCs	Antigen presenting cells
BMDCs	Bone marrow-derived dendritic cells
BMMϕ	Bone marrow-derived macrophages
ConA	Concanavalin A
CR1	One-step chemical reaction
CR2	Two-step chemical reaction
CL	Cutaneous leishmaniasis
CLRs	C-type lectin receptors
CTLD	C-type lectin-like domain
DCC	N-(3-dimethylaminopropyl)-N'-ethylcarbodiimide hydrochloride
DCL	Diffuse cutaneous leishmaniasis
DCM	Dichloromethane
DCs	Dendritic cells
DLS	Dynamic light scattering
DMEM	Dulbecco's modified Eagle's medium
DMSO	Dimethyl sulphoxide
E.E.	Encapsulation efficiency
FACS	Fluorescence activated cell sorting
FBS	Fetal bovine serum
FITC	Fluorescein isothiocyanate isomer I
FTIR	Fourier transformed infrared spectroscopy
Gal	Galactose
GalNAc	N-acetyl galactosamine
GM-CSF	Granulocyte macrophage colony-stimulating factor
HEPES	4-(2-hydroxyethyl)-1-piperazineethanesulfonic acid
HIV	Human immunodeficiency virus
HPLC	High-performance liquid chromatography
IFN-ɣ	Interferon-gamma
IL	Interleukin
LCCM	L929 cell conditioned medium
LPS	Lipopolysaccharide
LUC	Luciferase
M	Mannose
MCL	Mucocutaneous leishmaniasis
MFI	Mean fluorescence intensity
MN	Mannan
MN-PLGA	Mannan-coated poly(lactic-co-glycolic acid)

M-PLGA	Mannose-coated poly(lactic-co-glycolic acid)
MPS	Mononuclear phagocytic system
MR	Mannose receptor
Ms	Manossamine
Ms-PLGA	Mannosamine-coated poly(lactic-co-glycolic acid)
MTT	[3-(4,5-dimethylthiazol-2-yl)-2,5-diphenyltetrazolium bromide]
MW	Molecular weight
NHS	N-hydroxysuccinimide
NPs	Nanoparticles
OD	Optical density
PA	Physical adsorption
PACA	Poly(alkylcyanoacrylate)
PBS	Phosphate-buffered saline
PCL	Poly-ε-caprolactone
PDI	Polidispersity index
PEG	Poly-ethylene-glycol
PFA	Paraphormaldehyde
PGA	Poly(glycolic acid)
PKDL	Post kala-azar dermal leishmaniasis
PLA	Polylactic acid
PLA_2R	M-type phospholipase A_2 receptor
PLGA	Poly(lactic-co-glycolic acid)
PMA	Phorbol 12-myristate 13-acetate
PRR	Pattern recognition recepors
PVA	Poly (vinyl alcohol)
RLU	Relative light units
TEM	Transmission electron microscopy
TNF-α	Tumor necrosis factor - alpha
UPLC	Ultra-performance liquid chromatography
VL	Visceral leishmaniasis
WHO	World Health Organization

I. INTRODUCTION

1.1. Nanotechnology

The research interest in the area of developing nanotechnology suffered a huge growth in the last years. Thus, the concept of “magic bullet” proposed by Paul Ehrlich, Nobel Prize for medicine in 1908, is now a reality with the use of nanoparticles as drug targeting systems in the treatment of infectious and oncological diseases. Since the first descriptions of the use of liposomes [9] and polymeric nanoparticles [10] as drug delivery systems until now, a high number of different nanosystems made of lipids or polymers emerged (Fig.1). It’s important to note that each of these nanosystems have different physicochemical properties and distinct sizes that ranges in the nanoscale, *e.g.* liposomes (80-200 nm), nanoparticles (20-1000 nm), polymer therapeutics (5-25 nm), block copolymer micelles (50-200 nm), gold nanoparticles (5-50 nm) and nanosized crystals (100-1000 nm) [11]. The use of these nanosystems for therapeutic purposes, to carry a drug in the body in a controlled manner from the site of administration to the therapeutic target, has been explored at the level of pharmaceutical research.

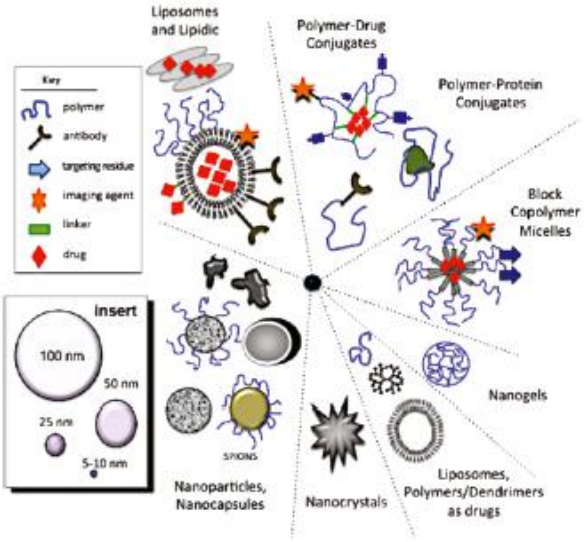

Figure 1 - Main classes of nanosystems used for drug delivery and targeting. Adapted from [11].

The nanotechnology has allowed making great advances in the development of drug targeting systems for therapeutic applications, however still far from the “magic bullet”.

1.2. Nanoparticles

Nanoparticles are colloidal systems with a particle size in the range of 10 nm - 1 µm and are composed of synthetic (polylactic acid (PLA), poly(lactic-co-glycolic acid) (PLGA), *etc*) or natural (*e.g.* gelatin, albumin and chitosan) polymers. A wide variety of drugs can be incorporated in the nanoparticles, including hydrophilic and hydrophobic small drugs, vaccines and biological macromolecules [12-13]. To allow their use as drug delivery system their components should be biocompatible, biodegradable, non-immunogenic and non-toxic. As a result of their small size, nanoparticles present unique properties in terms of appearance and application. For example, their small size allows them to be maintained in suspension by Brownian motion of the water molecules and they can have a closure contact with tissues and cells as a result of their large surface areas [12]. According to the process used for their preparation, they can be classified as nanocapsules or nanospheres. Nanocapsules are vesicular systems composed by a polymeric shell and an inner core where the drug can be dissolved. Nanospheres have a matrix like structure where the drug can be entrapped or dispersed [12].

The use of nanoparticles and most precisely polymeric nanoparticles, for encapsulation and controlled release of different pharmacological active agents, has been extensively studied in the last decades, since they favors a controlled release of the drugs, have a sub-cellular size, are biocompatible with tissues and cells, biodegradable, non-toxic, non-thrombogenic, non-immunogenic, non-inflammatory and can be used to deliver small molecules, proteins, peptides or nucleic acids [14-15]. In addition, the use of nanoparticles in drug delivery has many advantages over the use of other nanosystems, such as liposomes: higher encapsulation efficiencies, higher stability in physiological conditions and improvement of the bioavailability of the drug. Furthermore, the simplicity and low cost of the preparation processes make them a highly attractive drug delivery system [16].

1.3. Preparation of polymeric nanoparticles

1.3.1. Polymers used in nanoparticles preparation

The polymeric composition of the nanoparticles, including their hydrophobicity, surface charge, biocompatibility and biodegradation profile, should be taken into consideration when preparing nanoparticles for drug delivery purposes. Different polymers, either natural or synthetic, can be used in the preparation of biodegradable polymeric nanoparticles. The natural polymers commonly used in nanoparticles preparation are albumin, gelatin and chitosan [12]. The use of these polymers has several advantages including their low cost, biocompatibility with both biological systems and drugs and aqueous solubility. However, their use could be limited by the presence of contaminants,

the variability from batch to batch, their low hydrophobicity that make them inappropriate for the encapsulation of lipophilic drugs, and by the fact that they promote a short duration release of the drug [12, 15]. Synthetic polymers are widely used in the preparation of nanoparticles as a result of their reproducible manufacture and stability. Furthermore, they promote a sustained release of the encapsulated drug for a period of days to several weeks [15]. Their limited solubility in aqueous solutions and the need to use surfactants to form stable nanoparticle suspensions are some of the drawbacks in the use of this type of polymers [17]. Depending on the application of the nanoparticles and to favor a better performance, the molecular weight, copolymer composition and degradation rate could be changed. Moreover to allow a more precise drug release to target places within the body the nanoparticles can be designed with additional properties, like thermo- or pH-sensitivity [18]. The most extensively used and studied synthetic polymers for drug delivery are PLA, poly(glycolic acid) (PGA) and their copolymers with different ratios of lactic and glycolic acid (PLGA) [19-20]. The latter was selected for the studies conducted for this master thesis and will be detailed on section 1.3.1.1. Since they are polyesters in nature, and as a result of the presence of ester linkages in their backbones, these polymers suffer an hydrolysis upon implantation into the body, with the consequent formation of products that are easily metabolized in the Krebs cycle and eliminated as carbon dioxide and water [12, 21].

Poly-ε-caprolactone (PCL) is a biodegradable, non-toxic and synthetic polymer also used in nanoparticle preparation. Since it has a slow degradation rate in comparison with PLA and PLGA their use is more adequate for long-term drug delivery [12]. Other synthetic polymer used is the poly(alkylcyanoacrylate) (PACA) whose properties can be controlled by the side chains introduced, being that the longer the side-chains the longer the half-life of the nanoparticles [12].

1.3.1.1. Poly(lactic-co-glycolic acid) (PLGA)

PLGA has generated a huge interest on the development of nanocarriers due to its excellent biocompatibility, biodegradability and mechanical strength. This polymer is degraded in the body by hydrolytic cleavage of ester linkage with the production of two metabolite monomers, lactic acid and glycolic acid that are effectively metabolized in the body through the Krebs cycle (Fig.2) [12, 21-22].

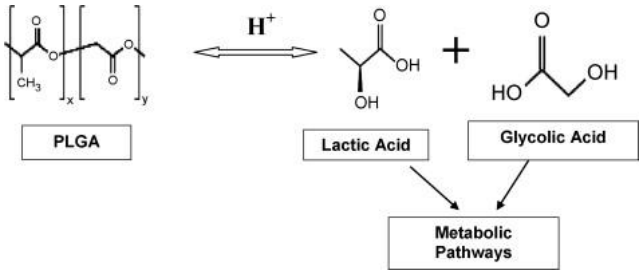

Figure 2 – Hydrolysis of PLGA nanoparticles. Adapted from [21].

Several factors influence the degradation of PLGA, including the method of preparation, the type of encapsulated drugs, intrinsic properties (molecular weight and copolymer composition), physicochemical parameters (pH, temperature and ionic strength) and site of implantation. The degradation time can go from months to years being that will be shorter for polymers with low molecular weight and composed by copolymers with higher glycolide content [23]. The degradation of PLGA nanoparticles can occur by two mechanisms, bulk erosion or surface erosion (Fig.3). The bulk erosion that is the main degradation pathway comprises three phases. Initially it is observed a significant decrease in the molecular weight of the polymer as a result of a random scission of ester bonds, that is followed by the formation of soluble monomeric and oligomeric products, being that the latter's in the final phase originate more soluble monomeric products, thus favoring the complete degradation of the polymer [22].

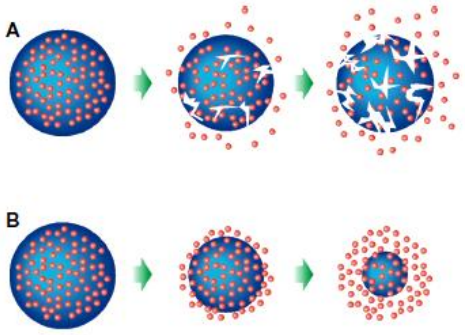

Figure 3 – Degradation mechanisms of PLGA nanoparticles **(A)** bulk erosion and **(B)** surface erosion. Adapted from [23].

PLGA nanoparticles are internalized mainly through clathrin-mediated endocytosis and have a mechanism that allow them to escape the endo-lysosomes and enter the cytoplasm in a short period of time (Fig.4), which is extremely advantageous for the use of this nanoparticles as cytoplasmic delivery systems [24]. The mechanism responsible for the endo-lysosomal escape of the nanoparticles is the surface charge reversal of nanoparticles as a result of the acidic pH of these compartments [15, 25].

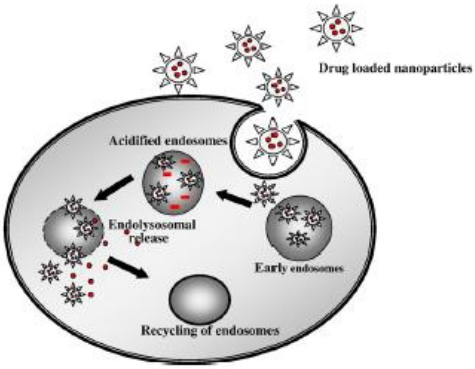

Figure 4 – Schematic representation of endo-lysosomal escape mechanism. Adapted from [25].

The use of PLGA in different drug delivery systems and its application at clinical level was approved by US Food and Drug Administration and European Medicine Agency [13, 19]. As a result, several drugs used in the treatment of different diseases were successfully encapsulated into PLGA microparticles and commercialized in the market [26].

1.3.2. Methods used in the preparation of polymeric nanoparticles

Different methods for the preparation of polymeric nanoparticles are currently available and to choose the most appropriate is necessary to take into account the type of polymer, the drug to be encapsulated and, the intended use of the nanoformulation. In the conventionally used methods, namely emulsification solvent evaporation, nanoprecipitation, the method used in this work and that is described in more detail in section 1.3.2.1., emulsification solvent diffusion and emulsification reverse salting-out, the polymeric nanoparticles were prepared directly from polymers synthesized by conventional polymerization techniques, which allows a better control of physicochemical and biological properties of the nanoparticles that are formed. Normally, these methods include two steps: a first step, that is common to all methods, in which the polymer is dissolved in an organic solvent and then emulsified in an aqueous phase, and a second step in which the nanoparticles are formed by the evaporation of the organic solvent [12, 23, 27]. In other methods, such as interfacial poly-condensation, polymeric nanoparticles were prepared by the polymerization of the monomers in an emulsion or micelle system [12, 27].

1.3.2.1. Nanoprecipitation or solvent displacement method

The nanoprecipitation method (or solvent displacement method), developed by Fessi *et al.* [5] is a simple method in which the nanoparticles are prepared in only one-step. Briefly, the polymer and the drug are dissolved in a volatile organic solvent, that is also miscible in water (*e.g.* acetone), and then added dropwise to an aqueous phase that normally has a stabilizing agent (*e.g.* polyvinyl alcohol (PVA)) under magnetic stirring. The rapid

formation of the nanoparticles and the drug entrapment are favored by the diffusion of the organic solvent to the aqueous phase, being that the organic solvent is then removed by slow evaporation. The produced nanoparticles usually have a small size (100-300 nm) and a narrow unimodal distribution. The application of this method in the preparation of polymeric nanoparticles has some advantages, including the fact of do not involve aggressive steps, like sonication, high temperatures and extended stirring rates, surfactants are not always needed and the organic solvents normally used are not toxic. However, one of the major problems of this technique is the low encapsulation efficiency of hydrophilic drugs, since they tend to diffuse into the aqueous phase [23, 28].

1.3.3. Nanoparticles characterization

The capability of nanoparticles to effectively target organs and tissues are influenced by morphological characteristics, particle size, surface charge and chemistry, and efficiency with which the drug is encapsulated and released. Thus, their use as drug delivery systems implies that a systematic characterization is made, in order to verify if their properties are the most suitable for pharmaceutical applications.

1.3.3.1. Morphology

Morphology of nanoparticles could be readily assessed by imaging techniques like scanning electron microscopy [10] used mostly for surface characterization (shape, distribution and aggregation), transmission electron microscopy (TEM) [29] used for shape, aggregation and internal details and, atomic force microscopy (AFM) [29] used mostly for size and morphology.

1.3.3.2. Size and polidispersity index

Size is a very important parameter in the characterization of nanoparticles that will be used as drug delivery systems, not only because it will influence the release profile and degradation rate of the nanoformulations, but also because it will determines their uptake by the cells of the mononuclear phagocytic system (MPS) and their biodistribution [30]. Although different techniques based on different physical principles can be used to measure nanoparticles size, the one that is widely used is dynamic light scattering (DLS), also called photon correlation spectroscopy. DLS measures the hydrodynamic diameter and is based on the dispersion of light caused by the Brownian motion of the particles, which is the random movement of particles due to the bombardment by the solvent molecules that surround them. In this technique, the calculation model assumes that all particles have a spherical shape, thus if some aggregates are present in the suspension the mean size will increase significantly. To have a more accurate measure several

parameters such as viscosity, pH, temperature and refractive index of the suspension medium should be previously known [30]. DLS also give us an idea of the size distribution through the polidispersity index (PDI). Size distributions can be monomodal (one population) or plurimodal (several populations) and monodisperse (narrow distribution) or polydisperse (broad distribution) (Fig.5). Assuming that the PDI values are in a range from 0 to 1, values below 0.1 are normally associated to populations with a narrow size distribution [30].

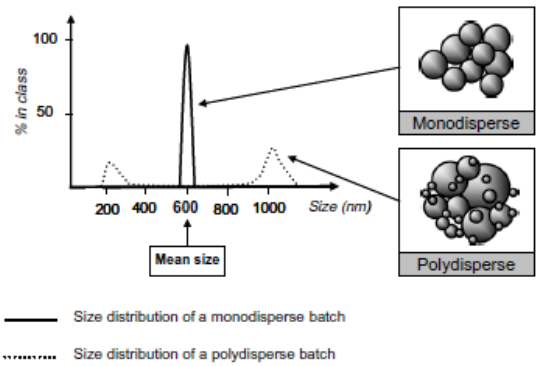

Figure 5 – Representation of the curves obtained for two nanoparticles batches of a monodisperse and polydisperse population after analysis by DLS. Adapted from [30].

Other techniques like TEM, AFM, analytical ultracentrigutation, capillary electrophoresis, *etc*, can be used for size determination although their high cost, difficulty to perform and the time consumed make their use slightly disadvantageous [30].

1.3.3.3. Surface properties

Zeta potential corresponds to the overall charge that the particles acquire in a particular medium, being an important parameter in the characterization of nanoparticles since it will determine if they will cluster in blood circulation or interact with oppositely charged cells membrane [31]. Nanoparticles in a liquid suspension are surrounded by a liquid layer composed by two parts: an inner layer (Stern layer) where the ions are strongly bound to each other and with nanoparticles and an outer (diffuse) layer where they are not so firmly bound. Within the diffuse layer exists an imaginary boundary, in which ions and particles form a stable entity [32]. The potential formed at this boundary surface is designated zeta potential and its determination is achieved through the monitoring of the mobility of charged particles by application of an electrical potential [16]. Zeta potential give us information on the stability of the particles in suspension, being that its value may be positive or negative depending on the nature of the polymer used and the occurrence or not of a surface modification. If the particles in a suspension have a high negative or positive value the tendency is to repel each other, however when the value is close to

zero the particles tend to aggregate. In general, if the zeta potential is above +30 mV or below -30 mV the particle suspension is considered stable [16, 32].

The chemical characterization analysis is important mostly in the cases where a surface modification was made, and the methods usually used include Fourier transformed infrared spectroscopy (FTIR) [29], nuclear magnetic resonance [33] and X-ray photoelectron spectroscopy [34].

The determination of the hydrophobicity/ hydrophilicity of nanoparticles is also an important parameter in the characterization of nanoparticles, since it will determines the distribution of nanoparticles in the body after administration. This parameter could be determined by hydrophobic interaction chromatography [35].

1.3.3.4. Encapsulation efficiency and drug release profile

When a drug is entrapped into the nanoparticles two parameters should be taken into consideration: encapsulation efficiency (E.E.) that corresponds to the percentage of drug retained in the nanoparticle matrix relatively to the total amount of drug initially used in the preparation process; and, drug loading which is the theoretical percentage of loaded amount of drug relatively to the total amount of polymer used in the preparation process [36]. Ideally, nanoparticles should have high E.E. and a high drug loading in order to reduce the quantity of nanoformulation required for administration. Precise determination of drug loading is not easy because nanoparticles are colloidal systems and requires a previous separation of nanoparticles from non- encapsulated drug, normally by ultracentrifugation [21]. To determine E.E. usually a drug extraction is made through the dissolution of the nanoparticles in an organic solvent (*e.g.* acetonitrile). Then the drug concentration in the solution can be measured by chromatographic (ultra-performance liquid chromatography (UPLC) [37], high-performance liquid chromatography (HPLC) [29]) or spectroscopic techniques (fluorescence [38] or ultraviolet spectroscopy [36]). Instead it can be determined the quantity of non-encapsulated drug that remains in the aqueous phase after preparation and recuperation of nanoparticles being that the value of E.E. is calculated as the difference between the amount of drug added to the nanoparticles solution and the quantity of non-entrapped drug that remain in the aqueous phase [39-40].

The *in vitro* drug release profile is also an important parameter because of the application of nanoparticles in sustained drug delivery. Depending on the type of polymer, on the preparation method, on the loading efficiency and on the size of nanoparticles, the drug release can occur by four mechanisms: desorption from the surface, diffusion through water-filled pores, diffusion through the polymer matrix or as result of polymer dissolution, being that in most cases a combination of the erosion and diffusion processes can occur [12-13, 41]. In the case of most of the PLGA-based drug delivery systems the drug

release follows a biphasic pattern with an initial burst of release that are mainly controlled by mechanisms of diffusion, followed by a more slow and controlled liberation that occurs as a result of the polymer degradation [42]. Despite the biphasic pattern is most common some authors already demonstrate that some drug delivery systems have a triphasic release profile [43-45]. Drug release studies are normally performed *in vitro* using centrifugation [43-44] or dialysis methods [42]. Usually in these methods and in order to simulate the biological conditions in which the drug delivery system will act, different buffers at different pHs are used and the samples are placed at physiological temperature (37ºC).

1.4. Modification of surface properties

One of the major issues in the use of polymeric nanoparticles as drug delivery systems is their hydrophobicity. After an intravenous administration, hydrophobic nanoparticles are rapidly recognized by the body as foreign and cleaned up from the systemic circulation by the MPS, ending up on liver, spleen or lymph nodes [46]. If the goal is to use nanoparticles for the treatment of a condition in any of the previous referred organs the use of hydrophobic nanoparticles is the better choice, however if a sustained systemic circulation is required, in order to increase the probability for the nanoparticles reach their target, then the surface of hydrophobic nanoparticles must be modified to avoid the occurrence of phagocytosis. The aim of these surface modifications is the production of nanoparticles that are not recognized by the MPS, as a result of the hydrophilic nature of their surface, which favors a longer circulation and the reduction of nonspecific distribution [47-48]. Different hydrophilic polymers such as poly-ethylene-glycol (PEG), poly-vinyl pyrrolidone, pluronics (poly-ethylene oxides), poloxamers, vitamin E TPGS, polysorbate 20, polysorbate 80, polysaccharides (*e.g.* dextran) and different types of copolymers can be used to promote the surface modification of nanoparticles [49]. These polymers can be introduced at the surface of nanoparticles using adsorbed or grafted shielding groups leading to the formation of a hydrophilic protective layer that repels plasma proteins, being that in the case of biodegradable nanoparticles, PEG can be incorporated as copolymers [46, 50-51]. PEG is the polymer most widely used for the surface modification of various polymeric nanoparticles not only because of its hydrophilic, neutral and flexible chains but also as a result of the presence of functional groups that are able to efficiently prevent the binding of plasma proteins to hydrophobic nanoparticles [52]. It is described that coating of polymeric nanoparticles with PEG decreases significantly the opsonization process of the particles and the consequent recognition and uptake by macrophages which result in an improvement of the long-term systemic circulation of nanoparticles and, higher uptake of drug when compared to non-PEGylated ones [53-55].

1.5. Nanoparticles as drug delivery systems – applications in infections therapy

The application of polymeric nanoparticles as drug delivery systems in the treatment of different diseases has been extensively investigated [56-58]. However, despite these formulations have more advantages over the use of other nanocarriers like liposomes and microparticles, until now only one polymeric-based formulation has reached the market, Abraxame®. This polymeric-based nanocarrier consists of a paclitaxel-loaded albumin nanoparticles, able to overcome the major drawbacks associated with the use of chemotherapeutic agents and effectively against metastatic breast cancer [59]. In fact, the main application of polymeric nanoparticles as drug delivery systems is in cancer therapy. The effect of chemotherapy in the treatment of different types of cancer is limited by the toxic side effects and multidrug resistance [13].

Besides nanoparticles application as drug transporters leading to a sustained and controlled release of the drug directed to the target site, these systems are also useful to improve imaging techniques that allows, for example, an early diagnosis of tumors [13]. In that way, and since that it was already demonstrated that polymeric nanoparticles have applications in different areas of medicine, is important to continue research related to the use of these nanoparticles in the treatment of different diseases (*e.g.* cancer, infectious diseases, metabolic diseases, auto-immune diseases, *etc*).

Another field in which nanoparticles are widely applied includes infectious diseases as a result of parasitic (*e.g.* leishmaniasis and malaria), viral (*e*.g. human immunodeficiency virus (HIV)) and bacterial infections (*e.g.* chlamydia). The treatment of infectious diseases has evolved greatly in the last century as a result of the discover of antibiotics and the application of a large program of vaccinations. Even tough, as a result of the development of resistances and the side effects that many of the compounds used have, infections are still a major public health problem and is urgent try to find alternative therapeutics [60]. So in that way polymeric nanoparticles constitute themselves as good alternative to defeat some of these drawbacks. An example is the encapsulation of saquinavir in PACA nanoparticles, which leads to an increase in the cellular uptake of the drug by HIV-infected macrophages and to a reduction in viral activity [56].

In metabolic diseases, like diabetes and osteoporosis, since the treatments used are based on multiple daily injections of peptides and proteins that could limit the success of the therapy, the use of polymeric nanoparticles seems to constitute a promising alternative to overcome this problem [57].

The treatment of autoimmune diseases is based on the use of immunosuppressive agents that will modulate the immune response, being that one of the major problems of these compounds is poor bioavailability in the target site. However, some studies already

demonstrate that the use of polymeric nanoparticles leads to an improvement of the local bioavailability of the immunosuppressive agents [58].

1.6. Nanoparticles and targeting of immune system – application in immunotherapy

Functionalization of nanoparticles through the conjugation of ligands that are specifically recognized by surface receptors of target cells may favor the stimulation of the immune system. Several studies have demonstrated that the use of these nanoparticles induces antigen-presenting cells (APCs) maturation, which is evaluated by the expression of co-stimulatory molecules and by cytokines production, with the simultaneous activation of T-cell responses and breaking of self-tolerance [6-7, 61].

The different ligands that are currently used to functionalize nanoparticles and which sometimes mimics the ones that exist in the surface of pathogens includes proteins, peptides, antibodies, polysaccharides, glycolipids, glycoproteins and lectins [62]. APCs (*e.g.* dendritic cells (DC) and macrophages) are cells of the innate immune system that play a major role in connecting innate and adaptive immunity, which is important to favor the development of a protective response. These cells express a wide variety of pattern recognition receptors (PRRs) in their surface that are involved in the recognition of pathogen-associated molecular patterns and is involved in the development of the immune response. Some examples of PRRs expressed by these cells are Toll-like receptors, nucleotide oligomerization domain-like receptors, scavenger receptors and C-type lectin receptors (CLRs) [62].

Active targeting of nanoparticles into the endocytic receptors expressed by APCs, such as CLRs, is a good strategy to improve their efficiency as drug delivery systems. Among CLRs, mannose receptor (MR), which is described in more detail on section 1.6.1, has been extensively studied as nanoparticles-target receptor due to its capacity to recognize mannosylated conjugates. Hamdy *et al*. [7] have demonstrated that PLGA nanoparticles decorated with mannan (MN), a polymannose isolated from the cell wall of *Saccharomyces cerevisiae*, have a strong binding affinity to MR and enhance antigen-specific T-cell responses, when compared to non-decorated nanoparticles. In another study it was demonstrated that mannose-functionalized polyanhydride nanoparticles induce and enhance DC activation by specific interactions with MR [6].

In theory, the use of functionalized nanoparticles allows targeting specific cell types of the immune system (*e.g.* macrophages and DCs) and most probably enhance the cellular uptake by these cells and induce the activation of mechanisms of innate and adaptive immunity as a result of the formation of a “danger signal”.

1.6.1. Mannose receptor

MR, also known as CD206 was identified in the late 1970s as a 175 kDa endocytic receptor on rabbit alveolar macrophages involved in the recognition of endogenous glycoproteins [63] and sugar chains terminated in D-mannose, L-fucose or N-acetyl glucosamine [64-65]. This receptor is a member of the MR family which is a subgroup of the C-type lectin superfamily and comprises three additional members: M-type phospholipase A_2 receptor (PLA_2R), DEC-205/gp200-MR6 and Endo180/uPARAP [66]. MR is a type I transmembrane receptor composed by an extracellular region containing three domains: a cysteine-rich domain that is capable of binding to sulphated sugars terminated in SO_4^{-3}-galactose (Gal) or $SO_4^{-3/4}$-N-acetyl galactosamine (GalNAc), acting as a second lectin domain; a fibronectin type II domain that is involved in collagen binding; and multiple C-type lectin-like domains (CTLDs) within a single polypeptide backbone where occurs the binding of sugars terminated in D-mannose, L-fucose or N-acetyl glucosamine. It has also a transmembrane domain and a short cytoplasmatic tail that contain motifs that mediate receptor internalization and recycling (Fig. 6) [66-67]. Although the four members of MR family share structural similarities they differ in the number of CTLDs, being that MR, PLA_2R and Endo180 have eight and DEC205 has ten. They have also a different range of functions, for example, MR has an important role in the innate and adaptive immunity, PLA_2R is involved in the internalization of soluble PLA_2 enzymes, DEC-205 internalize antigens for presentation to T cells and Endo180 is involved in the extracellular matrix remodeling [66].

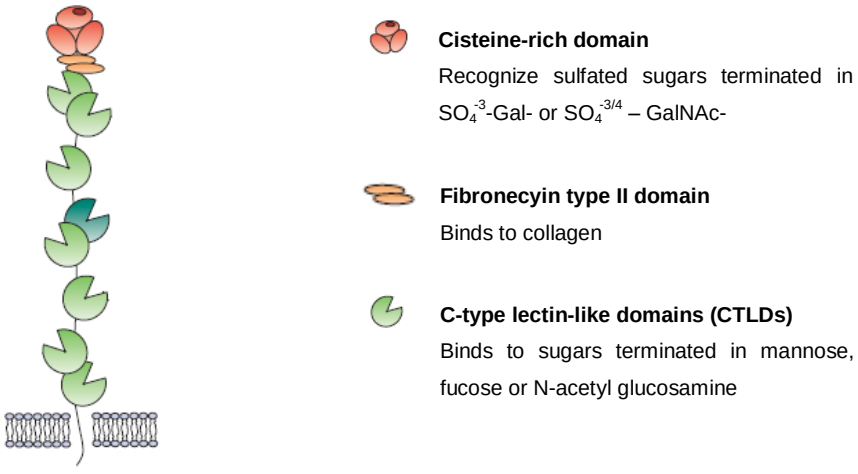

Figure 6 – MR structure – extracellular domains include cisteine-rich domain (red), fibronectin type II domain (orange) and eight CTLDs (green). Among the CTLDs, CTLD4 is shown in dark green, since it is the main responsible for sugar binding. Adapted from [67].

1.6.1.1. MR expression

Although the MR was originally termed as macrophage MR its expression is not restricted to tissue macrophages. Is now known that it is also expressed on immature murine [68] and human [69-70] monocyte-derived DCs, lymphatic and hepatic endothelial cells [71], tracheal smooth muscle cells [72], retinal pigment ephitelium [73] and kidney mesangial cells [71]. MR expression is modulated by different factors such as cytokines [74-77], immunoglobulin receptors [78] and, pathogens and their products [79], which suggest that its expression is dependent on the functional state of the cell. Studies of the role of cytokines in the regulation of MR expression demonstrate that interleukin (IL) -4 [74], IL-13 [75] and IL-10 [76] increase the expression of receptor in macrophages, which contrasts to the effect induced by interferon-gamma (IFN-ɣ) that stimulates the activation of macrophages and down-regulate the MR expression [77]. It was also demonstrated that other agents such as dexamethasone [80], prostaglandin E [81] and 1,25-dihydroxyvitamin D3 [82] also promote an increase in MR expression.

1.6.1.2. MR as an endocytic receptor

MR is constitutively internalized into early endosomes and sent back to the plasma membrane even in the absence of any ligand. At steady state 10-30% of MR are found at the cell surface and the remaining ones (70-90%) have an intracellular localization [66]. The internalization and deliver of MR into endosomal compartment is possible due to the presence of motifs in their cytoplasmic domain that are capable of interact with the components of clathrin-mediated endocytic machinery [66]. Clathrin-mediated endocytosis is a mechanism mediated by small intracellular vesicles (<0.2 μm) in which a wide variety of extracellular components are internalized. Briefly, MR is recruited into clathrin-coated pits through motifs present in their cytoplasmatic domain and is automatically internalized into early endosomes. In these compartment receptors are targeted to be recycled and to go back to the plasma membrane or delivered into late endosomes, which are characterized by abundant intravesicular membranes and the presence of active lysosomal hydrolases. When they achieve lysosomes, the last compartment of the endocytic pathway, the final degradation of internalized cargo occurs as a result of acidic pH and high content of active lysosomal hydrolases in this compartment (Fig.7) [66].

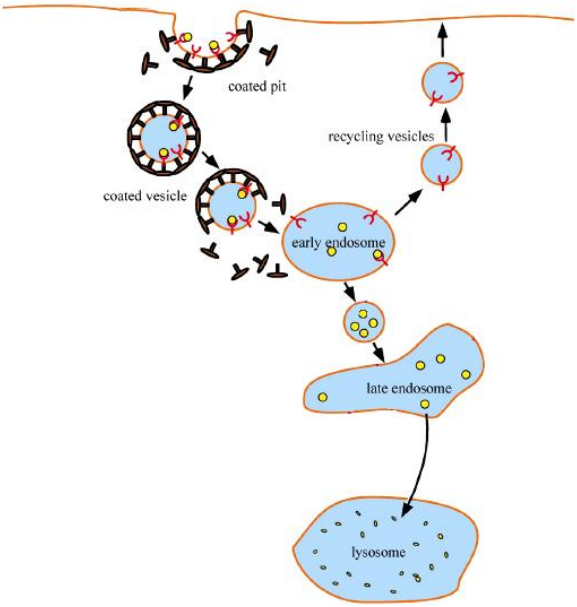

Figure 7 – Schematic representation of the clathrin-mediated endocytosis mechanism. Adapted from [66].

The role of MR in phagocytosis is still unclear, and the existent data in the literature is contradictory. Some authors have demonstrated that MR can function as a professional phagocytic receptor although they do not know what the mechanism behind this process [67, 83]. Other authors have shown that MR does not act as a phagocytic receptor and consider that this receptor *per se* is not able to mediate phagocytosis, proposing that it requires a partner to trigger phagocytosis, which means that although MR binds to particles that have terminal mannose residues then it need to recruit a phagocytic receptor to drive the phagocytic machinery [84].

1.6.1.3. Role of MR in immunity

MR has an important role in innate immunity that is the first line of defense of an organism. In this type of immunity macrophages have an important function since they are one of the first cells to arrive at the site of infection and are the main responsible for the uptake and degradation of foreign organisms [66]. MR is widely expressed on macrophages and act as a PRR since it has highly conserved CTLDs that binds, in a calcium-dependent manner, to sugar molecules (*e.g.* mannose, fucose and N-acetyl glucosamine) present on the surface of a wide variety of pathogens, including *Candida albicans* [85]*, Leishmania donovani* [86] and *Mycobacterium tuberculosis* [87]. Although, it is assumed that MR favor the pathogen uptake and, consequently degradation by macrophages, in literature there are only a few examples that corroborate this fact [85-87]. The absence of signaling motifs in MR cytoplasmatic domain suggest that the clearance promoted by this receptor does not lead to cell activation or production of pro-inflammatory cytokines, however several studies suggest that although the receptor

appears to require the assistance of other receptors, is capable to trigger a signaling cascade [88-90]. Shibata *et al.* have demonstrated that the use of chitin and mannose-coated beads stimulate the production of tumor necrosis factor-alpha (TNF-α), IFN-ɣ and IL-12 by murine spleen cells, while non-coated beads did not induce any change in cytokine production [90].

Some evidences suggest that MR may be important in antigen recognition and processing and, the fact of this receptor be abundantly expressed on DCs, which are the main APCs in the organism, reinforces the idea that this receptor mediates the antigen-internalization mechanism in these cells. Studies in which were demonstrated that mannosylation of bovine serum albumin leads to an increased internalization and presentation of this antigen to T cells [91-92], corroborates this assumption.

1.7. *Leishmania* parasite

1.7.1. History and taxonomy

William Leishman and Charles Donovan were the first ones to describe, separately but simultaneously in 1903, the protozoan parasite actually known as *Leishmania donovani* in the spleen from patients in India suffering from a life-threatening disease nowadays known as visceral leishmaniasis (VL) [93-94].

Leishmania spp. is a diverse group of organisms that belongs to the order *Kinetoplastidae*, characterized by the presence of a kinetoplast in their members, and to *Trypanosomatidae* family. The *Leishmania* genus can be divided into two subgenera, *Leishmania (Leishmania)* spp. and *Leishmania (Viannia)* spp. (Table 1). These parasites are the causative agents of leishmaniasis, existing more than 20 species that can promote the development of the disease. They are transmitted by the bite of female sandflies, belonging to the genus *Phlebotomus* in the Old World and *Lutzomyia* in the New World [93, 95].

Table 1 - Human pathogenic *Leishmania* species, clinical manifestations and geographical distribution [95]

Species	Clinical manifestation	Geographical distribution
Old World, subgenus *Leishmania*		
L. donovani	VL; PKDL	Africa, India
L. infantum	VL; CL (rare)	Mediterranean, Asia, Sub-Saharan
L. tropica	CL; VL (rare)	Middle East, India, Mediterranean
L.major	CL	Africa, Middle East, India, China
L. aethiopica	CL; DCL	East Africa
New World, subgenus *Leishmania*		
L. chagasi*	VL; CL (rare)	Latin America
L. mexicana	CL; DCL	Central America
L. amazonensis	CL; DCL; MCL; VL (rare)	Central and South America
New World, subgenus *Viannia*		
L.braziliensis	CL; MCL	South America
L. guyanensis	CL	South America
L. panamensis	CL	South America
L. peruviana	CL	Central and South America

VL, visceral leishmaniasis; PKDL, post kala-azar dermal leishmaniasis; CL, cutaneous leishmaniasis; DCL, diffuse cutaneous leishmaniasis; MCL, mucocutaneous leishmaniasis.

*There are growing evidences suggesting that *L. infantum* and *L. chagasi* are the same species [96]

1.7.2. Life cycle

Leishmania parasites have a digenetic life cycle, which means that they can successfully develop in two hosts, vertebrate (humans, dogs and other mammals) and invertebrate (insects (*e.g*. sand fly)). In the life cycle two main morphological forms of the parasite can be distinguished: an extracellular and motile promastigote form found within the sand-fly and an intracellular, non-motile and proliferative amastigote form that lives in a variety of mammalian cells, mostly within professional phagocytes such as macrophages [93, 97].

Promastigotes (Fig. 8A) are the elongated (10-20 μm), motile and flagellated form of the parasite, that are found within the alimentary tract of the sand fly where progress through

a differentiation process, known as metacyclogenesis, to ultimately form the non-dividing and highly infectious form of the parasite, the metacyclic form [93, 97].

Amastigotes (Fig. 8B) are the round or oval, non-motile and aflagellated form of the parasite (3-7 µm in diameter) and are able to survive and replicate inside the phagolysosome of the host mononuclear phagocytes. Contrarily to other pathogens *Leishmania* amastigotes survive and divides in the adverse conditions of phagolysosome (acidic pH, presence of hydrolytic enzymes and reactive species of oxygen and nitrogen) [93, 97].

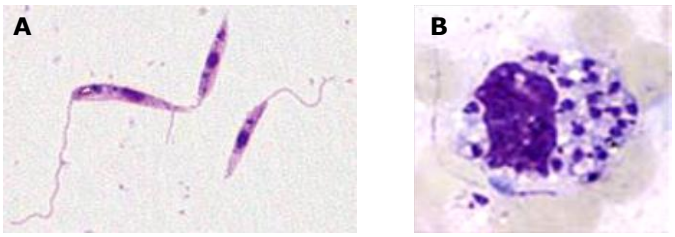

Figure 8 – *Leishmania m*orphological forms: **(A)** *Leishmania* promastigotes (Adapted from [98]) ; **(B)** *Leishmania* intracelular amastigotes stained with Giemsa (Adapted from [99])

Infection of the mammalian host is initiated when an infected *Phlebotominae* female sand fly, during blood feeding, inoculate metacyclic promastigotes together with various salivary components in dermis. Once in the vertebrate host the metacyclic promastigotes are rapidly internalized by the resident dermal or recruited phagocytic cells (*e.g*. neutrophils, macrophages and DCs), either directly or indirectly based on *Trojan Horse* model, according to which neutrophils are initially recruited to the sand fly bite and infected by *Leishmania* promastigotes suffering, shortly after infection, spontaneous apoptosis, being that the clearance by macrophages allows the indirect entry of the parasites into their final host cells [100]. Promastigotes are targeted to phagosomes in the macrophages that fuse with lysosomes forming a phagolysosome, within which they differentiate to the amastigote form. The change in temperature (from 25ºC in sandfly to 37ºC in the host) and the acidic environment (pH around 5) in the phagolysosome induces the differentiation of the promastigote form into the amastigote form. Then amastigotes proliferate by binary cell division within the host cells, which leads to their lysis when too many amastigotes are present, allowing the infection of other macrophages as wells as other phagocytic cells (*e.g*. DCs) and non-phagocytic cells (*e.g*. fibroblasts). When a sand fly ingests infected phagocytes with the blood meal, initiates the insect stage of the parasite life cycle. In this stage, after the ingestion of infected macrophages, the amastigotes are converted in flagellated and slight motile procyclic promastigotes that multiply by binary fission. On a later stage of metacyclogenesis *Leishmania* procyclic promastigotes differentiate into infective, non-dividing metacyclic promastigotes that

migrates to the sand fly salivary glands and are able to infect a mammalian host, mainly due to high expression of virulence factors like, lipophosphoglycan and glycoprotein 63 (Fig.9) [93, 97, 101-102].

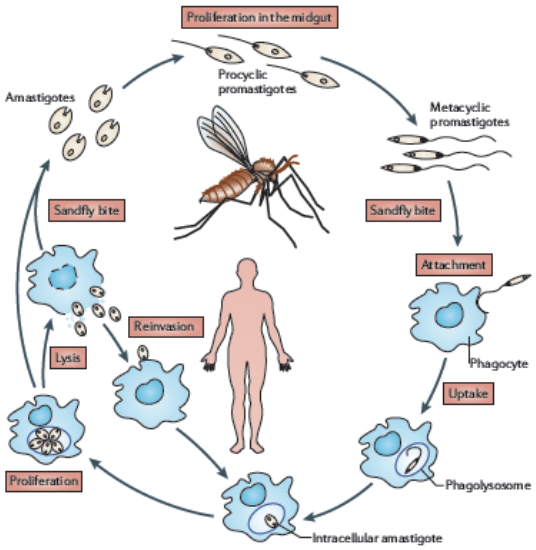

Figure 9 - *Leishmania* life cycle. Adapted from [97]

1.8. Leishmaniasis

Leishmaniasis is a neglected tropical disease that is caused by infection with one of several different species of protozoan parasites of the genus *Leishmania*. (Table 1). This is a poverty-related disease and its high prevalence is normally associated with malnutrition, poor housing, illiteracy, weakness of the immune system, lack of resources and environmental changes.

1.8.1. Epidemiology and geographical distribution

World Health Organization (WHO) has classified leishmaniasis as an emerging and uncontrolled disease, which causes 70,000 deaths each year. Currently, this disease is considered to be endemic in 88 countries (16 developed countries and 72 developing countries) on four continents. Leishmaniasis is mainly distributed in tropical and subtropical regions that include, Africa, Middle East, Southweast Asia, Southern Europe and, Central and South America (Fig.10), which is in agreement with the fact that these regions have a high prevalence of sand fly vectors [103]. It is estimated that about 350 million people are living at risk of developing one of the many forms of the disease and there are 12 million people currently infected worldwide. There are 2 million new cases of leishmaniasis per year, although there are reasons to believe that the number is increasing as a result of man-made environmental changes that promote an increased humane exposure to the sand fly vector and migration [94, 104].

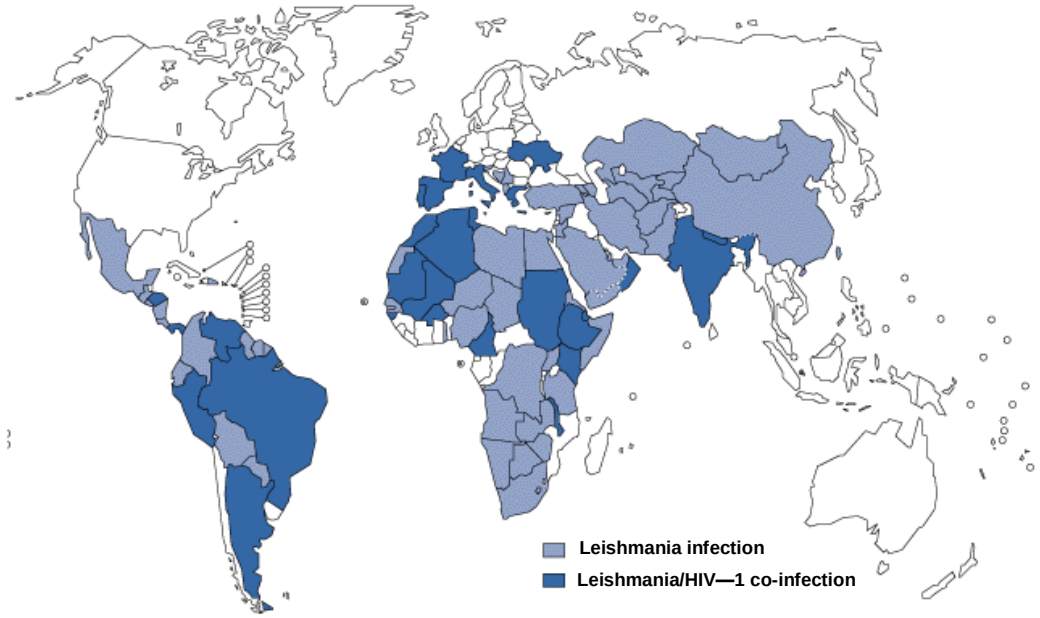

Figure 10 - Geographical distribution of reported cases of *Leishmania* infection and *Leishmania*/HIV-1 co-infection from 1990 to 1998. Adapted from [105].

Leishmaniasis has emerged as one of the main opportunistic infections that affect HIV-infected individuals, being the visceral form the one that most contribute to co-infection. According to the WHO, until now 35 countries around the world have reported cases of *Leishmania*/HIV-1 co-infection (Fig. 10). The increment in the number of cases of co-infection is a result of the increase overlap in the geographical areas with high risk of HIV-1 infection (urban areas) and leishmaniasis (rural areas). *Leishmania* and HIV-1 act synergistically on the immune system weakening it so that lead to death of the individual [105].

1.8.2. Clinical manifestations

Leishmaniasis has a large spectrum of clinical manifestations that goes from contained cutaneous ulcers to fatal, if left untreated, visceral disease. The clinical presentation of the disease depends on the causative agents and on the host immune response. The different clinical manifestations of leishmaniasis, as well as the fact that this disease could be caused by more than 20 protozoan species transmitted by approximately 30 different species of phlebotomine sandflies, reflects its diversity and complexity [106].

Leishmaniasis consists of three main clinical forms: cutaneous leishmaniasis, mucocutaneous leishmaniasis and visceral leishmaniasis.

1.8.2.1. Cutaneous leishmaniasis

Cutaneous leishmaniasis (CL) is caused by a number of species from both subgenera (*Leishmania and Viannia*) belonging to Old and New World (Table 1). Patients with this disease generally present one or several ulcer(s) or nodule(s) in the exposed areas of the skin, such as the face, arms and legs (Fig.11A). These ulcers normally self-heal in immune-competent individuals, leaving disfiguring scars, being that the time necessary to complete healing will depend on the immune status of the host [93, 107-108]. Despite CL be endemic in more than 70 countries worldwide, 90% of cases occur in Afghanistan, Brazil, Iran, Peru, Saudi Arabia and Syria [109-110].

Diffuse cutaneous leishmaniasis (DCL), a more severe and chronic form of CL, is caused by *L. aethiopica, L. mexicana* and *L. amazonensis* and is characterized by the spread of the primary lesions to multiple areas of the skin [108].

1.8.2.2. Mucocutaneous leishmaniasis

Leishmania brazilienses is responsible for most cases of mucocutaneous leishmaniasis (MCL), also known as espundia (Table 1). This disease is characterized by the formation of progressively destructive ulcerations in the mucosal membranes of the nasal and buccal cavities, which then spread to the pharynx and larynx (Fig. 11B). The lesions don't heal spontaneously and are very difficult to treat. Since this disease can develop as a result of an inadequate treatment of a cutaneous infection which can result in the appearance of mucosal metastasis in nasopharynx, it is recommended that CL is promptly treated [93, 107-108]. 90% of MCL occurs in Bolívia, Brazil and Peru [110].

1.8.2.3. Visceral leishmaniasis

Visceral leishmaniasis (VL), also known as kala-azar, is a systemic disease that is fatal when left untreated and is caused by species of the *Leishmania donovani* complex, namely *L. donovani* and *L. infantum* (Old World) and *L. chagasi* (New World) (Table 1). The causative agents could have two ways of transmission, zoonotic (*L. infantum* and *L. chagasi*), which means that is transmitted from animal to vector to human or anthroponotic (*L. donovani),* which means that is transmitted from human to vector to human. The development of the disease is a consequence of the dissemination of VL causing species to internal organs such as the liver, spleen and bone marrow, which results in the appearance of different symptoms of persistent systemic infection, including prolonged fever, anemia, loss of appetite and weight and polyclonal hypergammaglobulinaemia and, symptoms of parasitic invasion of the blood and reticulo-endothelial system, like swelling of spleen (splenomegaly), liver (hepatomegaly) and lymph nodes (Fig. 11C). Although the infection produces only moderate toxic

symptoms, as a result of severe weight loss, anemia and systemic impairment, the patient dies if is not conveniently treated. Although patients that recovered from VL have lifelong immunity, in some cases the reactivation can occur (*e.g*. HIV infection) [1, 93, 107-108].

Most of the VL cases (90%) occurs in Bangladesh, Brazil, India, Nepal, Sudan and Ethiopia [110]. There are 500,000 new cases of VL per year, being that the increased incidence of this disease is associated with migration, lack of control measures and VL-HIV co-infection. This disease is responsible for more than 50,000 deaths per year [107].

Post kala-azar dermal leishmaniasis (PKDL) is a complication of VL, frequently observed in patients a few months or years after treatment and is characterized by a macular, macula-papular or nodular rash in the face and limbs (Fig. 11D). As a result of the high number of parasites present in nodular lesions, PKDL patients are more susceptible to infections [93, 107-108].

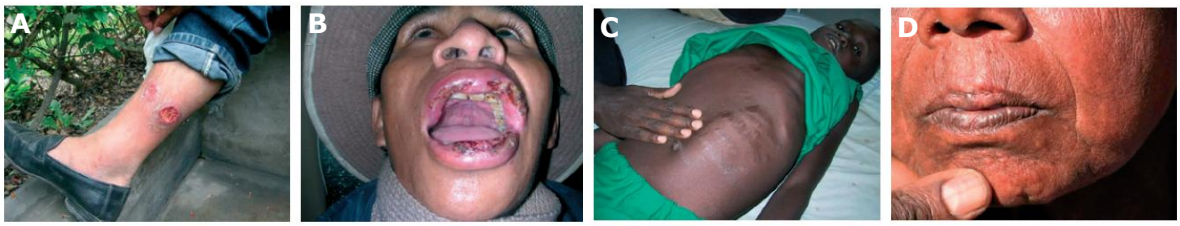

Figure 11 - Clinical manifestations of leishmaniasis. Patients with **(A)** cutaneous leishmaniasis, **(B)** mucocutaneous leishmaniasis, **(C)** visceral leishmaniasis, and **(D)** post kala-azar dermal leishmaniasis. Adapted from [107].

1.9. Treatment of leishmaniasis

Leishmaniasis has higher incidence in less developed countries where, for economic reasons, exist serious limitations in diagnosis, disease control and treatment. Since there is no commercially available human vaccine against leishmaniasis the control of this disease is dependent on drug therapy and vector control. The drugs currently used in the treatment of leishmaniasis have severe side effects, are poorly tolerated, induce the emergence of resistances, most of them involve a long period of treatment, close medical supervision, and are ineffective in situations of disease exacerbation [1-3, 111]. Thus it is of great importance to develop new drugs and/or formulations that replace or complement the ones that are current available.

1.9.1. Current treatment options

1.9.1.1. Pentavalent antimonials

Pentavalent antimonials, which were developed in 1945, are still the drugs recommended by the WHO as first-line of treatments against CL and VL. The compounds from

pentavalent antimonial family, namely the commercially available sodium stibogluconate (Pentostam®) and meglumine antimoniate (Glucantime®), remain as the main therapy for leishmaniasis in most regions with the exception of Bihar State, India, because of the high prevalence of resistance (more than 60%) and, in Europe, not related to drug resistance, but because of the availability of highly effective forms of treatment. [3, 112]. Although the compound is used for a long time in the treatment of leishmaniasis their mechanism of action is not yet completely understood. Antimonials have several disadvantages including the long duration of the treatment, the requirement of a parenteral administration and consequently a close medical supervision, the toxic effects (nausea, abdominal pain, chemical pancreatitis and cardiotoxicity) and the emergence of resistances [3].

1.9.1.2. Pentamidine

Pentamidine (isethionate or methansulphonate) is an aromatic diamine, previously used, in areas of antimonial resistance, as a second line treatment for VL, however as a result of its toxic side effects (hypoglycemia, nephrotoxicity, hypotension, *etc*) and emergence of resistant strains, the use of this drug, in India, for the treatment of VL was abolished [3, 113]. However for CL was demonstrated that the low doses of pentamidine and a short course period of treatment promotes a high cure rate, making this drug a good alternative in cases of CL [114].

1.9.1.3. Amphotericin B

Amphotericin B (AmB) is a polyene antifungal antibiotic agent, discovered in 1956, from a bacterium of genus *Streptomyces*, widely used to treat systemic fungal infections. AmB have a high affinity for ergosterol that is the main component of the cell membrane of fungi and *Leishmania* parasite. The antileishmanial activity of this compound is due to its interaction with ergosterol. Although in a lesser extent AmB also interacts with cholesterol of host macrophages inhibiting the bind of the parasite to cells, being that at higher concentrations (<0.1M) it induces the formation of aqueous pores in leishmanial cell membranes leading to parasite death [1, 111]. AmB constitutes a second line of treatment, except in areas of antimonial resistance, like Bihar State in India, where it is the drug of choice. The major drawbacks associated with the use of AmB are the higher costs, the limited availability in some areas, difficulties associated with the administration (slow infusions), prolonged duration of therapy (up to 30 days) and the severe side effects (fever, bone pain, chills, hypokalemia, renal impairment and anemia) [1, 3-4]. To overcome some of these issues, especially the high toxicity, three effective lipid-associated formulations of this compound, unilamellar liposomal formulation (AmBisome®), colloidal dispersion (Amphocil) and lipid complex (Abelcet), were

implemented. These lipid formulations not only retain the fungal activity of AmB but are also more effective and well tolerated since their physicochemical properties favors their uptake by the reticuloendothelial cells in the liver, spleen and bone-marrow that are the main targets of VL [1, 3, 111]. They have been evaluated in clinical trials for VL and CL and the results showed that AmBisome® and Amphocil are more effective than Abelcet in the treatment of VL and the reduction of the size of the lesions in CL is more significant with the use of AmBisome® [115]. Despite its efficacy the high costs limits its use in less developed countries. Some studies have demonstrated that the effectiveness of AmB treatment is dependent of the patient immunity status and that successive relapse could favor the appearing of clinical resistances against the compound. Thus, although until now doesn't exist any report of clinical resistance against AmB, these studies supports the possibility of their development [116-117].

1.9.1.4. Miltefosine

Miltefosine (hexadecylphosphocholine) is a membrane activating alkyl phospholipid that was originally developed as an antineoplastic agent. After clinical studies, it was approved as Impavido™ and become the first commercial available oral drug for the treatment of VL. This drug has many advantages including its high efficiency, low cost, the short course of the treatment, reduced side effects and the fact of be orally administered and well tolerated allowing it to be made an ambulatory treatment without the need of a close monitoring. However miltefosine has some disadvantages related to its teratogenicity, which limit its use in women that are pregnant or in reproductive age and, to its long half-life (≈7 days) that increases the possibility of development of resistances [113, 118].

1.9.1.5. Paramomycin

Paramomycin (aminosidine) is an aminoglycosidic antibiotic with antileishmanial activity. This antibiotic can be used for the treatment of both VL and CL, however the poor oral absorption led to the development of parenteral and topical formulations, for VL and CL, respectively [119]. The results of phase III clinical trials conducted in Bihar, India revealed that this drug have a high efficacy, not inferior to AmB, and safety since treated patients do not present nephrotoxicity, and only a small percentage present damage of the inner ear and a significant increase in hepatic transaminases [120]. Furthermore, paramomycin have other advantages namely the fact that it is active against different pathogens, including bacteria, the short duration time of its administration and its low cost in comparison to the other treatments currently available for leishmaniasis [107].

1.9.2. Combined therapy

The implementation of a combined therapy aims to increase treatment efficacy, prevent the development of drug resistances, reduce treatment duration and if possible, the treatment cost [121]. It was demonstrated that the use of a combination therapy with sodium stibogluconate and paramomycin in the treatment of VL was more safe and effective than the therapy with sodium stibogluconate alone. These clinical studies conducted in India and East Africa also showed that combined therapy allows a reduction in the duration of the treatment, from 30 to 17 days [122]. A combination therapy including liposomal AmB and miltefosine is being currently studied in India [107].

1.9.3. New formulations in the treatment of leishmaniasis

Leishmania spp. are characterized by its ability to survive and replicate inside the host phagocytes and by its capacity to disseminate for different locations, which constitutes a great challenge to drug discovery and delivery since the intracellular localization protects them against the action of drugs that are not able to diffuse readily into cells. The use of some drug carriers, including emulsions, liposomes and nanoparticles is of great interest, because it allows the selective distribution to phagocytic cells, prevent the action of drugs in uninfected tissues and consequently reduce the toxicity and increase the efficiency of the antileishmanial compounds.

Liposomes and polymeric nanoparticles were already tested as drug delivery systems for antileishmanial compounds showing a great potential to improve the efficacy and tolerability of these compounds [123]. Liposomes are widely used as drug carriers since they are capable to entrap hydrophilic and hydrophobic drugs reducing its toxicity, are highly versatile, their surface can be easily modified and when administered intravenously are rapidly captured by the phagocytic cells present on liver and spleen that are the main target organs in VL [62]. One of the first applications of liposomes was the treatment of leishmanial infections [124]. Although it has been demonstrated that the encapsulation of some antileishmanial drugs, namely pentavalent antimonials and miltefosine, in liposomes increases its effectiveness in the treatment of leishmaniasis [125-127], the most successful example is AmBisome®, the only liposomal product approved and commercially available for treatment of VL. The AmBisome® has the advantage of reducing the toxicity associated with free drug. In fact, its small size (<100 nm) prevents its immediately uptake by macrophages of liver and spleen allowing their circulation in the blood to reach other infected tissues, like lungs, kidney and brain. These formulations also have the advantage of killing microorganisms that were not phagocytised. Nowadays, AmBisome® is considered an excellent treatment option not only for VL but also for fungal infections, however the high costs associated with the use of this formulation limits its

application in developing countries. Another liposomal formulation of AmB (Abelcet®) is commercially available, however it is less effective when compared with AmBisome®[128]. The most promising strategy to overcome the problems associated with the costs of these liposomes-based treatments appears to be the development of formulations using polymeric nanoparticles.

Polymeric nanoparticles can be useful in the treatment of macrophage-mediated diseases, like leishmaniasis, since the small size of these formulations favors its efficient cross through biological barriers, improved cellular uptake and the delivery of the therapeutic agents in infected sites. The main advantage of polymeric nanoparticles when compared to liposomes is the ability that they have to withstand physiological stress or improved biological stability and possibility of oral delivery [128]. When polymeric nanoparticles are used for treatment of leishmaniasis is fundamental to consider the type of polymer used because it hydrophobicity will influence the uptake by macrophages, that are the main targets in leishmaniasis. Several studies [129-133] demonstrate the efficacy of polymeric nanoparticles in the treatment of VL. Primaquine loaded- PACA and PLA nanoparticles showed an increase on efficacy and reduced toxicity when compared with the free drug. Moreover, unloaded PACA nanoparticles have, *per se*, an antileishmanial activity equivalent to free primaquine, which is not verified in the case of unloaded PLA nanoparticles [129-130]. The incorporation of pentamidine in polymethyl methacrylate and of AmB in PCL biodegradable nanoparticles improves their antileishmanial activity and reduces the side effects of the free compounds [131-132]. The antileishmanial activity of 2',6'-Dihydroxy-4'-methoxychalcone, a compound of natural origin, was improved ≈ 2.3-fold when it is encapsulated in PLA nanoparticles [133].

The surface of both liposomes and polymeric nanoparticles can be modified by the use of targeting ligands that are recognized by specific receptors presents on phagocytic cells, which will direct their internalization and posterior action, at a specific cell/ site. In a recent study the use of AmB-loaded mannose-coated liposomes was explored for selective delivery of drug to macrophages in the treatment of VL and it was demonstrated that functionalization of this formulations with mannose leads to a higher uptake in the liver and spleen which favors the direct action of the drug in the region where the parasite resides, and at the same time prevent the action of drugs in other organs reducing its toxicity [134]. In another study the use of functionalized polymeric nanoparticles in the treatment of VL was explored [29]. Taking into account that MR are present mainly in the surface of macrophages and DCs the authors have prepared AmB-loaded PLGA nanoparticles containing the MR specific ligand (mannose). The results showed that the functionalization of polymeric nanoparticles with mannose leads to a higher uptake and increased antileishmanial activity [29].

II. AIMS

In the last decades significant progresses were made in understanding the immunopathogenesis of leishmaniasis, however until now, no effective and safe treatment was discovered. Moreover, currently available drugs for the treatment of this disease are associated with emerging resistance and elevated toxicities. In that way it is of great importance to develop alternative treatments, like nanotechnology-based drug delivery systems, that replace or complement the ones that are current available. Furthermore, it has been demonstrated that the efficiency of PLGA-based drug delivery systems in the treatment of leishmaniasis could be improved by their functionalization with ligands that specifically target MR, a member of CLR family that is highly expressed on APCs, the target cells in VL. In that way, the first purpose of the present work was to develop a mannosylated nanoparticulate system for efficient delivery of AmB, being that the strategy chosen involves: (1) the preparation of unloaded mannose-coated PLGA (M-PLGA) nanoparticles by three different techniques physical adsorption (PA), one-step chemical reaction (CR1) and two-step chemical reaction (CR2), their biophysical characterization and evaluation of their cytotoxicity towards macrophages and intracellular *Leishmania infantum* amastigotes, to determine which of those techniques are more suitable for the preparation of nanoparticles; (2) use the developed nanoparticulate system to encapsulate AmB and evaluate the *in vitro* efficacy of the new delivery systems against *Leishmania* –infected macrophages; (3) assessment of the new nanoformulation differential uptake by APCs, through *ex vivo* and *in vivo* studies, using splenocytes isolated from Balb/c mice.

Functionalization of nanoparticles through the conjugation of ligands that are specifically recognized by surface receptors on target cells may favor the stimulation of the immune system. Several studies have demonstrated that the use of these nanoparticles induces DCs maturation, which is evaluated by the expression of co-stimulatory molecules and by cytokines production, with the simultaneous activation of T-cell responses [6-7, 61]. Thus, the second purpose of this work was to identify the optimum mannosylated nanoformulation for efficient delivery to APCs, using PLGA nanoparticles functionalized with three different sugars, mannose (M), mannan (MN) and mannosamine (Ms) and evaluate the extent in which these formulations affect the activation status of the cells, as well as the type of response that they will modulate in APCs.

III. MATERIALS AND METHODS

3.1. Chemical reagents

PVA [87-89 % hydrolysed , molecular weight (MW) 13 000 – 23 000 g/mol], D-(+)-mannose (MW 180.16 g/mol), mannan, from *Saccharomyces cerevisiae*, D-mannosamine hydrochloride (MW 215.64 g/mol), N-hydroxysuccinimide (NHS) (MW 115.09 g/mol), N-(3-dimethylaminopropyl)-N'-ethylcarbodiimide hydrochloride (DCC) (MW 191.7 g/mol), AmB, from *Streptomyces* (MW 924.1 g/mol) and fluorescein isothiocyanate isomer I (FITC) (MW 389.38 g/mol). All reagents were purchased from Sigma-Aldrich (Sintra, Portugal). PLGA (70:30) (MW 10 000 g/mol) was purchased from Polysciences, Inc .(Valley Road, Warrington).

3.2. Preparation of nanoparticles

3.2.1. Preparation of PLGA nanoparticles loaded with AmB or FITC

PLGA nanoparticles were prepared by the nanoprecipitation method [5] in the presence of a specific amount of AmB or FITC (% drug loading (w/w)). Briefly, a mass of ± 10 mg of PLGA was rigorously weighted (Analytical Balance Kern ABS) and dissolved in approximately 1 mL of acetone, in a glass tube. To obtain the desired % drug loading (mass of compound per mass of polymer) a defined volume of a stock solution of 10 mg/mL AmB or 50 mg/mL FITC, both in dimethyl sulphoxide (DMSO) was added to the previous solution. Then, the formed organic phase was added dropwise to an aqueous solution of 1% (w/v) PVA using a 19G syringe. The emulsion was left under magnetic stirring for 10 minutes, followed by slow evaporation of the organic solvent using a rotator evaporator over-night. After that, the nanoparticles were recovered and washed by centrifugation. An initial centrifugation at 5,000 *xg* for 5 minutes at 20ºC (Sigma 3K18 Laboratory Centrifuge; Philip Harris Scientific, Lutterworth, UK) was performed to remove larger particle aggregates. The resulting supernatant was recovered and centrifuged at 20,000 *xg* for 20 minutes at 20ºC in order to obtain the nanoparticle sediment that is then washed twice, with distilled water, by centrifugation at 20,000 *x g* for 20 minutes at 20ºC. The final sediment was re-suspended in 2 mL of phosphate-buffered saline (PBS) (137 mM NaCl, 2.7 mM KCl, 10 mM Na_2HPO_4 and 2.0 mM KH_2PO_4; pH 7.4) and the supernatants obtained from the washing steps (S1, L1 and L2) were stored at 4ºC for quantification of drug encapsulation. Plain (empty) PLGA Nanoparticles were prepared using the same procedure without the addition of compound. Nanoparticle suspensions were sterilized by exposure to ultraviolet light (20 minutes) and stored at 4ºC until further use.

The FITC-loaded PLGA nanoparticles were prepared in aseptic conditions. All reagents, glass and plastic equipment's were sterilized by autoclaving, exposure to ultraviolet light or filtration and all the steps involved in the preparation of the nanoparticles (stirring, mixing and suspending) were done inside a biosafety cabinet. All FITC-nanoformulations were tested for the presence of endotoxin using a kit (CellTox^{TM}, Promega, Madison, USA) accordingly to the manufacturer instructions, and were shown to be endotoxin free.

3.2.2. Mannose incorporation

Mannose was attached to PLGA nanoparticles (M-PLGA nanoparticles) by three different techniques: PA, CR1 andCR2. For PA 20 mg of mannose were added to 10 mg of PLGA nanoparticles dispersed in 5 mL acidic PBS (pH 5.0), and the mixture was then stirred at room temperature over-night. The PLGA nanoparticles with adsorbed mannose were then collected and washed off from soluble mannose by successive centrifugations as described on section 3.2.1. In CR1 a mixture of 20 mg of mannose, 153 µg DCC and 0,459 µg NHS were added to 10 mg of PLGA nanoparticles dispersed in 5 mL acidic PBS (pH 5.0) and in CR2, first 10 mg of PLGA dispersed in 5 mL acidic PBS (pH 5.0) were incubated with the activators of PLGA carboxyl groups (NHS and DCC), in the same quantities that we use for CR1, during 2 hours, followed by the incubation with 20 mg mannose over-night. In both types of chemical reaction the excess reagents and soluble by-products were washed away at 20,000 *xg* for 20 minutes at 20ºC. The final sediment was re-suspended in 2 mL of pH7.4 PBS and the supernatants obtained from the washing steps (S1, L1 and L2) were stored at 4ºC for quantification of drug encapsulation. Nanoparticle suspensions were sterilized by exposure to ultraviolet light (20 minutes) and stored at 4ºC until further use.

3.2.3. Mannan and mannosamine incorporation

In the case of FITC-loaded nanoparticles the coating were made not only with M, but also with MN and Ms. These two sugars were attached to PLGA nanoparticles (MN-PLGA and Ms-PLGA nanoparticles) by CR1, following the same procedure described on the previous section.

3.3. Characterization of nanoparticles

3.3.1. Size, polydispersity index and zeta potential

Size, polydispersity index and zeta potential determinations were performed by dynamic light scattering methods using a Zetasizer Nano ZS (Malvern Instruments, Malvern, UK) with a detection angle of 173º. Measurements were made in triplicate at 25ºC. The

samples for dynamic light scattering analysis were prepared by diluting the nanoparticle suspension in distilled water to a final concentration of 1 mg/mL in polymer.

3.3.2. Transmission Electron Microscopy

The morphology of prepared nanoparticles was determined by TEM (Jeol JEM-1400, Tokyo, Japan). About 10 µL of the aqueous dispersion of nanoparticles was placed on carbon coated copper grids and after 1 minute excess was removed and the sample stained with an aqueous solution of 3% uranyl acetate for 30 seconds. Samples were then observed in a microscope at the accelerating voltage of 60 kV.

3.3.3. Fourier Transform Infrared Spectroscopy

The molecular structure of uncoated and M-PLGA nanoparticles was confirmed using FTIR (Perkin Elmer 2000 FTIR/ RAMAN system, Massachusetts, USA). For FTIR analysis the nanoparticles were freeze-dried using 5% trehalose, followed by vacuum dried at 25ºC. Then the obtain solid samples were milled with potassium bromide, in a proportion of 1:100, to form a very fine powder, that is then compressed within two stainless steel disks using hydraulic pressure. After that, the formed film, which should be homogenous and transparent in appearance, was removed and used to obtain the FTIR spectrum.

3.3.4. Lectin Binding Assay

In order to assess the surface orientation and availability of mannose ligand after formation of coated PLGA nanoparticles, an agglutination test was carried out using Concanavalin A (ConA) lectin (Sigma Aldrich, Sintra, Portugal) [135]. Briefly, 200 µL of M-PLGA nanoparticles were diluted 10 times with PBS pH 7.4 containing 5 mM of calcium chloride and 5 mM of magnesium chloride (both from Sigma Aldrich, Sintra, Portugal), then ConA was added to a concentration of 25 µg/mL and time-dependent increase in turbidity at 550 nm was monitored spectrophotometrically (Sinergy 2, BioTek) for 90 minutes.

3.3.5. Quantification of mannose, mannan and mannosamine

The effect of polymer type and coating method on the incorporation level of the used sugars was investigated by indirect quantification using phenol-sulfuric acid reaction. M, MN or Ms that are present in larger particle aggregates were extracted using a dichloromethane (DCM)/water extraction system. Briefly, 5 mg of aggregates were dissolved in 500 µL DCM in an eppendorf tube by vortexing. Then 700 µL of water was added and the two phases were mixed thoroughly. The aqueous phase was separated and heated in a horizontal lab shaker at 40ºC to evaporate the remaining DCM, which is

followed by a centrifugation at 14,000 *xg*, for 15 minutes at 20ºC to remove the insoluble fractions. The sugar dissolved in the supernatant previously obtained and in the supernatants obtained from the washing steps (S1, L1 and L2) was then quantified by phenol-sulfuric acid reaction [136]. In this colorimetric assay, to 50 µL of supernatant in a flat 96-well microplate, 150 µL of concentrated sulfuric acid (96%) were rapidly added to favor maximum mixing. Immediately after that, we add 30 µL of 5% (w/v) phenol solution and then the plate was incubated in a heated static water bath for 5 minutes at 90ºC to favor the color development. The plate was then cooled down at room temperature to stop reaction and the absorbance was read at 490 nm in a microplate reader (Sinergy 2, BioTek). Linear calibration curves relating sugar concentration and absorbance at 490 nm were made in the range of 4.50-0.03 mg/mL and the extent of sugar incorporation in nanoparticles was expressed as the amount of mannose, mannan or mannosamine (mg/ mg of polymer) and was calculated as:

$$\textbf{Amount of sugar (mg/mg polymer)} = \frac{m_{\text{initial solution}} - m_{\text{Agregattes+ S1+L1+L2}}}{m_{\text{initial solution}}} \times 100$$

3.3.6. Storage Stability

Storage condition assays were performed in order to evaluate the stability of empty M-PLGA nanoparticles, prepared by CR1, at -20ºC, 4ºC and 37ºC. Nanoparticle suspensions were divided in aliquots of 100 µL, stored at -20ºC, 4ºC and 37ºC and over a period of 8 weeks an aliquot was periodically diluted in distillated water to give a final concentration in polymer of 1 mg/mL. This sample was then analyzed for size, polydispersity index and zeta potential by dynamic light scattering methods using a Zetasizer Nano ZS.

3.3.7. Encapsulation efficiency

3.3.7.1. AmB

E.E. of AmB in uncoated and M- PLGA nanoparticles was determined directly by UPLC (Acquity Ultra Performance LC™, Waters Corp., Milford, MA, USA) using an Ethylene Bridged Hybrid C18 column (Acquity UPLC®, Waters) (150 x 2.1 mm, 1.7 µm particle size; Waters Corp., Milford, MA, USA) maintained at 20ºC. The autosampler temperature was maintained at 4ºC. The conditions established for the gradient elution program used in the analysis of AmB are shown in Table 2. The mobile phase was comprised of (A) 0.1 M ammonium acetate pH 4 and (B) acetonitrile at a flow rate of 0.1 mL/min. The injection volume was 10 µL when the full loop mode was selected for sample injection.

The detection was performed at a 407 nm wavelength using a photodiode array detector with total running time of 6 min. The retention time was found to be 4.3 minutes. Data acquisition, data handling and instrument control were performed by MassLynx software (Waters Corp., Milford, MA, USA).

Table 2 – Gradient elution program for the analysis of AmB

Time (minutes)	Mobile phase A[a] (%)	Mobile phase B[b] (%)	Flow rate (mL/min)
0.00	60	40	0.1
0.01	60	40	0.1
4.00	0	100	0.1
5.50	0	100	0.1
6.00	60	40	0.1

[a] 0.1 M Ammonium acetate pH4; [b] Acetonitrile

Linear calibration curves relating AmB concentration and peak area were made using AmB standard solutions in the range of 2 – 0.1 ppm. The quantity of encapsulated AmB in uncoated and mannose-coated PLGA nanoparticles was determined by interpolation of the peak area, obtained for each sample, in the calibration curve.

3.3.7.2. FITC

E.E. of FITC in uncoated and M-, MN- and Ms - coated PLGA nanoparticles was determined indirectly by quantification of the non-encapsulated compound that stays in the aqueous phase after particle recovery (Aggregates, S1, L1 and L2). FITC have intrinsic fluorescence properties exhibiting an excitation and emission wavelength of 485 nm and 528 nm, respectively, which allows its quantification by measurement of fluorescence intensity in a microplate reader. Linear calibration curves relating FITC concentration and fluorescence were made in the range of 0.400– 0.003 mg/mL. Encapsulation efficiency was determined as:

$$\textbf{Encapsulation Efficiency (\%)} = \frac{m_{\text{FITC initial solution}} - m_{\text{FITC Agregattes+ S1+L1+L2}}}{m_{\text{FITC initial solution}}} \times 100$$

3.3.8. *In vitro* drug release

The release of AmB from M-PLGA nanoparticles was determined over time at two pH conditions, 5.5, to simulate the release in the endosomal compartment of macrophages, and 7.4, to simulate the physiological conditions, and using two different buffers PBS and HEPES (4-(2-hydroxyethyl)-1-piperazineethanesulfonic acid) (20 mM). The nanoparticle suspension was diluted in the appropriate buffer to a final concentration of 1 mg/mL in

polymer and incubated at 37ºC in a horizontal lab shaker (Thermomixer compact – Eppendorf (Hamburg, Germany)) at 500 rpm. At determined intervals samples were centrifuged at 20,000 *xg* for 15 minutes at 4ºC, the supernatants were collected and stored at 4ºC for quantification of the released compound by UPLC, in the conditions previously described. The resulting nanoparticle sediment was re-suspended in fresh buffer and re-incubated in the same conditions until next sampling time.

The release of FITC from uncoated and M-, MN- and Ms -coated PLGA nanoparticles was determined over time at pH 7.4, using PBS. The nanoparticle suspension was diluted in the appropriate buffer to a final concentration of 1 mg/mL in polymer and incubated at 37^0 C in a horizontal lab shaker at 500 rpm. At known intervals samples were centrifuged at 20,000 *xg* for 15 minutes at 4ºC, the supernatants were collected and stored at 4ºC for quantification of the released compound by measurement of fluorescence intensity in a microplate reader. The resulting nanoparticle sediment was re-suspended in fresh buffer and re-incubated in the same conditions.

3.4. Parasites and cell culture

3.4.1. Parasites

A cloned line of *Leishmania infantum* (MOM/MA671TMAP263) promastigotes, stably expressing the luciferase gene (*LUC*), were maintained in culture in RPMI 1640 medium supplemented with 10% heat-inactivated fetal bovine serum (FBS), 2 mM L-glutamine, 20 mM HEPES, 100 U/mL penicillin and 100 µg/mL streptomycin (all from BioWhittaker, Verviers, Belgium) at 26ºC by sub-passage (10^6 parasites/mL) every 5 days. Selection of *LUC*-positive parasites was done by adding geneticin sulphate (Sigma-Aldrich, St Louis, MO) to the culture media at a final concentration of 5 µg/mL.

Leishmania infantum axenic amastigotes stably expressing the *LUC*- gene were derived from promastigotes, in stationary phase, by culturing them in MAA (Medium for Axenic Amastigotes), that is composed by modified medium 199 with Hank's balanced salt solution (Gibco Invitrogen, Barcelona, Spain) supplemented with 0.5% trypto-casein-soy broth (Bio-Rad, Bath, UK), 15 mM D-glucose anhydrous (Panreac, Barcelona, Spain) and 4 mM $NaHCO_3$ (Sigma Aldrich, St Louis, MO). The pH was adjusted to 5.8 and the media was 0.2 µM sterilized by filtration and further supplemented with 0.023 mM bovine hemin (Fluka, St Louis, MO), 5 mM L-glutamine and 25% heat-inactivated FBS. Axenic amastigotes were maintained in culture at 37ºC in an atmosphere containing 5% CO_2 by sub-passage (10^5 parasites/mL) every 5 days.

3.4.2. Human leukaemia monocytic cell line (THP-1 cells)

The human leukaemia monocytic cell line THP-1 was grown in RPMI 1640 medium supplemented with 10% heat-inactivated FBS, 2 mM L-glutamine, 100 U/mL penicillin and 100 µg/mL streptomycin. Cells were maintained in culture at 37ºC in a humidified atmosphere containing 5% CO_2 by sub-passage every 4 days. The cells were counted in a haemocytometer (Marienfeld, Germany) in the presence of trypan blue to exclude non viable cells. Human THP-1 cells (10^5 cells/mL) were differentiated in the presence of 20 ng/mL phorbol 12-myristate 13-acetate (PMA) (Sigma Aldrich, Sintra, Portugal) for 18h at 37^0 C and were left for another 24h with fresh medium containing no PMA.

3.4.3. Murine bone marrow-derived macrophages (BMMϕ) – Isolation and culture

Macrophage primary cultures were generated from murine bone marrow precursors from femurs and tibias of Balb/c mice in Dulbecco's modified Eagle's medium (DMEM) (BioWhittaker, Verviers, Belgium), supplemented with 10% heat-inactivated FBS, 2mM L-glutamine, 100 U/mL penicillin and 100 µg/mL streptomycin in the presence of L929 cell conditioned medium (LCCM), as described by [137]. Briefly, femurs and tibias were removed from Balb/c mice with 8-10 weeks and in order to promote their disinfection, the intact bones were put in 70% ethanol and then washed with PBS. Then both ends of the femur were cut with sterile scalpel, and the bone marrow was flushed with cold DMEM using a 25G syringe. The obtained cell suspension was cultured in DMEM and after 5 h of incubation at 37ºC non-adherent cells were recovered by centrifugation at 300 *xg* during 10 minutes at room temperature and cultured in 24-well plate at $4x10^5$ cells/mL in 5% LCCM-supplemented DMEM. For BMMϕ differentiation 5% LCCM was added at days 0 and 4. If we want to extend further cultured, at day 7 we renew half of the culture medium with 5% LCCM-supplemented DMEM.

3.4.4 Murine bone marrow-derived dendritic cells (BMDCs) – Isolation and culture

Primary cultures of DCs were generated from murine bone marrow precursors from femurs and tibias of Balb/c mice in RPMI 1640 medium supplemented with 10% heat-inactivated FBS, 2 mM L-glutamine, 100 U/mL penicillin, 100 µg/mL streptomycin and β-mercaptoetanol (Sigma Aldrich, Sintra, Portugal), in the presence of granulocyte macrophage colony-stimulating factor (GM-CSF) obtained from the supernatant of transfected J558 cells. The isolation of bone-marrow cells from femurs and tibias were made as described on 3.4.3. section. The obtained cell suspension was cultured at a cell density of $5x10^6$ cells in a final volume of 25 mL of complete medium

containing 10% GM-CSF. At day 3, more 25 mL of complete medium with 10% GM-CSF was added to the culture flasks and at days 6 and 8, half of the culture supernatant was collected, centrifuged at 300 *xg* during 10 minutes, and the cell pellet was re-suspended in 25 mL of fresh medium containing 5% GM-CSF and put back into the original flask.

3.5. Toxicity of free AmB and nanoformulations to macrophages

Differentiated THP-1 macrophages and BMMϕ were incubated in 96-well plates at a cell density of 10^5 cells/mL. Serial dilutions of free AmB and empty or AmB-loaded PLGA nanoparticles in culture medium were added to the wells, in quadruplicate, and were incubated for 72h at 37ºC in 5% CO_2. Cell viability was assessed by the MTT [3-(4,5-dimethylthiazol-2-yl)-2,5-diphenyltetrazolium bromide] assay as previously described [138]. Briefly, after the incubation period, culture media was removed and cells were incubated with the MTT reagent (thyazolyl blue tetrazolium bromide) (Sigma Aldrich, St Louis, MO) in culture medium (at 0.5 mg/mL) for 4 hours. After that, we remove the medium and add 200 µL of isopropanol to dissolve the formed formazan crystals. Optical density (OD) was read at 570 and 660 nm in a microplate reader (Sinergy 2, BioTek). Cell viability for each sample was calculated as:

$$\textbf{\% cell viability} = \frac{(OD_{570\text{-}660})\ \text{treated cells}}{(OD_{570\text{-}660})_{\text{untreated cells}}} \times 100$$

The AmB concentration, either free or in PLGA nanoparticles, necessary to decrease cell viability to 50% (EC_{50}) of the untreated control, was determined by linear regression analysis.

3.6. Growth inhibition assays against intracellular *Leishmania infantum* amastigotes

Differentiated THP-1 macrophages and BMMϕ were incubated in 96-well plates at a cell density of 10^5 cells/mL and subsequently were infected with the stationary phase *LUC*-expressing *L.infantum* axenic amastigotes at a parasite: cell ratio of 10:1, for a period of 4h, after which the cells were washed with culture medium to remove non-internalized parasites. Serial dilutions of free AmB and empty or AmB-loaded PLGA nanoparticles in culture medium were added to the wells, in quadruplicate, and were incubated for 72h at 37ºC in 5% CO_2. After the incubation period, the luciferase activity of intracellular amastigotes was determined as previously described [139]. Briefly, culture media was removed and cells were incubated during 10 minutes under constant agitation with 100 µL of PBS pH7.4 and 25 µL of Glo Lysis Buffer (Promega, Madison, USA) in order to promote the cell lysis. After that the luciferase substrate (Steady-Glo® Luciferase) (Promega, Madison, USA) was added to the samples (50 µL/well) and incubated under constant

agitation and in the dark during 15 minutes. Luminescence was measured in a luminometer (Sinergy 2, BioTek) and the values were expressed as relative light units (RLU). The percentage of growth inhibition was calculated as:

$$\textbf{\% growth inhibition}=(1-\frac{\text{RLU treated cells}}{\text{RLU untreated cells}}\times 100)$$

The AmB concentration, either free or in PLGA nanoparticles, necessary to decrease parasite viability to 50% (EC_{50}), was determined by linear regression analysis.

3.7. *Ex vivo* and *in vivo* uptake studies

3.7.1. Mice

Six to eight week old male Balb/c mice were obtained from Instituto de Biologia Molecular e Celular (IBMC, Porto, Portugal) animal facilities. The animals were maintained in sterile cabinets and water and food pellets were provided *ad libitum*. Animal care and procedures were in accordance with institutional guidelines. All conducted experiments were done in accordance with the IBMC.INEB Animal Ethics Committee and the Portuguese Veterinary Director General guidelines. Sofia Costa Lima has an accreditation for animal research given from Portuguese Veterinary Direction (Ministerial Directive 1005/92) and conducted the experiments.

3.7.2. *Ex vivo* uptake studies

Splenocytes isolated from the control group (group I), use in the *in vivo* studies, were incubated in 24-well plates at a cell density of $2x10^6$ cells/mL and incubated with FITC-loaded PLGA (0.5 mg/mL in polymer) and M-PLGA nanoparticles (1 mg/mL in polymer) during 24h. After incubation with nanoparticles, the supernatants were recovered, washed by centrifugation (300 *xg*, 10 min at room temperature) with fluorescence activated cell sorting (FACS) buffer (PBS pH 7.4, 2% FBS, 1% P/S and 0.01% sodium azide) and stained, with CD8-PB, CD4-PerCP, CD3-PeCy7, CD19-APC, Ly6C-PerCPCy5.5, Ly6G-PB, CD11b-PeCy7, CD11c-PE and CD206-APC (BioLegend, San Diego, CA), at room temperature, during 30 minutes in the dark. The cells were then washed and suspended in 200µL of FACS buffer. Data were collected by a BD FACS CANTO II flow cytometer and analysed by FlowJo software.

3.7.3. Experimental groups

For the *in vivo* uptake studies animals were divided into 3 groups, each comprised of 2-3 mices, and submitted to different treatments, as follows:

Group I : Control group – mice treated with PBS;

Group II : Intravenously (i.v.) administration of 0.5 mg/mL in polymer of FITC-loaded PLGA nanoparticles;

Group III: Intravenously (i.v.) administration of 1 mg/mL in polymer of FITC-loaded M-PLGA nanoparticles.

3.7.4. *In vivo* uptake studies

Two hours after the administration of the nanoparticle formulations (groups II-III) and PBS (groups I), mice were euthanized and spleens were isolated, washed in PBS and weighted. After that, spleen was homogenized, centrifuged at 300 *xg* during 10 minutes and the final pellet was resuspended in RPMI 1640 medium supplemented with 10% FBS, 2 mM L-glutamine, 20 mM HEPES, 100 U/mL penicillin and 100 µg/mL streptomycin. The number of viable cells was determined by the trypan blue dye exclusion method. Splenocytes were then incubated in 96-well plates at a cell density of 10^6 cells/mL, washed thoroughly with cold FACS buffer and stained with the same antibodies used for *ex vivo* uptake studies, at room temperature, during 30 minutes in the dark. The cells were then washed and suspended in FACS buffer. Data were collected by a BD FACS CANTO II flow cytometer (BD Bioscience, San Jose, California, USA) and analysed by FlowJo software.

3.8. Flow cytometry studies

3.8.1. Mannose Receptor expression in BMMϕ and BMDCs

The expression of MR on different days of cell differentiation was evaluated by flow cytometry. At days 6, 7, 8 and 9, adherent cells, in the case of BMMϕ, and semi-adherent and non-adherent cells, in the case of BMDCs, were recovered and washed by centrifugation (300 *xg*, 10 minutes at room temperature) with cold FACS buffer. Thus, BMMϕ were stained with F4/80-FITC and CD206-APC (BioLegend, San Diego, CA), and BMDCs with CD11c-PE and CD206-APC (BioLegend, San Diego, CA) at room temperature, during 30 minutes in the dark. The cells were then washed and suspended in 200 µL of FACS buffer. Data were collected by a BD FACS Calibur flow cytometer and analysed by FlowJo software.

3.8.2. *In vitro* uptake and activation studies in BMMϕ and BMDCs

3.8.2.1. Uptake studies in BMMϕ

At day 8 of culture, BMMϕ were incubated with uncoated and M-, MN and Ms- coated PLGA nanoparticles (0.5 mg/mL in polymer) at different times (30 min, 2h, 6h, 20h and 24h), in order to study the differential uptake of the nanoparticles. After each time of incubation with the nanoparticles adherent cells were washed thoroughly with cold FACS buffer, to remove non-internalized nanoparticles, recovered, centrifuged at 300 *xg* during 10 minutes and the final pellet was re-suspended in 200µL of FACS buffer. Data were collected by a Becton-Dickinson FACS calibur flow cytometer and analysed by FlowJo software.

3.8.2.2. Cell surface markers

To study the surface co-stimulatory molecules of BMMϕ and BMDCs non-stimulated cells and lipopolysaccharide (LPS) (10 µg/mL) (Sigma Aldrich, Sintra, Portugal) treated cells were used as negative and positive controls, respectively.

At day 8 of culture, BMMϕ were incubated with uncoated and M-, MN- and Ms-coated FITC-loaded PLGA nanoparticles at a concentration of 1mg/mL in polymer, during 20h. After incubation with nanoparticles, cells were washed thoroughly with cold FACS buffer to remove non-internalized nanoparticles and then recovered for surface co-stimulatory markers analysis. Thus, BMMϕ were stained with CD40-PE, CD86-BV, CD80-PerCP/Cy5.5, MHCII-Alexa 647, CD206-APC and CD11b-PeCy7 (BioLegend, San Diego, CA) at room temperature, during 30 minutes in the dark. The cells were then washed and suspended in 200 µL of FACS buffer. Data were collected by a BD FACS CANTO II flow cytometer and analysed by FlowJo software. Dead cells were excluded by staining with 7-AAD and the intensity of the expression of each cell surface marker was reported as mean fluorescence intensity (MFI) of $CD11b^+/7\text{-}AAD^-$ cells.

At day 8 of culture, BMDCs were incubated in a 24-well plate at a cell density of 10^6 cells/mL and left over-night at 37ºC in an atmosphere containing 5% CO_2. At day 9, cells were incubated with uncoated and M-, MN- and Ms-coated FITC-loaded PLGA nanoparticles at a concentration of 1mg/mL in polymer, during 20h. After incubation with nanoparticles, semi-adherent and non-adherent cells were recovered, washed thoroughly by centrifugation (300 *xg*, 10 minutes at room temperature) with cold FACS buffer to remove non-internalized nanoparticles, and then recovered for surface co-stimulatory markers analysis. Thus, BMDCs were stained with CD40-PeCy7, CD86-BV, MHCII-Alexa 647, CD206-APC, CD11c-PE and 7-AAD-PerCPCy5 (BioLegend, San Diego, CA) at room temperature, during 30 minutes in the dark. The cells were then washed and suspended

in 200 µL of FACS buffer. Data were collected by a BD FACS CANTO II flow cytometer and analysed by FlowJo software. Dead cells were excluded by staining with 7-AAD and the intensity of the expression of each cell surface marker was reported as MFI of $CD11c^{+}/7\text{-}AAD^{-}$ cells.

3.8.2.3. Intracellular cytokines

In order to study the production of intracellular cytokines by BMMϕ and BMDCs co-cultured with mannosylated PLGA nanoparticles we perform the procedure described in section 3.8.2.2., being that, in this case, after 20h of co-culture with nanoparticles and the cells were incubated with 50 ng/mL of PMA and 500 ng/mL Ionomycin (Sigma Aldrich, Sintra, Portugal) during 2h at 37ºC, 5% CO_2. The cells were then incubated for more 2h, at 37ºC, 5% CO_2, with 10 µg/mL of brefeldin A. After that, the cells were recovered and in the case of BMMϕ the surface staining was performed during 30 minutes in the dark using the CD11b-PeCy7 antibody. The fixation of the cells were achieved by incubation during 20 minutes at room temperature with paraphormaldehyde 2% (PFA) (Merck , Darmstadt, Germany) and after that time the cells were washed and permeabilized using a permeabilization buffer (10% saponin and FACS buffer). Thus cells were stained with IL-12 - APC, IL-6 - APC, IL-4 - PE and TNFα – PerCPCy5.5 (BioLegend, San Diego, CA) at room temperature, during 30 minutes in the dark. The cells were then washed and suspended in 200µL of FACS buffer. Data were collected by a BD FACS CANTO II flow cytometer and analyzed by FlowJo software.

3.9. Fluorescence microscopy analysis of nanoparticle uptake by BMMϕ

At day 8 of culture, BMMϕ, previously platted in coverslips at a cell density of $4x10^{5}$, were incubated with uncoated and M-, MN- and Ms-coated FITC-loaded PLGA nanoparticles at a concentration of 1mg/mL in polymer, during 20h. After that time cells were washed three times with PBS pH 7.4, to remove extracellular and non-adherent nanoparticles, and fixed for 20 minutes with 2% PFA in PBS. Then the fixed cells were washed and the coverslips were mounted on glass slides using mounting medium with DAPI, VectaShield (Vector Laboratories). Cells were examined in the fluorescence microscope AxioImager Z1 (Carl Zeiss, Germany).

3.10. Statistical Analysis

Statistical analysis was performed by one-way ANOVA followed by Tukey test or Dunnett's multiple comparison test.

IV. RESULTS

4.1. Mannosylated nanoparticles for VL therapy

Since current therapies against VL have several drawbacks it is of great importance to develop alternative treatments, like nanotechnology-based drug delivery systems, that replace or complement the ones that are already available. Thus, one of the aims of this work was to prepare a targeting delivery system to overcome some of the weaknesses and allowing a more efficient delivery of drugs, namely of AmB.

The MR is a member of CLR family, highly expressed on APCs, that was selected to functionalize nanoparticles for targeting and delivery of drugs towards *Leishmania*-infected macrophages. Three different techniques, PA, CR1 and CR2, were conducted to prepare unloaded M-PLGA nanoparticles. After the physicochemical characterization of the produced nanoparticles, AmB was encapsulated on the M-PLGA nanoparticles and their efficiency as drug delivery system evaluated *in vitro* in *Leishmania*-infected macrophages. *Ex vivo* and *in vivo* studies, using splenocytes isolated from Balb/c mice, were also performed, in order to verify if M-PLGA nanoparticles effectively target APCs.

4.1.1. Preparation and characterization of unloaded M-PLGA nanoparticles

Unloaded M-PLGA nanoparticles were prepared by three different techniques, PA, CR1 and CR2, and were evaluated based on the physicochemical characterization of the produced nanoparticles, in order to see which of those techniques is/are more suitable for their preparation.

Physicochemical characterization of the nanoformulations included size, PDI, zeta potential, mannose coating efficiency, morphology, confirmation of the molecular structure of nanoparticles and assessment of mannose surface orientation.

4.1.1.1. Size, PDI, zeta potential and mannose quantification

Table 3 summarizes the physicochemical characteristics of the prepared nanoformulations before and after mannose functionalization.

Table 3 - Physicochemical characteristics of M- PLGA nanoparticles [a]

Nanoparticles	Coating Reaction	Size (nm)	PDI	ζ- Potential (mV)	Mannose (mg/mg polymer)[b]
PLGA	-	205.5 ± 7.3	0.072 ± 0.001	-12.50 ± 0.90	-
M-PLGA	PA	221.9 ± 2.6	0.060 ± 0.002	-16.80 ± 0.01*	1.87 ± 0.01
	CR1	195.0 ± 8.2	0.036 ± 0.001	-27.00 ± 2.50***	1.90 ± 0.01
	CR2	199.8 ± 1.8	0.061 ± 0.011	-22.20 ± 0.07**	1.87 ± 0.01

PA, physical adsorption; CR1, one-step chemical reaction; CR2, two-step chemical reaction

[a] Values are presented as mean ± standard deviation of three independent experiments

[b] Indirect quantification by phenol-sulfuric acid reaction

*P<0.05; **P<0.01; ***P<0.001 compared with ζ-potential of uncoated PLGA nanoparticles

The uncoated PLGA nanoparticles prepared by the nanoprecipitation method [5] presented a mean diameter of 205.5 ± 7.3 nm and a low PDI (<0.1) that suggests an homogeneous distribution of nanoparticle size.

Mannosylated nanoformulations prepared by the three different techniques (PA, CR1 and CR2) exhibited a mean diameter in the range of 195 – 222 nm and a low PDI (<0.1). No statistically significant differences in size were observed between the M-coated and the uncoated nnoparticles.

Uncoated PLGA nanoparticles have an anionic surface charge of -12.5 ± 0.9 mV. The coating of these nanoparticles with mannose leads to a statistically highly significant increase (P<0.001), in absolute value, of zeta potential for values in the -16 to -27 mV range. The M-PLGA nanoparticles produced by PA (-16.80 ± 0.01 mV) has a statistically significant surface charge when compared with uncoated nanoparticles (P<0.05), while the chemical reaction methods (CR1 and CR2) lead to statistically highly significant anionic charges (-27.00 ± 2.50, P<0.001 and -22.20 ± 0.07 mV, P<0.01; respectively) on the M-PLGA nanoparticles surface. Anionic surface charge in M-PLGA nanoparticles followed this trend: CR1 > CR2 > PA.

The effect of the coating method on the incorporation level of mannose was investigated by indirect quantification using phenol-sulfuric acid reaction. The quantity of mannose present in larger particle aggregates and supernatants obtained from the washing steps was very low, leading to a yield around 94% for each of the three techniques.

4.1.1.2. Transmission electron microscopy

The morphology of M-PLGA nanoparticles prepared by the each different technique was observed using TEM. The photographs suggested that M-PLGA nanoparticles prepared by PA and CR1 (Fig.12B-C) exhibit spherical shape, whereas the ones that are prepared by CR2 (Fig.12D) were relatively less spherical and smooth. The nanoparticles prepared

by PA tend to form aggregates, which can be explained by the fact of this nanoparticles have a lower, in absolute value, zeta potential value (-16.80 ± 0.01 mV).

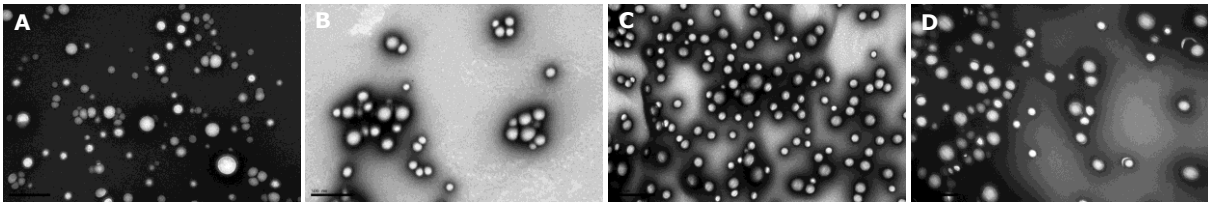

Figure 12 - TEM photomicrographs of uncoated PLGA **(A)** and PLGA coated with mannose by physical adsorption **(B)**, one-step chemical reaction **(C)** and two-step chemical reaction **(D)** at 50,000 magnifications. *Bars* represent 500 nm.

4.1.1.3. Fourier transformed infrared spectroscopy

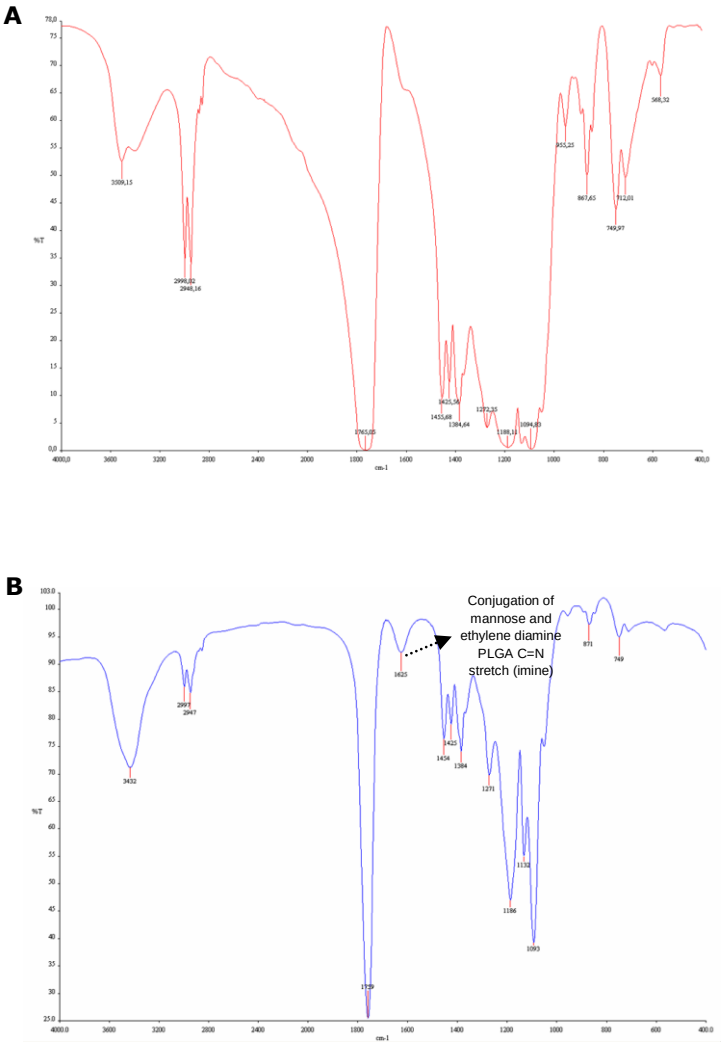

Figure 13 - FTIR spectrum of uncoated **(A)** and mannose-coated by chemical reaction **(B)** PLGA nanoparticles.

FTIR is a technique used for chemical characterization of nanoparticles, being particularly important in cases where there is a surface modification. Through this technique it is possible to detect strong chemical bonds (*e.g.* covalent bond). Thus, in this work a FTIR analysis was performed to confirm the presence of mannose linked to the polymer, by CR1 and CR2, and verify if the covalent binding between this ligand and PLGA occurred.
According to the literature, the peak correspondent to the covalent binding between mannose and PLGA is around 1630 cm^{-1} [29].
The FTIR spectrum obtained for M-PLGA nanoparticles prepared by CR1 and CR2 were similar, and in Fig.13B is possible to see a more prominent peak at 1625 cm^{-1}, representing the covalent binding of mannose and PLGA, that is not observed in the FTIR spectrum of uncoated PLGA nanoparticles Fig. 13A.

4.1.1.4. Lectin binding assay

To assess the surface orientation and the availability of mannose ligand after formation of coated PLGA nanoparticles, an agglutination assay using ConA lectin was conducted.

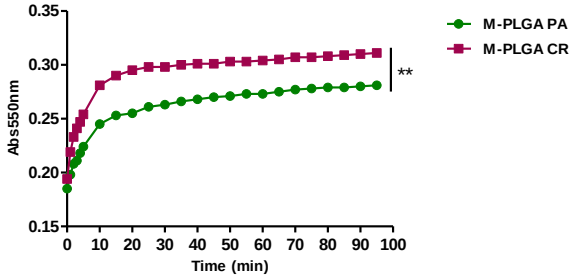

Figure 14 - *In vitro* ligand agglutination of M-PLGA nanoparticles using 25 µg/mL of ConA (PA – physical adsorption; CR – chemical reaction). Values represent mean ± standard deviation of two independent experiments. Comparison of absorbance values, measured at 550 nm, of M-PLGA nanoparticles prepared by PA and CR (** P<0.01).

Following exposure to 25 µg/mL of ConA an increase in the absorbance at 550 nm was observed for M-PLGA nanoparticles prepared by either PA or CR (Fig.14). The extent of agglutination, for nanoformulations prepared by any of the three techniques, rapidly increases up to 10 minutes and from here after remains almost constant, which may be due to saturation of the binding sites.
It is clear by statistically significant higher absorbance (P<0.01) that mannose in nanoparticles prepared by either CR1 or CR2 interact in a greater extent with ConA when compared with mannose in nanoparticles prepared by PA.

4.1.2. *In vitro* evaluation of M- PLGA nanoparticles

4.1.2.1. Toxicity of M- PLGA nanoparticles to macrophages

The toxicity of unloaded M-PLGA nanoparticles, prepared by PA, CR1 and CR2, was evaluated in *Leishmania*-host cells (THP-1 differentiated macrophages), used later in the infection assays, by the MTT assay. As illustrated in Fig.15 the THP-1 cells exhibited more than 80% viability after 3 days in the presence of 0.25 – 2.0 mg/ml of any of the three nanoformulations, which means that these do not exhibit significant toxicity towards mammalian cells.

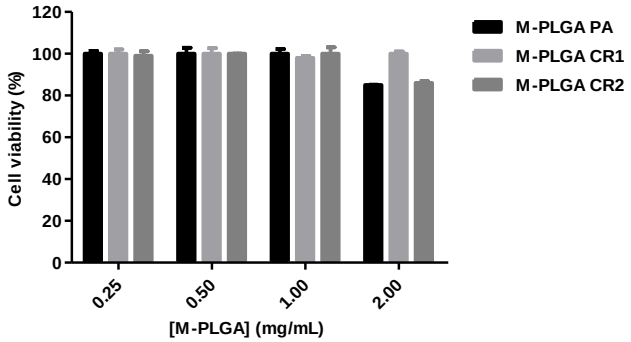

Figure 15 - Viability of human THP-1 differentiated macrophages following treatment with increasing concentrations of unloaded M-PLGA nanoparticles prepared by three different techniques. Values represent mean ± standard deviation of three independent experiments.

4.1.2.2. Antileishmanial activity of M-PLGA nanoparticles against L. infantum intracellular amastigotes

The ability of unloaded M-PLGA nanoparticles, prepared by PA, CR1 and CR2, to inhibit the growth of *L. infantum* intracellular amastigotes was evaluated through the determination of the parasites luciferase activity.

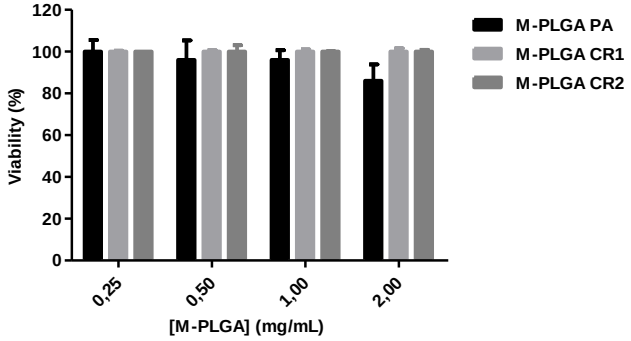

Figure 16 - Biological activity of unloaded M-PLGA nanoparticles prepared by each of the three different techniques against intracellular *L. infantum* amastigotes. Values represent mean ± standard deviation of three independent experiments.

As illustrated in Fig.16 M-PLGA nanoparticles prepared by any of the three techniques are not able, *per se*, to inhibit the growth of *L. infantum* intracellular amastigotes at concentration below 2 mg/ml in polymer within a 72h period of incubation.

4.1.3. Storage stability of unloaded M-PLGA nanoparticles prepared by one-step chemical reaction

CR1 was the reaction chosen to prepare M-PLGA nanoparticles, since the nanoparticles prepared using this reaction, in comparison with the others, exhibit a small mean diameter (195.0 ± 8.2 nm), a low PDI (0.036 ± 0.001), good stability (-27.00 ± 2.50 mV), were spherical in shape and interact in a greater extent with ConA. So, the next step was conducted to evaluate the storage stability of these nanoparticles at different temperature conditions: -20ºC, 4ºC and 37ºC. From the same batch of nanoparticles, aliquots were stored at different temperatures and periodically analyzed for size, PDI and zeta potential by DLS.

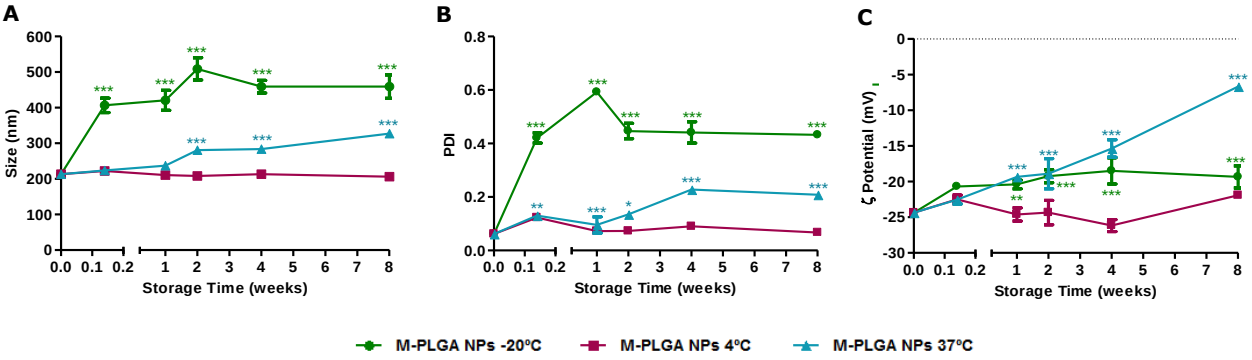

Figure 17 – Storage stability at -20ºC, 4ºC and 37ºC of unloaded M-PLGA nanoparticles prepared by one-step chemical reaction. **(A)** Size; **(B)** PDI; and **(C)** Zeta Potential. Values are presented as mean ± standard deviation of two measurements. **P*<0.05; ***P*<0.01; ****P*<0.001 compared with values at day 0 of each measured parameter.

As illustrated in Fig.17A no significant changes in size, with a mean of 212.4 ± 5.6 nm, was observed when M-PLGA nanoparticles were stored for a period of 8 weeks at 4ºC. However, a statistically highly significant (*P*<0.001) increase on average size was observed for M-PLGA nanoparticles stored at -20ºC, thus verifying that at the end of 1 day of storage, at this temperature, the nanoparticles already present a ≈2-fold increase in their size (406.5 nm compared with the 213.2 nm at day 0). This trend is maintained over the 8 weeks of storage. Although in the case of M-PLGA nanoparticles stored at 37ºC we also see a statistically highly significant (*P*<0.001) increase in size, this only occurs at the end of 2 weeks of storage (280.2 nm compared with the 213.2 nm at day 0).

In what concerns PDI values (Fig. 17B), once again, no significant changes was observed for nanoparticles stored at 4ºC, with the values remaining more a less the same over the 8 weeks of storage (0.062 at day 0 and 0.067 after 8 weeks of storage). On the other hand, a statistically highly significant (P<0.001) increase was observed for M-PLGA nanoparticles stored at -20ºC (PDI > 0.40) and 37ºC (PDI > 0.15), being that increase more prominent in the ones stored at negative temperatures.

Zeta potential of M-PLGA nanoparticles (Fig.17C) stored at 4ºC doesn't significantly change with the time of storage (-24.4 mV at day 0 and -22.0 mV after 8 weeks of storage). At -20ºC and 37ºC the zeta potential becomes less negative with time, being this decrese more prominent for the nanoparticles that are stored at 37ºC (-24.4 mV at day 0 and -6.7 mV after 8 weeks of storage).

4.1.4. Characterization of AmB-loaded M-PLGA nanoparticles

The application of the mannose-coated nanoparticulate system developed previously in section 4.1.1., for efficient delivery of AmB, was evaluated *in vitro* using *Leishmania*-infected macrophages. AmB was successfully incorporated into uncoated PLGA nanoparticles by the nanoprecipitation method [5] and mannose was both physically and chemically conjugated to PLGA nanoparticles.

Physicochemical characterization of the nanoformulations included size, PDI, zeta potential, mannose coating efficiency, E.E., morphology and *in vitro* drug release.

4.1.4.1. Size, PDI, zeta potential, mannose quantification and E.E.

Table 4 summarizes the physicochemical characteristics of the prepared AmB-loaded nanoformulations before and after mannose coating.

Table 4 - Physicochemical characteristics of uncoated and coated PLGA nanoparticles loaded with AmB [a]

Nanoparticles	Coating Reaction	Size (nm)	PDI	ζ- Potential (mV)	Mannose (mg/mg polymer)[b]	E.E. (%)[c]
PLGA AmB	-	208.0 ± 0.3	0.083 ± 0.003	-12.58 ± 0.23	-	20.0 ± 1.1
M-PLGA AmB	PA	200.2 ± 10.7	0.085 ± 0.004	-14.66 ± 0.25**	1.90 ± 0.02	1.8 ± 0.0***
	CR1	190.8 ± 6.4*	0.076 ± 0.002	-16.21 ± 0.90***	1.96 ± 0.02	4.1 ± 0.0***

PA, physical adsorption; CR1, one-step chemical reaction

[a] Values are presented as mean ± standard deviation of three independent experiments

[b] Indirect quantification by phenol-sulfuric acid reaction

[c] Direct quantification by UPLC

*P<0.05, **P<0.01, ***P<0.001 compared with AmB-loaded PLGA nanoparticles

The incorporation of AmB in PLGA nanoparticles leads to a statistically significant increase (P<0.01) in their size (208.0 ± 0.3 nm) (Table 4), when compared to empty PLGA nanoparticles (205.5 ± 7.3 nm) (Table 3). The AmB-loaded PLGA nanoparticles presented a low PDI (<0.1) that suggests a homogeneous distribution of the nanoparticle size. The mannose-coating of this nanoparticles by PA does not lead to a significant change in the mean diameter (200.2 ± 10.7 nm), however when the CR1 is used a statistically significant decrease (P<0.05) (190.8 ± 6.4 nm) was observed. Both mannosylated nanoformulations present a low PDI (<0.1).

AmB-loaded PLGA nanoparticles have an anionic surface charge of -12.6 mV. The coating of these nanoparticles with mannose, either by PA or CR1, leads to a statistically significant increase, in absolute value, of zeta potential for values of -14.7 mV (P<0.01) and -16.2 mV (P<0.001), respectively.

The coating level of mannose was investigated by indirect quantification using phenol-sulfuric acid reaction. The quantity of mannose present in larger particle aggregates and supernatants obtained from the washing steps was very low, leading to a yield around 95% for nanoparticles prepared by PA and around 98% for the ones prepared by CR1.

E.E. of AmB in uncoated and mannose-coated PLGA nanoparticles was determined directly by UPLC, as described in section 3.3.7.1. Uncoated PLGA nanoparticles have an E.E. of 20%, being that the coating of these nanoparticles with mannose, either by PA or CR1, leads to a statistically highly significant decrease (P<0.001) on the E.E., for values of 1.8% and 4.1%, respectively.

4.1.4.2. Transmission electron microscopy

The morphology of AmB-loaded PLGA nanoparticles, either uncoated or mannose-coated by PA and CR1, was observed by TEM (Fig.18).

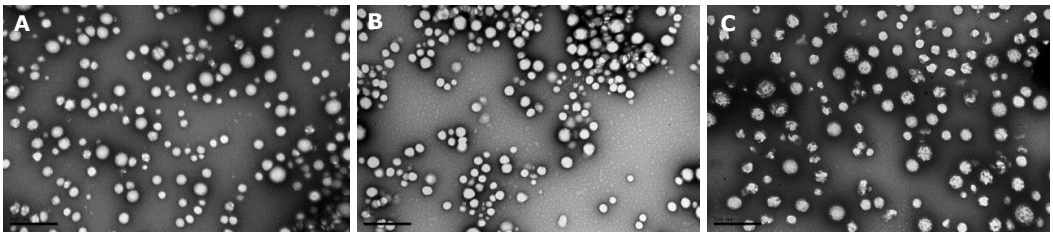

Figure 18 - TEM photomicrographs of AmB-loaded uncoated **(A)** and mannose-coated by PA **(B)** and CR1 **(C)** PLGA nanoparticles at 50,000 magnifications. *Bars* represent 500 nm.

TEM photographs showed that although all nanoformulations were spherical in shape the AmB-loaded M-PLGA nanoparticles prepared by CR1 have a more heterogeneous surface, with some of them presenting a rough surface and others a smooth surface.

4.1.4.3. In vitro release of AmB

Release of AmB from M-PLGA nanoparticles, prepared either by PA or CR1, was determined over time at two pH conditions, 5.5, to simulate the release in the endosomal compartment of macrophages, and 7.4, to simulate the physiological conditions, and using two different buffers PBS and HEPES.

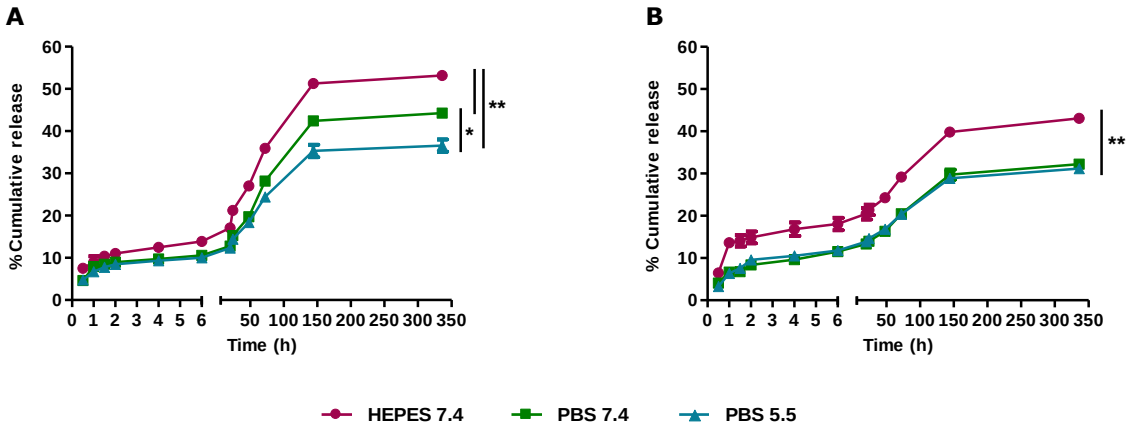

Figure 19 - *In vitro* release profile of AmB from M-PLGA nanoparticles prepared by PA **(A)** and CR1 **(B)** under physiological (HEPES and PBS pH 7.4) and acidic (PBS pH 5.5) conditions. Values are presented as mean ± standard deviation of two measurements. *P<0.05; **P<0.01 comparison of the % cumulative release of AmB from M-PLGA nanoparticles in different incubation conditions.

Table 5 - Comparison of the percentage of cumulative release of AmB from M-PLGA nanoparticles, prepared either by PA or CR1, after 2 weeks, incubated under the same conditions

Nanoformulation	Coating reaction	% Cumulative release		
		HEPES 7.4	PBS 7.4	PBS 5.5
M-PLGA AmB	PA	53.20 ± 0.02	44.25 ± 1.07	36.58 ± 1.45
	CR1	43.07 ± 0.41***	32.21 ± 0.96**	31.19 ± 0.09*

Values are presented as mean ± standard deviation of two measurements. *P<0.05; **P<0.01; ***P<0.001 comparison between % cumulative release of AmB from nanoparticles prepared by PA and CR1.

The AmB-loaded M-PLGA nanoparticles, prepared by PA or CR1, exhibited a triphasic release profile, that include an initial moderate release of 15 to 20% in the first 24 hours, a fast release, of 30 to 40% in the following 6 days, and a last phase in which we observe a sustained release of the drug lasting for 1 week (Fig.19).

The maximum release percentage of AmB in M-PLGA nanoparticles, prepared either by PA or CR1, was observed when these nanoformulations were incubated in HEPES pH 7.4, while significantly lower release was observed when incubated under acidic conditions, PBS pH 5.5 (Fig. 19).

Although the release profile of AmB is similar for M-PLGA nanoparticles prepared by PA and CR1, a slower and more controlled release is observed, for all experimental

conditions, in the ones prepared by CR1 (Fig.19 and Table 5), which is in accordance with the fact of these nanoparticles have a much more stable structure resulting from the covalent bond between mannose and PLGA.

4.1.5. *In vitro* evaluation of AmB-loaded M- PLGA nanoparticles

4.1.5.1. Toxicity of AmB-loaded M- PLGA nanoparticles to macrophages

The toxicity of free AmB, uncoated and mannose-coated AmB-loaded PLGA nanoparticles, was evaluated in human THP-1 differentiated macrophages and murine BMMϕ by the MTT assay (Table 6).

Table 6 - Cytotoxicity of free AmB and nanoformulations to human THP-1 differentiated macrophages and murine BMMϕ

Formulation	Coating reaction	EC_{50} (μM)[a]	
		THP-1	BMMϕ
Free AmB		19.8 ± 3.6	21.8 ± 2.8
PLGA AmB		>100	>100
M-PLGA AmB	**PA**	>50	>50
	CR1	>50	>50

EC_{50} (half maximal effective concentration), concentration of a compound necessary to decreased cell viability to 50% of the untreated control; PA, physical adsorption; CR1, one-step chemical reaction.

[a] Values are presented as mean ± standard deviation of three independent experiments

The incorporation of AmB into uncoated and mannose-coated PLGA nanoparticles decreased by ≈ 5- and 2.5-fold, respectively, its toxicity to human THP-1 differentiated macrophages and BMMϕ, in comparison with free AmB.

4.1.5.2. Growth inhibition of AmB-loaded M-PLGA nanoparticles against Leishmania infantum intracellular amastigotes

The antileishmanial activity of free AmB, uncoated and mannose-coated AmB-loaded PLGA nanoparticles was evaluated on human THP-1 differentiated macrophages and murine BMMϕ infected with *L.infantum* intracellular amastigotes (Table 7).

The incorporation of AmB into uncoated PLGA nanoparticles, leads to an increased statistically highly significant (P<0.001) of the efficacy of the compound in inhibiting intracellular amastigote growth, in comparison to free AmB. On the other hand, the values of EC_{50} obtained for AmB incorporated in mannose-coated PLGA nanoparticles, either by PA or CR1, show a statistically highly significant (P<0.001) improvement, both in THP-1 cells and BMMϕ, of the drug antileishmanial activity in the nanoformulations, perhaps related with a more efficient uptake.

Table 7 - Antileishmanial activity of free AmB and nanoformulations against *Leishmania infantum* intracellular amastigotes in human THP-1 differentiated macrophages and murine BMMϕ

Formulation	Coating reaction	EC_{50} (nM)[a]	
		THP-1	BMMϕ
Free AmB		1320.2 ± 151.5	1134.6 ± 91.0
PLGA AmB		140.8 ± 21.6***	146.1 ± 7.6***
M-PLGA AmB	**PA**	13.0 ± 2.2***	5.2 ±0.6***
	CR1	4.3 ± 0.3***	5.0 ± 0.1***

EC_{50} (half maximal effective concentration), concentration of a compound necessary to decreased intracellular parasite viability to 50% of the untreated control; PA, physical adsorption; CR1, one-step chemical reaction.

[a] Values are presented as mean ± standard deviation of three independent experiments

*** *P<0.001* compared with free AmB

4.1.6. Preparation and characterization of FITC-loaded nanoparticles

FITC-loaded uncoated and M-coated PLGA nanoparticles were prepared for *ex vivo* and *in vivo* studies by the nanoprecipitation method [5]. For the studies described later on section 4.2 (Mannosylated nanoparticles for immunotherapy) two other sugars (MN and Ms) were chemically conjugated to PLGA nanoparticles, using CR1 method, after encapsulation of FITC, being that their description will be included herein.

Physicochemical characterization of the nanoformulations included size, PDI, zeta potential, sugar coating efficiency, E.E. and *in vitro* drug release.

4.1.6.1. Size, polydispersity index, zeta potential, sugar quantification and E.E.

Table 8 summarizes the physicochemical characteristics of the prepared nanoformulations before and after the incorporation of different sugars.

Table 8 - Physicochemical characteristics of uncoated and coated PLGA nanoparticles loaded with FITC[a]

Nanoparticles	Size (nm)	PDI	ζ-Potential (mV)	Sugar (mg/mg polymer)[b]	E.E. (%)[c]
PLGA FITC	201.2 ± 7.5	0.057 ± 0.002	-12.17 ± 0.69	-	56.4 ± 4.1
M-PLGA FITC	188.5 ± 6.7	0.063 ± 0.002	-19.03 ± 1.10***	1.96 ± 0.01	56.1 ± 4.2
MN-PLGA FITC	191.5 ± 7.4	0.066 ± 0.004*	-18.03 ± 1.44***	1.82 ± 0.01	56.0 ± 4.2
Ms-PLGA FITC	184.0 ± 0.9*	0.084 ± 0.004***	-14.55 ± 0.57*	1.99 ± 0.01	56.1 ± 4.1

[a] Values are presented as mean ± standard deviation of three independent experiments.

[b] Indirect quantification by phenol-sulfuric acid reaction.

[c] Indirect quantification by fluorimetry

*P<0.05, ***P<0.001 compared with FITC-loaded PLGA nanoparticles.

FITC-loaded PLGA nanoparticles revealed a mean diameter of 201.2 ± 7.5 nm and a low PDI (<0.1) that suggests a homogeneous distribution of nanoparticle size. No statistically significant differences on the average diameter were observed between the M- and MN-PLGA and uncoated PLGA nanoparticles (Table 8). A statistically significant decrease in the size of Ms-PLGA (184.0 ± 0.9 nm, (P<0.05) when compared with uncoated PLGA nanoparticles was detected. Although mannose coating did not cause a significant change in the PDI (0.063 ± 0.002) of nanoparticles, when compared with uncoated PLGA nanoparticles (0.057 ± 0.002), the incorporation of MN and Ms lead to a statistically significant increase of the PDI values (0.066 ± 0.004 (P<0.05) and 0.084 ± 0.004 (P<0.001)), respectively.

FITC-loaded PLGA nanoparticles have an anionic surface charge of -12.2 ± 0.7 mV. The coating of these nanoparticles with M, MN and Ms leads to a statistically significant increase, in absolute value, of zeta potential for values of -19.0 ± 1.1 (P<0.001), -18.0 ± 1.4 (P<0.001) and -14.6 ± 0.6 mV (P<0.05), respectively.

The incorporation level of the different sugars was investigated by indirect quantification using the phenol-sulfuric acid reaction. The quantity of mannose present in larger particle aggregates and supernatants obtained from the washing steps was very low, leading to a yield around 98% for M-coated, 91% for MN-coated and 99% for Ms-coated PLGA nanoparticles.

E.E. of FITC was determined indirectly by quantification of the non-encapsulated compound as described in section 3.3.7.2.. An E.E. of FITC around 56% were achieved in all prepared nanoformulations, being that no significant differences were observed between uncoated and coated nanoparticles (Table 8).

4.1.6.2. In vitro release of FITC

Release of FITC from uncoated, M-, MN- and Ms-coated PLGA nanoparticles was determined over time at physiological conditions using PBS pH 7.4.

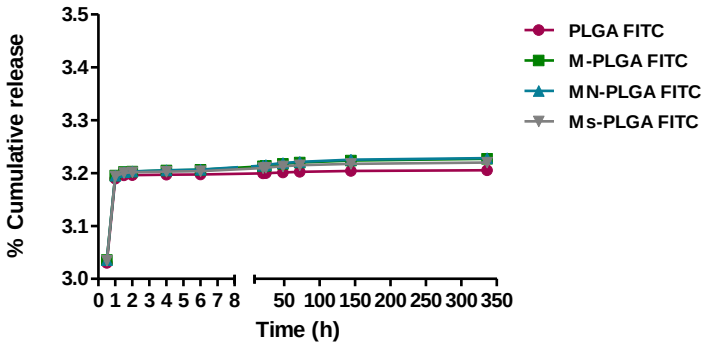

Figure 20 - *In vitro* release profile of FITC from uncoated, M-, MN- and Ms- coated PLGA nanoparticles under physiological conditions (PBS 7.4). Values are presented as mean ± standard deviation of two measurements.

No significant differences were observed in the release profiles of uncoated, M-, MN- and Ms-coated PLGA nanoparticles (Fig.20). The FITC-loaded nanoparticles presented a biphasic pattern of release with an initial burst of release of about 3.2 % in the first two hours that is followed by a constant release of the compound that at the end of the incubation period, 350h, remains ≈3.2%.

4.1.7. *Ex vivo* and *in vivo* uptake studies

To demonstrate that M-PLGA nanoparticles are directed to APCs (macrophages and DCs), *ex vivo* and *in vivo* studies, using splenocytes isolated from Balb/c mice were conducted in order to evaluate their differential uptake by lymphocytes (T cells ($CD4^+$ and $CD8^+$) and B cells), APCs (macrophages and DCs) and neutrophils.

4.1.7.1. Ex vivo uptake studies

Ex vivo uptake studies were performed using the splenocytes isolated from Balb/c mice that received intravenously PBS (control group). Splenocytes were co-cultured for 24h with FITC-loaded uncoated and mannose-coated PLGA nanoparticles. The differential uptake of nanoparticles by T cells, B cells, APCs (macrophages and DCs) and neutrophils was assessed by flow cytometry and the results are expressed in percentage and in total number of cells calculated relative to the total number of spleen cells.

Splenocytes were predominantly composed by lymphocytes, with a significant high number of B cells (35.5% of total cells), comparatively with $CD4^+$T cells (30.6%) and $CD8^+$T cells (10.6%). APCs and neutrophils represent, in turn, a small percentage of total cells in spleen (macrophages – 3.4%; DCs – 0.8% and neutrophils – 1.1%). The percentages values represent the mean of the percentages obtained for two independent experiments performed in duplicate. Fig.21 reveal that in splenocytes co-cultured with uncoated and M-coated PLGA nanoparticles, the uptake occurs preferentially by APCs and neutrophils (Fig.21B-F), with no significant differences in the number of cells containing each type of nanoparticles.

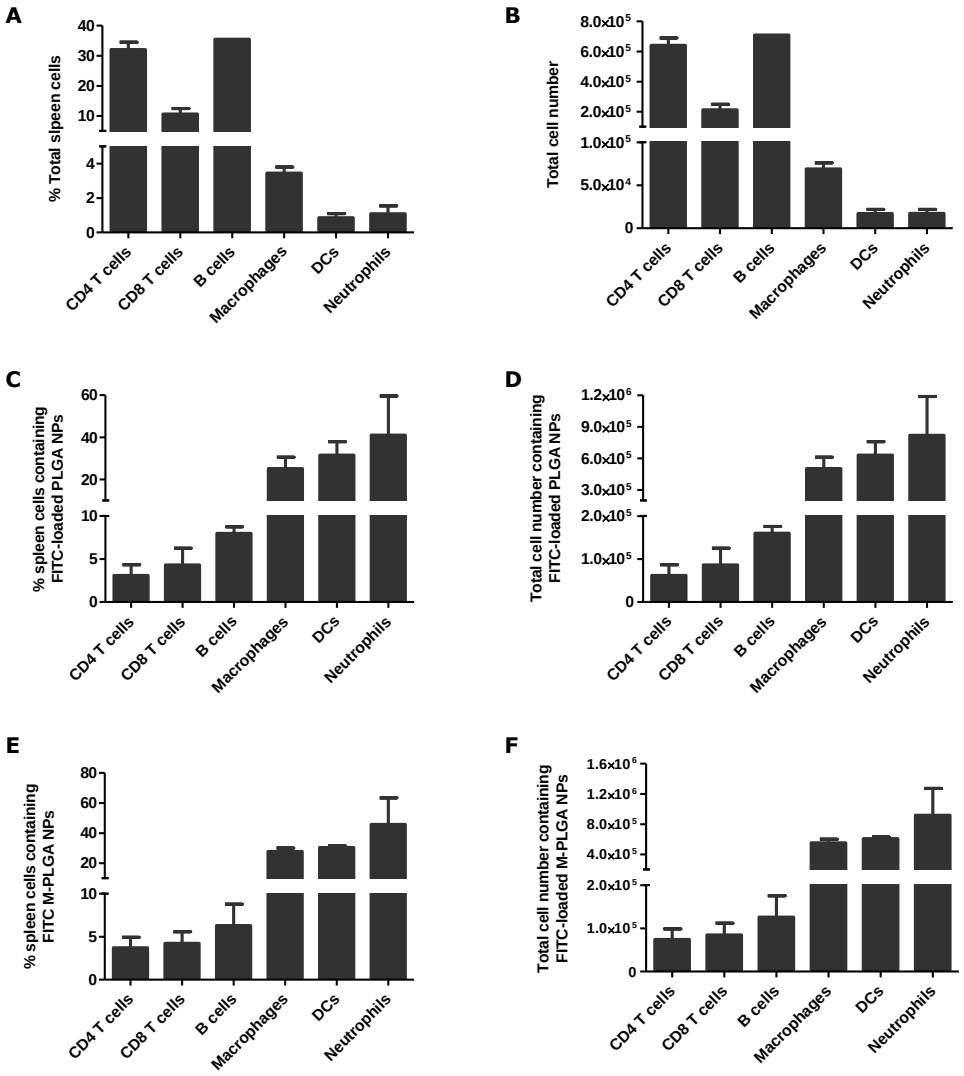

Figure 21 – *Ex vivo* evaluation of the differential uptake of FITC-loaded uncoated and M-coated PLGA nanoparticles by T cells ($CD4^+$ and $CD8^+$), B cells, APCs and neutrophils. **(A)** percentage of total spleen cells; **(B)** total cell number in the spleen; **(C)** percentage of spleen cells containing FITC-loaded PLGA nanoparticles; **(D)** total cell number containing FITC-loaded PLGA nanoparticles; **(E)** percentage of spleen cells containing FITC-loaded M-PLGA nanoparticles; **(F)** total cell number containing FITC-loaded M-PLGA nanoparticles. Results are expressed as the mean ± standard deviation of two independent experiments performed in duplicate.

4.1.7.2. *In vivo* uptake studies

For the *in vivo,* studies Balb/c mice were intravenously administered with PBS (control group) or FITC-loaded uncoated and mannose-coated PLGA nanoparticles. After 2h, the animals were euthanized and the spleen recovered to assess, by flow cytometry, the differential uptake of nanoparticles by T cells, B cells, APCs (macrophages and DCs) and neutrophils. The results are expressed in percentage and in total number of each type of cells calculated relative to total number of spleen cells.

Analysis of the cell composition of splenocytes revealed a predominance of lymphocytes, with a significant high number of B cells (32.1% of total cells), comparatively with $CD4^+$T cells (25.9%) and $CD8^+$T cells (8.7%). APCs and neutrophils represent, in turn, a small percentage of total cells in spleen (macrophages – 2.3%; DCs – 0.7% and neutrophils – 0.5%). The percentages previously shown represent the mean of the percentages obtained for one experiment performed in duplicate.

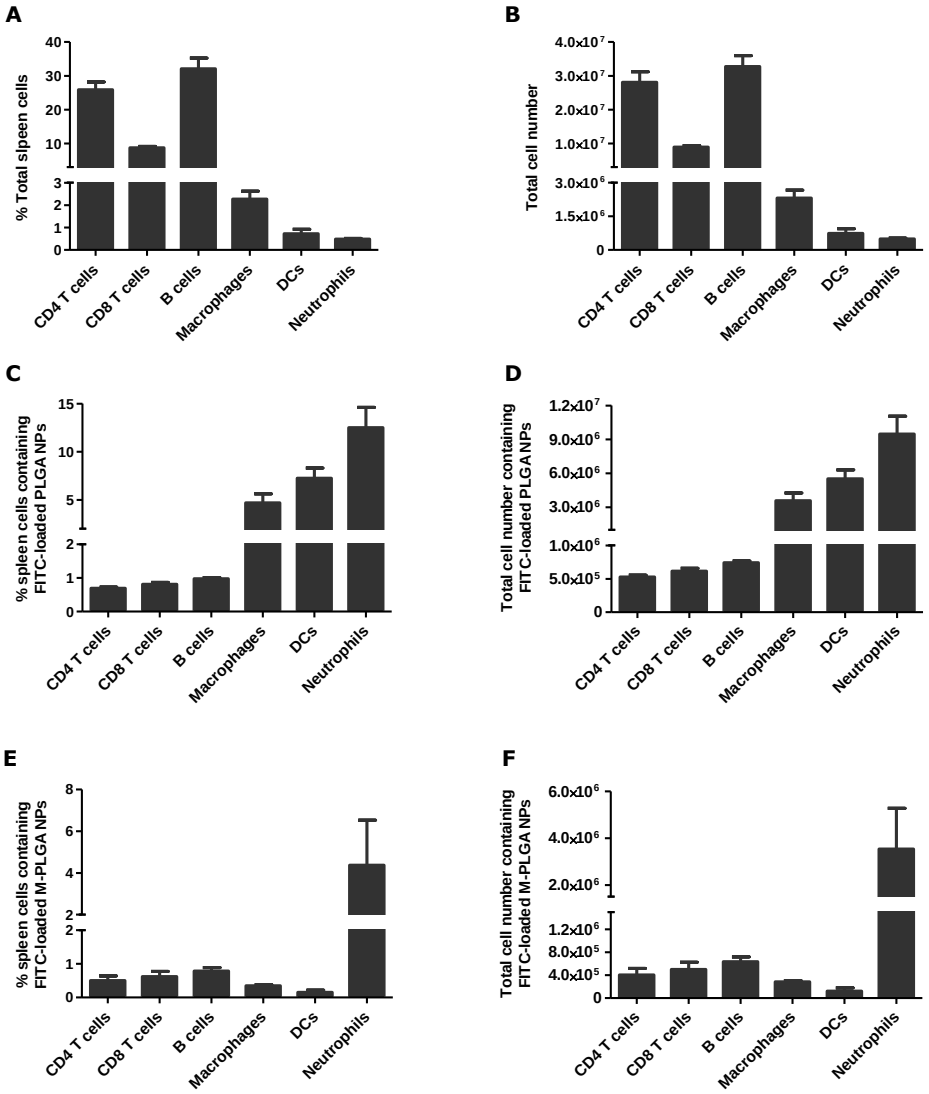

Figure 22 – *In vivo* evaluation of the differential uptake of FITC-loaded uncoated and mannose-coated PLGA nanoparticles by T cells ($CD4^+$ and $CD8^+$), B cells, APCs and neutrophils. **(A)** percentage of total spleen cells; **(B)** total cell number in the spleen; **(C)** percentage of spleen cells containing FITC-loaded PLGA nanoparticles; **(D)** total cell number containing FITC-loaded PLGA nanoparticles; **(E)** percentage of spleen cells containing FITC-loaded M-PLGA nanoparticles; **(F)** total cell number containing FITC-loaded M-PLGA nanoparticles. Results are expressed as the mean ± standard deviation of one experiment performed in duplicate.

In splenocytes isolated from mice treated with FITC-loaded PLGA nanoparticles it is observed that, although lymphocytes constitute the main population of cells in spleen, the uptake occurs preferentially by APCs and neutrophils (Fig.22C-D). In the case of mice treated with FITC-loaded M-PLGA nanoparticles, contrarily to what would be expected, APCs present an uptake similar to what is observed for lymphocytes (Fig.22E-F). On the other hand neutrophils present a higher uptake of nanoparticles comparatively with the other types of cells however it is significantly lower than that of PLGA formulations (Fig.22C-F).

The results of *in vivo* studies follow the same trend of the ones obtained on *ex vivo* studies.

4.2. Mannosylated nanoparticles for immunotherapy

Active targeting of nanoparticles to MR can potentially modulate macrophages and DCs improving their efficacy in the induction of an immune response [6-8].

In order to characterize the modulation of mannosylated nanoparticles on APCs, PLGA nanoparticles were functionalized with three different sugars, M, MN and Ms. Bone marrow derived macrophages and DCs were co-culture with each of these mannosylated nanoparticles and the expression of cell surface markers and intracellular cytokines production evaluated by flow cytometry.

4.2.1. Mannose receptor expression in BMMϕ

The expression of MR on different days of BMMϕ differentiation was evaluated by FACS. F4/80 was used as a macrophage marker in order to determine the percentage of BMMϕ expressing MR. Results in Fig.23A-D, representative of 3 independent experiments, showed that MR expression is time-dependent, being the maximum expression of this receptor observed on day 8 of differentiation (77.9% cells $F4/80^+$ / MR^+). At day 9 is possible to observe a significant reduction in the expression of MR (49.5% cells $F4/80^+/MR^+$).

Taking into consideration the previous results, in the following studies BMMϕ with 8 days of differentiation were used.

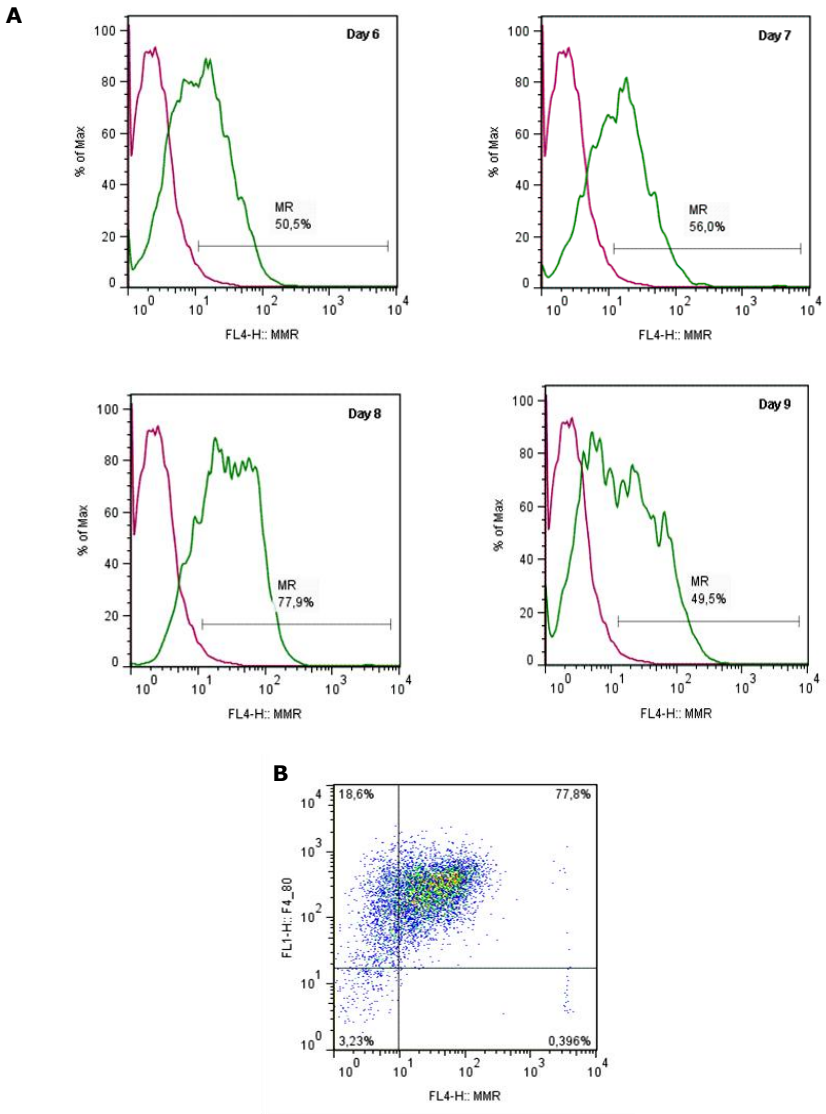

Figure 23 - Mannose receptor expression on different days of murine bone-marrow derived macrophages differentiation. **(A)** Histograms representing the MR expression at days 6, 7, 8 and 9. The pink and green colors represent F4/80^{+} control cells and F4/80^{+}/MR^{+} cells, respectively. **(B)** Dot plot of BMMϕ at day 8 of differentiation showing percentage of cells positive for F4/80 and MR. The results shown are representative of three independent experiments.

4.2.2. *In vitro* BMMϕ uptake studies

4.2.2.1. Uptake studies – Flow cytometry

Uptake studies were performed in BMMϕ with 8 days of differentiation co-cultured with each of the mannosylated nanoparticles (M-PLGA, MN-PLGA and Ms-PLGA).

Results (Fig.24A-D) show that after 30 minutes the non-functionalized and mannosylated nanoparticles had already been taken up by BMMϕ. In the subsequent times a slight shift of the fluorescence peak was observed, suggesting continuous cell uptake of the nanoformulations.

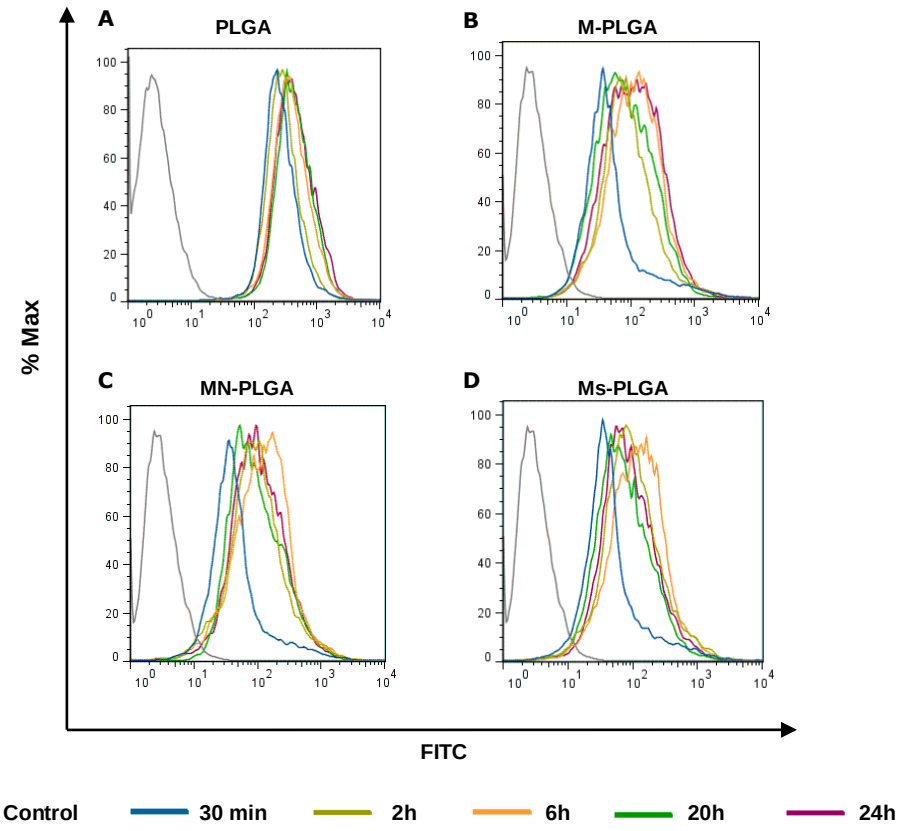

Figure 24 - Uptake of FITC-loaded **(A)** PLGA, **(B)** M-PLGA, **(C)** MN-PLGA and **(D)** Ms-PLGA nanoparticles by BMMϕ at different incubation times (30 min, 2h, 6h, 20h and 24h). The results shown are representative of two independent experiments.

In posterior *in vitro* studies an incubation time of 20h was used to assure that nanoparticles are in contact with cells enough time to modulate cell activation status. The differential uptake of non-functionalized and mannosylated nanoparticles is shown on Fig.25, revealing a significant higher fluorescence intensity for the uncoated nanoparticles (PLGA nanoparticles).

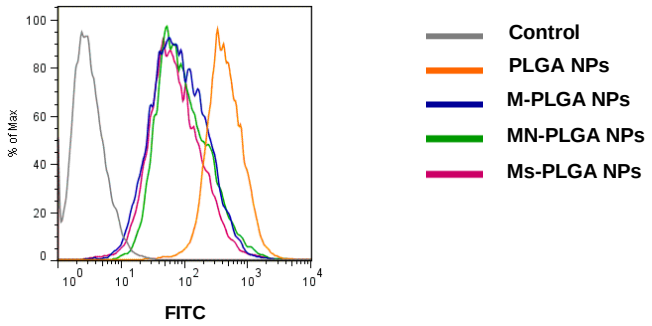

Figure 25 – Uptake of FITC-loaded PLGA and M-, MN- and Ms- PLGA nanoparticles by BMMϕ after 20h of incubation. The results shown are representative of two independent experiments.

4.2.2.2. Uptake studies - fluorescence microscopy

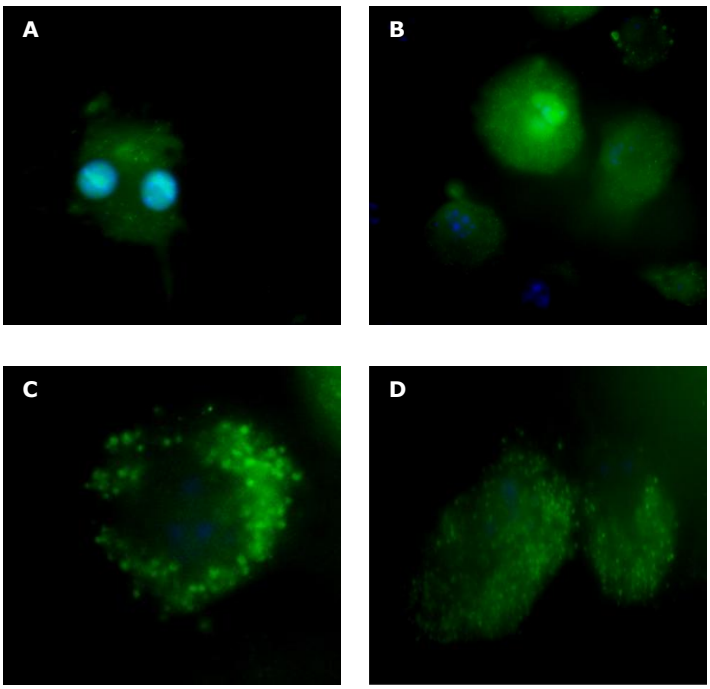

Figure 26– Internalization of uncoated **(A)**, M- **(B)**, MN- **(C)** and Ms- **(D)** coated PLGA nanoparticles, by BMMϕ, after 20h of incubation.

The images obtained by fluorescence microscopy demonstrate that all nanoformulations have an intracellular uptake after 20h incubation, evidenced by the presence of green fluorescence (FITC) within the cytoplasm. From the images it is possible to infer that in the case of uncoated (Fig.26A) and M-coated (Fig.26B) internalized PLGA nanoparticles the distribution pattern in the cytoplasm is more diffuse, whereas in cells that internalize MN- (Fig.26C) and Ms-coated (Fig.26D) PLGA nanoparticles small green dots are present distributed throughout the cytoplasm, which suggests that the uptake of these nanoparticles occurs by an endocytic way.

4.2.3. *In* vitro BMMϕ activation studies

4.2.3.1. Cell surface markers

Flow cytometry studies were performed to study in which way functionalization of PLGA nanoparticles with the different sugars (M, MN and Ms) influence the activation status of macrophages. For that BMMϕ with 8 days of differentiation were used and co-cultured for 20h with non-functionalized and M-, MN- and Ms-functionalized nanoparticles. The percentage of dead cells evaluated by FACS after staining with 7-AAD was 11.5%, being the expression of each cell surface marker reported as MFI of $CD11b^{+}/7\text{-}AAD^{-}$ cells.

In general, the results indicate that functionalization of PLGA nanoparticles with any of the three sugars, significantly enhanced the expression of co-stimulatory molecules

associated with the maturation of BMMϕ: CD40 (Fig.27A, Fig.28), CD86 (Fig.27B, Fig.28) and CD80 (Fig.27C, Fig.28), MHC II (Fig.27D, Fig.28), a molecule involved in antigen presentation, and increase also the surface expression of MR (Fig.27E), the target receptor of this study, as compared to non-functionalized nanoparticles. An interesting result is that MN- and Ms- functionalized nanoparticles induce a statistically highly significant (*P*<0.001) expression of all surface markers, with exception for MHC II, as compared with M-PLGA nanoparticles, which suggest that these two sugars influence more significantly the activation and maturation of BMMϕ.

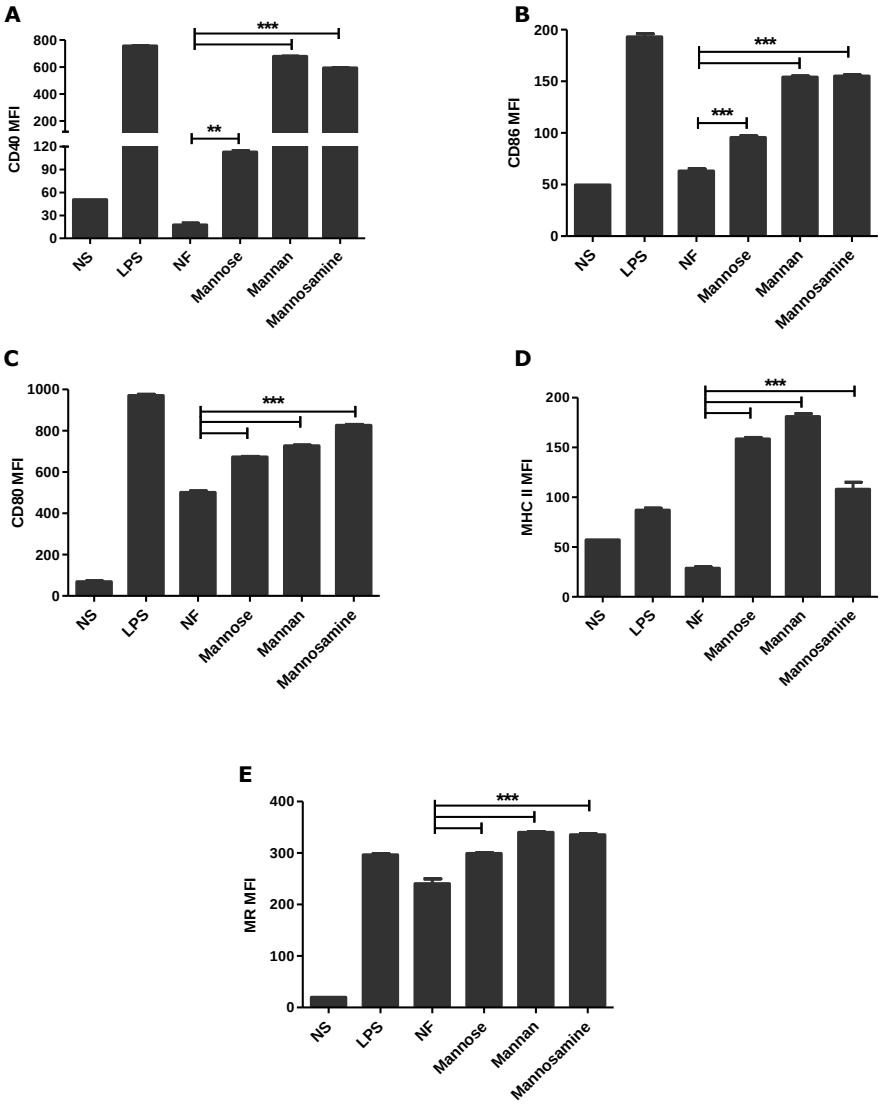

Figure 27 - Analysis of the surface expression of **(A)** CD40, **(B)** CD86, **(C)** CD80, **(D)** MHC II and **(E)** MR in BMMϕ with 8 days of differentiation and isolated from a Balb/c mice. Nonstimulated (NS) and LPS stimulated cells were used as negative and positive control, respectively. BMMϕ were also co-cultured with non-functionalized PLGA nanoparticles (NF) and M-, MN- and Ms-functionalized PLGA nanoparticles. Results are expressed as the mean ± standard deviation of three independent experiments performed in duplicate. ** *P*<0.01 and *** *P*<0.001 compared to NF; MFI – mean fluorescence intensity.

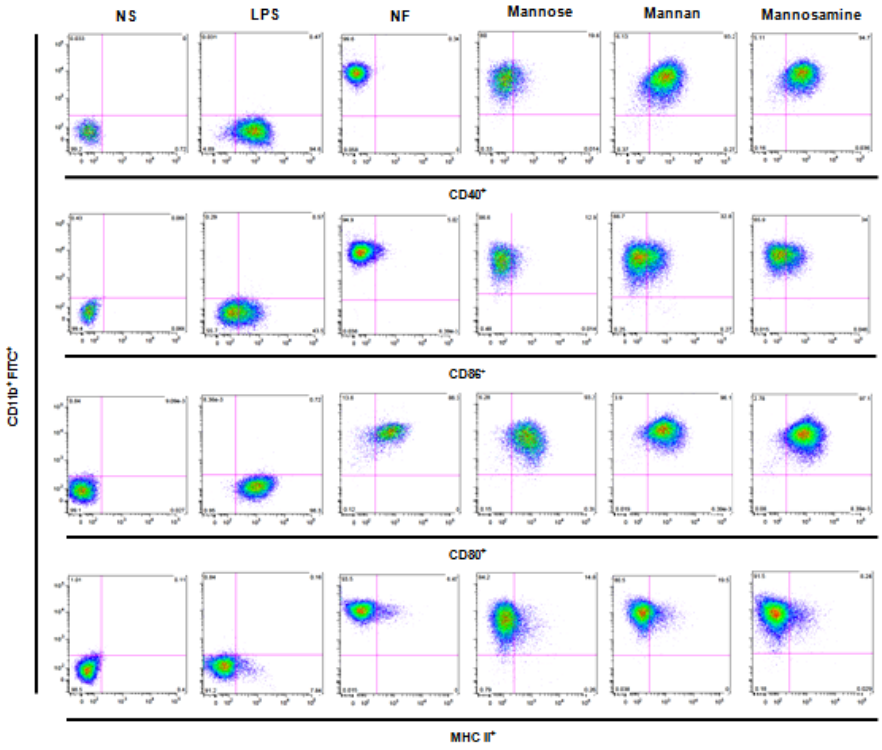

Figure 28 – Dot plots representing the surface expression of co-stimulatory molecules associated with macrophages maturation and antigen presentation, CD40, CD86, CD80 and MHC II, in BMMϕ with 8 days of differentiation and isolated from a Balb/c mice. The results shown are representative of three independent experiments.

4.2.3.2. Intracellular cytokines

The efficiency with which functionalized nanoparticles induces macrophage activation and maturation could be assessed not only by the expression of co-stimulatory molecules but also by cytokines production. The production of cytokines could be evaluated by ELISA using cell-free supernatants, or by the determination of the production of intracellular cytokines.

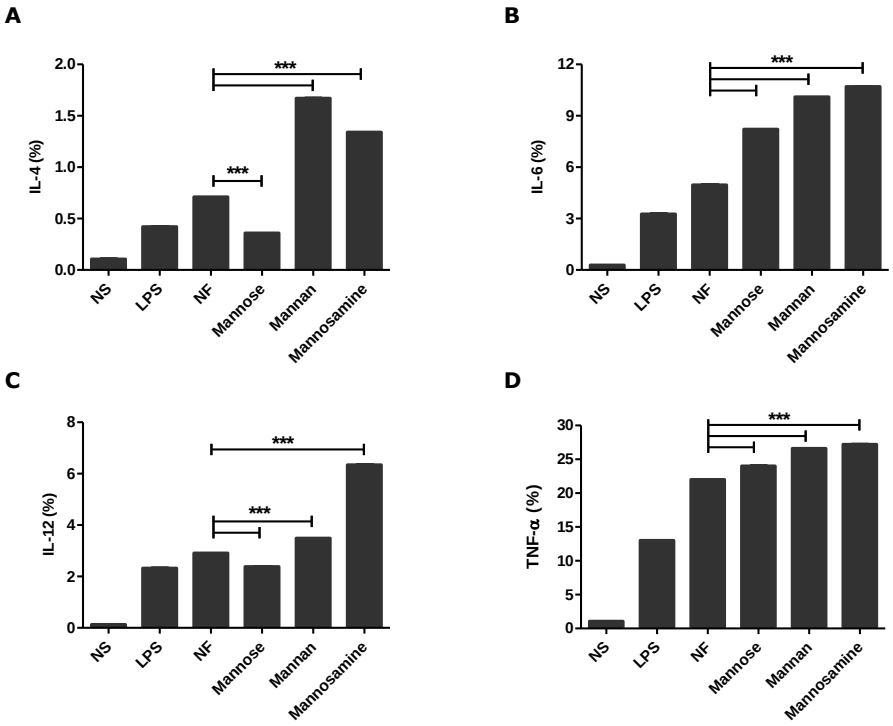

Figure 29 - Analysis of the production of **(A)** IL-4, **(B)** IL-6, **(C)** IL-12 and **(D)** TNF-α in BMMϕ with 8 days of differentiation and isolated from a Balb/c mice. Nonstimulated (NS) and LPS stimulated cells were used as negative and positive control, respectively. BMMϕ were also co-cultured with non-functionalized PLGA nanoparticles (NF) and M-, MN- and Ms-functionalized PLGA nanoparticles. Results are expressed as the mean ± standard deviation of three independent experiments performed in duplicate. ** P<0.01 and *** P<0.001 compared to NF.

BMMϕ production of cytokines IL-4, IL-6, IL-12 and TNF-α were measured in cells untreated and treated with non-functionalized and manosylated PLGA nanoparticles. Results show that co-culture of BMMϕ with PLGA nanoparticles functionalized with any of the three sugars, M, MN and Ms, increases statistically highly significant (P<0.001) the production of IL-6 and TNF-α (Fig.29B and D), in comparison with non-functionalized nanoparticles, being that, the greatest production of both pro-inflammatory cytokines was observed for cells co-cultured with Ms-PLGA nanoparticles. In what concerns the production of IL-4, a cytokine that induces the maturation of näive T cells to Th2 cells, it is possible observe in Fig.29A that BMMϕ, even the ones co-cultured with nanoparticles, produced small percentages of these cytokine (<2%). Despite the fact that production of IL-4 is low, it is possible to observe that cells co-cultured with MN- and Ms-PLGA nanoparticles exhibit a statistically highly significant (P<0.001) production of these cytokine, when compared with non-functionalized nanoparticles and even with M-PLGA nanoparticles, that curiously is the one that less efficiently stimulates the production of IL-4. The production of IL-12 (Fig.29C) is higher, when compared with IL-4 and, it follows the

same trend observed for that cytokine, being that, in this case, the higher production is observed for cells co-cultured with Ms-PLGA nanoparticles. These results suggest that PLGA nanoparticles functionalized with MN and Ms modulates more significantly the activation status of macrophages, with production of IL-6 and TNF-α, which is in accordance with the results presented in section 4.2.3.1..

4.2.4. MR expression in BMDCs

The expression of the MR on different days of BMDCs differentiation was evaluated to determine the most suitable day to perform the following *in vitro* studies. The CD11c was used as a DC marker to quantify the percentage of BMDCs expressing MR between the 7 and 9 day of differentiation. MHC II, a molecule highly expressed in mature DCs, was also assessed to gain additional information on the differentiation state of the cells.

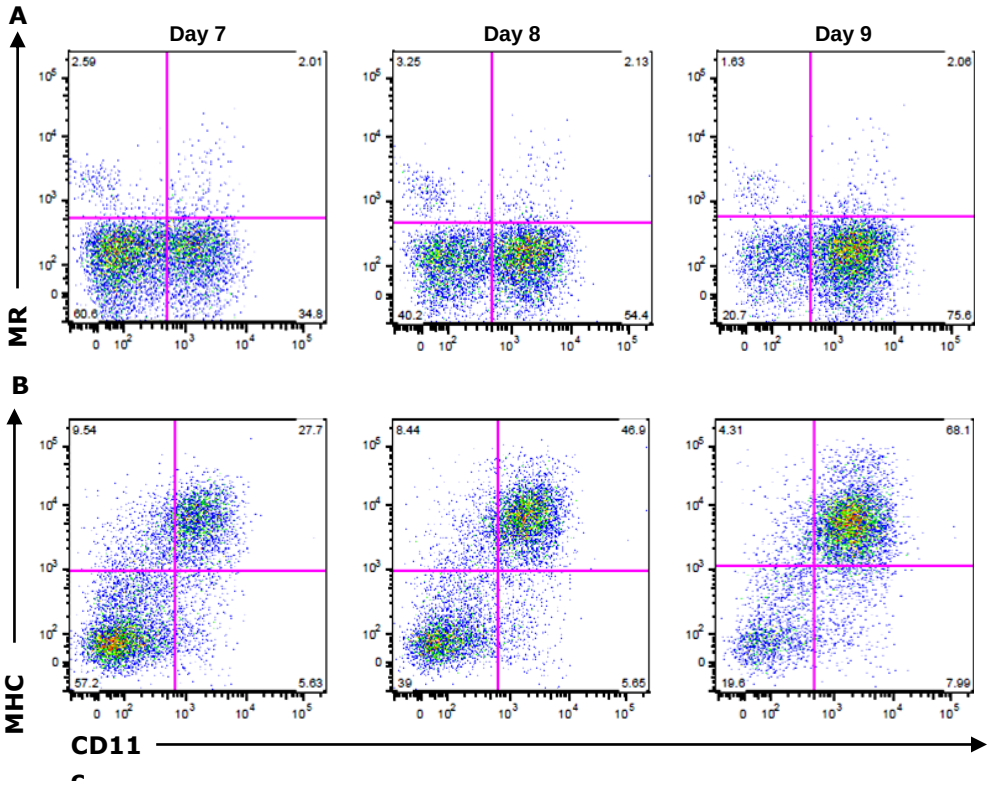

Figure 30 - Dot plots showing **(A)** MR and **(B)** MHC II expression on days 7, 8 and 9 of murine bone-marrow derived DCs differentiation. Numbers in the upper right quadrant represent the percentage of $CD11c^{+}MR^{+}$ or $CD11c^{+}$MHC II^{+}cells. The results shown are representative of one experiment.

No significant differences in MR expression were seen on different days of differentiation (Fig.30), and comparatively with BMMϕ (Fig 23), BMDCs have a significantly lower expression of these receptor. However, in what concerns MHC II expression (Fig.30B and F) we observe that the expression of these molecule is time-dependent, being the maximum expression observed on day 9 of differentiation, with 68.1 % cells $CD11c^{+}$/MHC II^{+}. Thus, taking into consideration these results BMDCs with 9 days of

differentiation were used to conduct *in vitro* activation studies, since, although the expression of MR is almost the same for the three days of differentiation, the percentage of mature DCs is significantly higher.

4.2.5. *In vitro* BMDCs activation studies

4.2.5.1. Cell surface markers

Flow cytometry was used to verify if mannosylated PLGA nanoparticles induce, as described in the literature [6, 140], the DC activation and maturation. For that BMDCs with 9 days of culture were co-cultured during 20h with non-functionalized and M-, MN- and Ms-functionalized nanoparticles. The percentage of dead cells evaluated by FACS after staining with 7-AAD was 9.1%, being the expression of each cell surface marker reported as MFI of $CD11c^{+}/7\text{-}AAD^{-}$ cells.

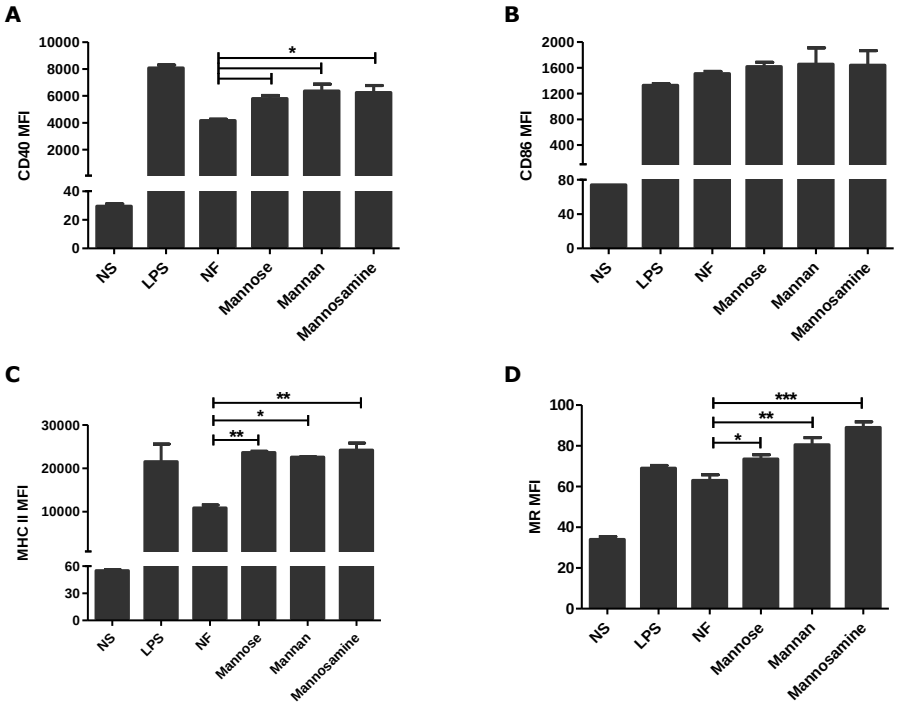

Figure 31 - Analysis of the surface expression of **(A)** CD40, **(B)** CD86, **(C)** MHC II and **(D)** MR in BMDCs with 9 days of differentiation and isolated from a Balb/c mice. Nonstimulated (NS) and LPS stimulated cells were used as negative and positive control, respectively. BMDCs were also co-cultured with non-functionalized PLGA nanoparticles (NF) and M-, MN- and Ms-functionalized PLGA nanoparticles. Results are expressed as the mean ± standard deviation of one experiment performed in duplicate. * P<0.05, ** P<0.01, *** P<0.001 compared to NF; MFI – mean fluorescence intensity.

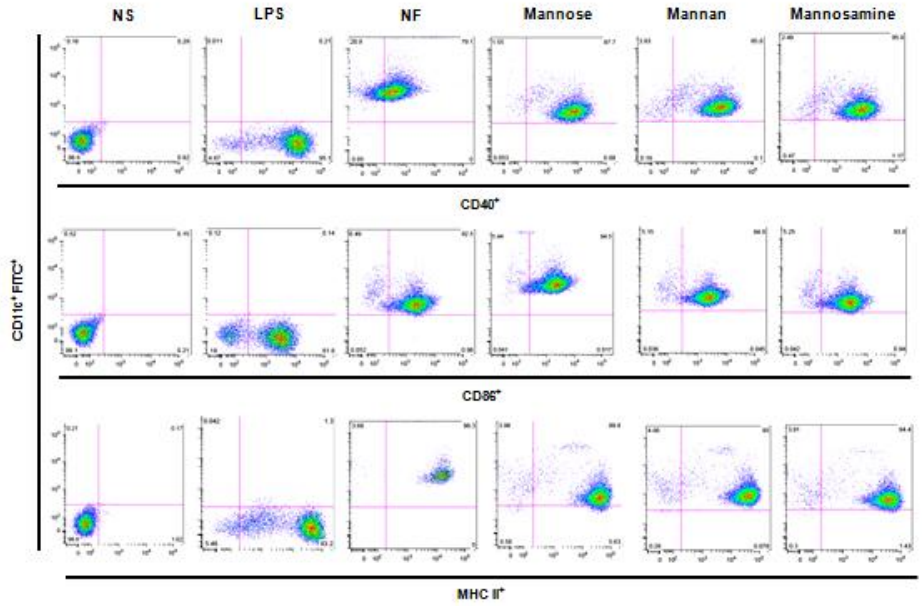

Figure 32 – Dot plots representing the surface expression of co-stimulatory molecules associated with DCs maturation and antigen presentation, CD40, CD86 and MHC II, in BMDCs with 9 days of differentiation and isolated from Balb/c mice. The results shown are representative of one experiment performed in duplicate.

Results show that PLGA nanoparticles functionalized with any of the three sugars significantly enhanced the expression of CD40 (Fig.31A and Fig.32) but not of CD86 (Fig.31B and Fig.32), both co-stimulatory molecules associated with the maturation of DCs. Moreover the mannosylation led to a significant increase in the expression of MHC II (Fig.31C and Fig. 32), a molecule involved in antigen presentation, and MR (Fig.31D), when compared to non-functionalized nanoparticles. The high MFI values obtained for MHC II molecule (Fig.31C), in comparison with the values obtained for the co-stimulatory molecules and even for MR is consistent with the fact that this molecule has a large expression in BMDCs. Contrary to what happen with BMMϕ, in this case the three sugars seem to stimulate equally the BMDCs activation and maturation.

4.2.5.2. Intracellular cytokines

As already mentioned for BMMϕ, the efficiency with which functionalized nanoparticles induce DC maturation could be assessed not only by the expression of co-stimulatory molecules but also by cytokines production.

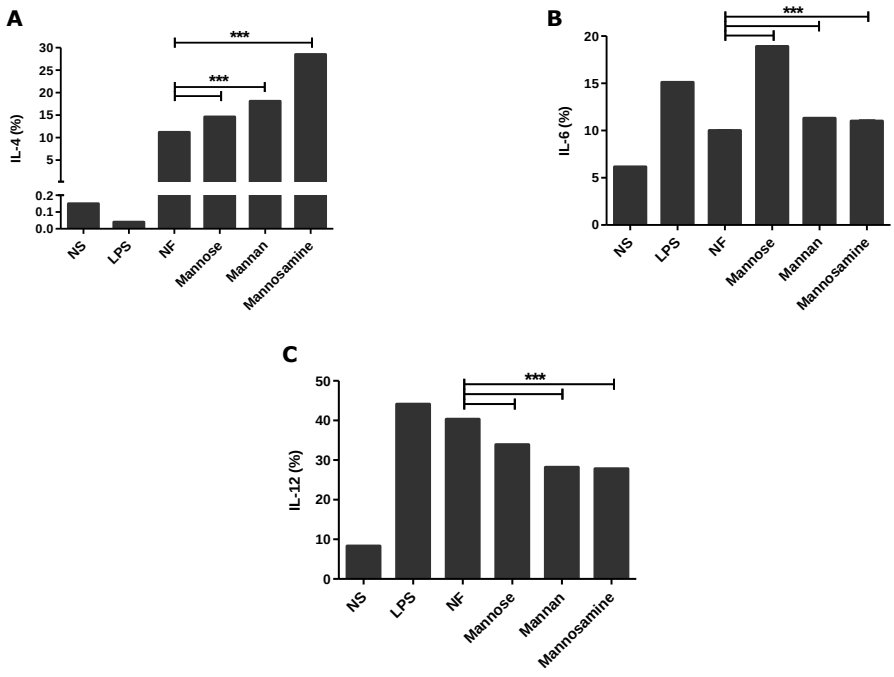

Figure 33- Analysis of the production of **(A)** IL-4, **(B)** IL-6 and **(C)** IL-12 in BMDCs with 9 days of differentiation and isolated from a Balb/c mice. Nonstimulated (NS) and LPS stimulated cells were used as negative and positive control, respectively. BMDCs were also co-cultured with non-functionalized PLGA nanoparticles (NF) and M-, MN- and Ms-functionalized PLGA nanoparticles. Results are expressed as the mean ± standard deviation of one experiment performed in duplicate. *** P<0.001 compared to NF.

BMDCs production of cytokines IL-4, IL-6 and IL-12 were measured in cells untreated and treated with non functionalized and sugar-functionalized PLGA nanoparticles by flow cytometry. Results show that stimulation of BMDCs with PLGA nanoparticles functionalized with any of the three sugars increases statistically highly significant (P<0.001) the production of IL-4 (Fig.33A), in comparison to non-functionalized nanoparticles, being that the greatest production of this cytokine is observed for cells stimulated with Ms-functionalized nanoparticles. Results also suggest that LPS is not capable of stimulating the production of IL-4, since the percentage of cytokine produced is almost zero. Fig.33B shows that functionalized nanoparticles increased significantly the IL-6 production being that, in this case, the greatest production of this cytokine is observed for cells stimulated with M-functionalized nanoparticles. Contrary to the trend observed so far, in the case of IL-12 production (Fig.33C), the higher levels were observed when BMDCs are stimulated with non-functionalized PLGA nanoparticles, with values almost identical to those observed for positive control (LPS). Among cells stimulated with functionalized nanoparticles, the ones that stimulate more efficiently the production of IL-12 are those with mannose.

V. DISCUSSION

5.1. Mannosylated nanoparticles for VL therapy

AmB, an amphiphilic polyene antibiotic, constitutes a second line of treatment against VL with a high cure rate [141]. However, the use of this compound have some drawbacks, including the high toxicity, the high costs associated with its use, the limited availability in some areas, difficulties associated with the administration, prolonged duration of therapy and the severe side effects [1, 4]. Thus in order to improve AmB efficacy as an antileishmanial drug and reduce its toxicity a nanoparticulate system targeting MR in APCs (macrophages and DCs), the target cells in VL, was developed and characterized.

5.1.1. Preparation and characterization of unloaded M-PLGA nanoparticles

In order to functionalize PLGA nanoparticles with mannose different approaches can be conducted. Initially three different techniques, PA, CR1 and CR2 were evaluated through their physicochemical characterization and *in vitro* studies to define the most suitable technique for the preparation of M-PLGA nanoparticles.

The use of nanoparticles as drug delivery systems implies that a systematic characterization is made, to verify if their properties are the most appropriate for the intended application. Size is the most important parameter in the characterization of a nanoparticulate system, since it will influence their release profile and degradation rate and also because, it is a major determinant of the uptake and biodistribution of nanoparticles [30]. Uncoated PLGA nanoparticles exhibited a mean diameter of 205.5 ± 7.3 nm, being that the incorporation of mannose does not lead to a statistically significant alteration in size, with M-PLGA nanoparticles presenting a mean diameter in the range of 195.0 ± 8.2 – 221.9 ± 2.6 nm (Table 3). All nanoformulations have low PDI values (<0.1) (Table 3) which suggest that homogenous populations with a narrow size distribution were produced.

Zeta potential is also an important parameter in the characterization of nanoparticles since it measures the surface charge of nanoparticles and gives information about their stability in a suspension, under defined conditions. In general, nanoparticles with high negative or positive values (≥ ± 30 mV) of zeta potential have a lower tendency to aggregate, due to electrical repulsion [16]. The negative surface charge of PLGA nanoparticles (-12.5 ± 0.90 mV) increased significantly, in absolute value, after mannose incorporation by PA (-16.8 ± 0.01 mV) (P<0.05), CR1 (-27.0 ± 2.50 mV) (P<0.001) and CR2 (-22.2 ± 0.07 mV) (P<0.01) (Table 3), which is not in accordance with previous findings, in which a reduction in zeta potential, in absolute value, was observed after coating with the same ligand [29]. It is known that, negative zeta potential of PLGA nanoparticles is due to

the presence of terminal carboxylic groups (COOH). According to the literature [29], it was expected that conjugation of the COOH- groups with mannose induced a decrease in zeta potential, however in our case that was not verified. M-PLGA nanoparticles prepared by CR1 are those with a more negative zeta potential, which indicates that these nanoparticles have a higher electrical charge in their surface that leads to a strong repulsion between the particles and a lower tendency to form aggregates (low PDI value (0.036 ± 0.001)). Based on that and in the obtained results, M-PLGA nanoparticles prepared by CR1 seems to be the more stable suspension.

The coating level of mannose was determined by indirect quantification of the ligand that was not adsorbed or chemically bound to PLGA, using the phenol-sulfuric acid reaction. Results demonstrate that an efficient coating of PLGA nanoparticles occur by any of the three techniques, being that the yields associated are around 94% (Table 3), which is not in accordance with data from literature [29]. Generally, the yields associated with mannose coating are much lower than the ones obtained in this work. This could be explained by the fact that in most articles, although the quantification method is the same, a direct measurement of mannose is made, which implies that mannose, physically or chemically incorporated, be effectively extracted through the use of techniques that requires the exposure of nanoparticles to harsh conditions, including high temperatures and organic solvents, leading to a great loss of the ligand, as a result of its destruction, and consequently the yields obtained will be lower. Thus the ideal would be to implement an alternative technique for quantification of mannose, like resorcinol sulfuric acid method [142], used as a complementary technique, to ensure that the yields obtained correspond to the real quantity of mannose that is present in the surface of nanoparticles.

FTIR was used to confirm the conjugation of mannose to the PLGA nanoparticles, through the occurrence of a carbodiimide reaction that will favor the formation of a covalent binding between the polymer and the ligand. In the FTIR spectrum obtained for M-PLGA nanoparticles, prepared by CR1 and CR2 (Fig.13B) is observed a more prominent peak at 1625 cm^{-1}, not observed in the FTIR spectrum of uncoated PLGA nanoparticles (Fig.13A), that confirms the occurrence of a covalent bound between PLGA and mannose, being that these results are in agreement with the literature [29].

To study the presence and orientation of mannose in the surface of PLGA nanoparticles, an agglutination assay using ConA lectin was conducted (Fig.14). Although the levels of mannose present are similar for nanoparticles prepared by PA, CR1 and CR2, the results clearly demonstrate that ConA interact in a greater extent with mannose present in the ones prepared by CR. This different agglutination behavior suggests that, probably, as a result of the weak interaction, mannose, in nanoparticles prepared by PA, will be oriented to the core of the nanoparticles and less accessible in the surface to interact with ConA.

The *in vitro* evaluation of empty M-PLGA nanoparticles, prepared by PA, CR1 and CR2, revealed that the three nanoformulations do not exert cytotoxicity on human THP-1 differentiated macrophages for concentrations up to 2 mg/ml (Fig.15). These results were expected since PLGA is a biodegradable, biocompatible and non-toxic polymer [12, 21].

Polymeric nanoparticles can be very useful in the treatment of leishmaniasis, due to its hydrophobic nature that allows their rapid uptake by macrophages, which are the main targets of *Leishmania* parasite, however they shouldn't have immunogenic properties, in order to avoid the non-specific activation of macrophages. Previous studies demonstrate that empty polymeric nanoparticles may have antileishmanial activity as a result of their uptake by macrophages and consequent activation of effector mechanisms. Venier-Julienne *et al* [143] have demonstrated, using an *in vitro* model of *L.infantum* infection, that empty PLGA nanoparticles are able, *per se*, to inhibit the growth of the parasite with the consequent release of hydrogen peroxide following the activation of macrophages. Another study report the same activity but for empty PACA nanoparticles [129]. Based on these facts it was important to verify if M-PLGA nanoparticles prepared by PA, CR1 and CR2 have immunogenic properties and are able, *per se*, to inhibit the growth of *L.infantum* intracellular amastigotes. The results obtained (Fig.16) indicate that nanoformulations do not have an inhibitory activity on parasite up to 2 mg/mL. Thus, it can be ensure that the antileishmanial activity observed when these nanoformulations are used as drug delivery systems is only due to the action of the drug.

Physicochemical characterization and *in vitro* evaluation of M-PLGA nanoparticles have demonstrated that CR1 is the most suitable reaction for the preparation of mannosylated nanoparticles, since the nanoparticles obtained by this reaction present a size (195.0 ± 8.2nm) adequate for animal administration, a low PDI (<0.1), good stability, were spherical in shape (Fig.12C), present more mannose groups oriented to the outer of the nanoparticle (Fig.14), and do not present toxicity against human THP-1 differentiated macrophages (Fig.15) or intracellular *L.infantum* amastigotes (Fig.16). The storage stability of chosen nanoparticles was then evaluated at different temperature conditions.

5.1.2. Storage stability of unloaded M-PLGA nanoparticles prepared by CR1

The storage of nanoparticles for long periods of time implies that the factors that could influence their stability should be controlled, including polymer properties (*e.g.* copolymer composition) and physicochemical properties (*e.g.* temperature, pH and ionic strength). It is described in the literature [144] that, more hydrophobic and crystalline polymers have slow degradation rates and consequently are more stable. Moreover, the stability of PLGA nanoparticles is influenced by the pH of the storage medium, since hydrolysis of ester groups is favored in acidic and basic media, as an example, the storage in a buffer with

pH 7.4 can slow their degradation and enhance their stability [144]. In this work a PLGA (70:30) polymer highly hydrophobic, as a result of the high percentage of lactic acid, is used and the nanoparticles are stored in PBS pH7.4. Another factor that influences significantly the storage stability of nanoparticles is temperature. Thus, the influence of different temperature conditions, -20ºC, 4ºC and 37ºC, in the storage stability of M-PLGA nanoparticles was evaluated, in order to determine the most suitable conditions for storage of these nanoformulations.

M-PLGA nanoparticles stored at 4ºC don't present significant changes in their size (Fig.17A), PDI (Fig.17B) and zeta potential (Fig.17C) over the 8 weeks of storage. On the other hand when storage assays are conducted at -20ºC at the end of only 1 day a highly significant increase in size (Fig.17A) was observed, possibly due to particle aggregation, being that high PDI values (Fig.17B) reinforce this idea. In storage assays performed at 37ºC a significant increase in size and PDI (Fig.17A-B) is also observed, however is not as prominent as observed at -20ºC. The zeta potential (Fig.17C) of nanoparticles stored at -20ºC and 37ºC becomes less negative with time, being that decreased more prominent for nanoparticles stored at 37ºC. Thus, nanoparticles stored at these temperatures will have a greater tendency to aggregate, being the suspension less stable.

The results from storage stability studies clearly demonstrate that the best storage temperature condition to maintain M-PLGA nanoparticles, prepared by CR1, for long periods of time is at 4ºC.

5.1.3. Preparation and characterization of AmB-loaded M-PLGA nanoparticles

The previous developed mannosylated nanoparticles were used to encapsulate AmB and their efficiency as drug delivery system, in the treatment of VL, was evaluated *in vitro* in *Leishmania*-infected macrophages.

AmB was successfully incorporated into uncoated PLGA nanoparticles by nanoprecipitation, a simple method usually employed to incorporate hydrophobic compounds into nanoparticles. Although we define CR1 as the most suitable reaction for the conjugation of mannose with PLGA nanoparticles, in this case, and in order to make a comparison in terms of physicochemical properties, mannose was both physically and chemically conjugated with nanoparticles.

The incorporation of AmB in PLGA nanoparticles leads to a statistically significant increase in size, possibly due to an expansion of their matrix following encapsulation of the compound, which is in accordance with data from literature [29]. AmB-loaded PLGA nanoparticles exhibited a mean diameter of 208.0 ± 0.3 nm (Table 4), being that the mannose-coating of these nanoparticles by PA does not lead to a significant alteration in

size (200.2 ± 10.7 nm), however when CR1 is used a statistically significant decrease (190.8 ± 6.4 nm) (Table 4), which is not in accordance with what is described in the literature [29]. All nanoformulations have lower PDI values (<0.1) (Table 4), which suggest that different populations have a narrow size distribution.

Zeta potential of PLGA nanoparticles is not significantly affected by the incorporation of AmB, which means that the compound has not influence in the surface charge of nanoparticles. On the other hand, the negatively surface charge of loaded nanoparticles (-12.6 ± 0.2 mV) increased significantly, in absolute value, after mannose incorporation by PA (-14.7 ± 0.2 mV) and CR1 (-16.2 ± 0.9mV) (Table 4), which is not, once again, in accordance with previous findings, in which a reduction in zeta potential, in absolute value, is observed after coating with the same ligand [29].

Similarly to what is observed previously for unloaded M-PLGA nanoparticles, also in AmB-loaded nanoparticles an efficient coating with mannose occur by PA and CR1, being that the yields associated are around 95% and 98%, respectively (Table 4).

AmB encapsulation in uncoated and M-coated PLGA nanoparticles was determined directly by UPLC. An E.E. of 20% was achieved for uncoated PLGA nanoparticles, being that the coating of these nanoparticles with mannose, either by PA or CR1, lead to a significant decrease on the E.E., for values of 1.8% and 4.1%, respectively. The observed decreased in the E.E. could be explained by a saturation of the polymeric matrix as a result of the high drug loading (20%) used. Besides that, it is demonstrated that different physicochemical properties of AmB, including limited solubility in water and in most organic solvents, with the need to use DMSO as co-solvent, as well as its aggregatory nature, could contribute for its low encapsulation in polymeric nanoparticles [145]. So, in further studies, to try to increase the E.E. of AmB it would be interesting decrease significantly the drug loading, *e.g*. 1% and employ the principle of co-solvency [4, 145].

Study of the mechanisms and physicochemical processes involved in drug release is important when we use polymeric nanoparticles, because of their application in sustained drug delivery. Release of AmB from M-PLGA nanoparticles, prepared either by PA or CR1, was determined over time at two pH conditions, 5.5, to simulate the release in the endosomal compartment of macrophages, and 7.4, to simulate the physiological conditions, and using two different buffers PBS and HEPES. Previous studies have demonstrated that in PLGA-based drug delivery systems, namely in the ones used for delivery of AmB, the drug release follows a biphasic pattern with an initial burst of release that are mainly controlled by mechanisms of diffusion, followed by a more slow and controlled liberation that occurs as a result of the polymer degradation [42, 146] (Lima, unpublished work). Despite the biphasic pattern is most common, some authors have already demonstrated that some drug delivery systems exhibited a triphasic release

profile [43-45, 147]. Although it has been demonstrated that AmB-loaded PLGA nanoparticles have a biphasic pattern (Lima, unpublished work), the coating of these nanoparticles with mannose, either by PA or CR1, leads to the exhibition of a triphasic release profile in all tested conditions (Fig. 19A-B), that include an initial moderate and continuous release of 15 to 20% of AmB, in the first 24 hours, caused by the controlled release of non-encapsulated drug molecules on the surface of nanoparticles; a second phase in which a fast release of about 30-40% occurs, in the following 6 days, that is more prominent in M-PLGA nanoparticles prepared by PA and which results from a swelling of PLGA by inward diffusion of water that will consequently favor the solubilization and rapid diffusion of AmB, either through the polymer or through the formed pores; and a last phase in which a sustained release of AmB was observed as a result of the slow polymer degradation, which means that the dissolution rate of the products formed as a result of the random scission of PLGA ester bonds and, the consequent creation of pores, through which AmB will diffuse, is very slow, as described on Fig 3. M-PLGA nanoparticles prepared by PA and CR1 have the same release profile (Fig.19A-B), however, for all experimental conditions, it is observed that nanoparticles prepared by CR1 have a slow and more controlled release of AmB (Table 5), which is in accordance with the fact of these nanoparticles have a much more stable structure resulting from the covalent bond between mannose and PLGA. Effectively, the less stable structure of nanoparticles prepared by PA, could explain the faster and significant release of AmB in the second phase of the release profile. Another interesting aspect is that M-PLGA nanoparticles prepared by both techniques present a significantly lower release of the compound when incubated in conditions that mimics the phagolysossomal compartment in macrophages (PBS pH5.0) (Table 5).

Thus, these results suggest that the use of M-PLGA nanoparticles prepared by CR1, as drug delivery system, is more advantageous, when compared to the ones prepared by PA, since besides having a higher encapsulation efficiency, they also favor a slow and controlled release of AmB, especially in acidic conditions, as a result of their stable structure.

The *in vitro* toxicity and efficacy of AmB and their nanoformulations were evaluated towards uninfected and *L. infantum*-infected macrophages (human THP-1 differentiated macrophages and BMMϕ). Results show that free AmB exhibited toxicities to human THP-1 differentiated macrophages and BMMϕ of 19.8 ± 3.6 μM and 21.8 ± 2.8 μM, respectively (Table 6). These elevated toxicities could be explained by the fact that even tough in a lesser extent, AmB interacts with cholesterol of host macrophages and can induce formation of pores leading to death of the cells, being these one of the possible mechanisms by which this compound cause cellular toxicity [1, 111, 148]. Encapsulation

of AmB on uncoated and M-coated PLGA nanoparticles significantly reduces its toxicity towards human THP-1 differentiated macrophages and BMMϕ (Table 6). These results are in accordance with *in vitro* and *in vivo* studies, in which was demonstrated that encapsulation of a drug into a nanoformulation effectively reduce their toxicity [4, 129-132].

Free AmB exhibit a higher antileishmanial activity against infected human THP-1 differentiated macrophages (1329.2 ± 151.5 nM) and BMMϕ (1134.6 ± 91.0 nM) (Table 7), being that, the incorporation of AmB into PLGA nanoparticles, increased significantly the efficacy of these compound in inhibiting intracellular amastigote growth in both types of cells, in comparison with free AmB (Table 7). On the other hand, when AmB is incorporated in M-PLGA nanoparticles, prepared either by PA or CR1, an improvement of the drug antileishmanial activity in the nanoformulations was also observed for both THP-1 cells and BMMϕ (Table 7), being that nanoparticles prepared by CR1 seems to be more efficient in that effect, which could be associated with the slow and more controlled release observed in these nanoparticles. Thus, the functionalization of PLGA nanoparticles seems to favor a higher uptake of nanoparticles and consequently a higher antileishmanial activity. Since we have already demonstrated that M-PLGA nanoparticles are not able, *per se*, to inhibit the growth of *L. infantum* intracellular amastigotes, the growth inhibition observed should be promoted by AmB released from the M-PLGA nanoparticles.

The results clearly have demonstrated that the use of polymeric nanoparticles, in particular the ones coated with mannose by CR1, for drug delivery of AmB is a good strategy, since they promote, as a result of a slow and sustained release, a significant reduction of the compound toxicity towards mammalian cells and, consequently allows the administration of higher doses in order to eliminate the parasite effectively.

5.1.4. Preparation and characterization of FITC-loaded nanoparticles

Encapsulation of FITC in PLGA nanoparticles was performed to produce fluorescently labeled nanoparticles, similar to the non-functionalized and mannosylated ones. To gain knowledge on the cell targeting of M-PLGA nanoparticles, *ex vivo* and *in vivo* studies were performed in splenocytes. On the other hand, in the second part of this work, to evaluate the immunotherapeutic effect of different mannosylated nanoformulations, in addition to the above mentioned nanoparticles, FITC-loaded MN- and Ms- coated PLGA nanoparticles were also prepared.

FITC was successfully incorporated into uncoated PLGA nanoparticles by the nanoprecipitation method and the different sugars were chemically conjugated to nanoparticles, using CR1 technique. FITC-loaded PLGA nanoparticles exhibited a mean

diameter of 201.2 ± 7.5 nm that is not statistically significant altered by the coating with M and MN, however a significant decrease ($P<0.05$) of size occurs after Ms incorporation (184.0 ± 0.9 nm) (Table 8). In what concerns PDI values (Table 8), results show that although the coating of PLGA nanoparticles with M did not cause a significant change (0.063 ± 0.002), as compared with uncoated PLGA nanoparticles (0.057 ± 0.002), the incorporation of MN and Ms favors a statistically significant increase of these values (0.066 ± 0.004 ($P<0.05$) and 0.084 ± 0.004 ($P<0.001$), respectively) that is more prominent in the case of Ms. This could be explained by the fact that the surface charge of Ms-PLGA nanoparticles (-14.6 ±0.6 mV) is less negative when compared with M- and MN-PLGA nanoparticles (-19.0 ± 1.1 and -18.0 ± 1.4, respectively) (Table 8), making them more prone to aggregate and present higher PDI values.

The coating level of M, MN and Ms was determined by indirect determination of the quantity of each sugar that was not chemically bound to PLGA, using phenol-sulfuric acid reaction. Results demonstrate that an efficiently coating of nanoparticles, with M-, MN- and Ms-, occurs, being the yields associated around 98%, 91% and 99%, respectively (Table 8), which is not in accordance with data from the literature [8, 29, 149]. Generally, the yields associated with the incorporation of any of the three sugars are much lower than the ones obtained for us. For M- and MN-PLGA nanoparticles, in most of the articles a direct quantification, using the phenol-sulfuric acid reaction, is made, which could lead as already mentioned to a great loss of ligand, as a result of the harsh techniques used to extract it from the surface of nanoparticles, leading to the achievement of very low yields. In the case of Ms-PLGA nanoparticles, the low yields normally presented in the articles could also be related with a direct quantification, however in this case, another important factor could explain this difference and, that is the method used for quantification, the O-phthalaldehyde fluorimetric assay [149]. Thus, the ideal would be to use two different techniques to quantify the same sugar in order to guarantee that the yields obtained are consistent and correspond to the real quantity of sugar present in the surface of nanoparticles.

FITC encapsulation was indirectly determined by quantification of the non-encapsulated amount that stays in the aqueous phase after particle recovery. An E.E. of around 56% was achieved in all prepared nanoformulations (Table 8). These results are in accordance with previous reports indicating that E.E. of hydrophobic compounds is higher when nanoparticles are prepared by the nanoprecipitation method, since this method will prevent the diffusion of the compound to the aqueous phase during particles formation[150]. The coating of PLGA nanoparticles, contrarily to what happens with AmB, does not lead to a significant decrease in the E.E. of FITC, which could be explained by the fact that the encapsulation of this compound is not dependent on the occurrence of an

interaction with COOH group of PLGA and, also by the fact that coating by CR1 leads to the formation of a stable structure that will favor the lost of only small quantities of FITC reaching good E.E..

Release of FITC from uncoated, M-, MN- and Ms-coated PLGA nanoparticles was determined, over time, at physiological conditions using PBS pH 7.4. A biphasic pattern release of FITC (Fig. 20) was observed for all nanoformulations, with an initial rapid release of about 3.2%, caused by the liberation of the drug deposited in the surface of nanoparticles, that is followed by a constant release during the rest of the incubation period, as a result of the constant diffusion of the compound through the channels that are created in the polymer matrix resulting from the inward diffusion of water and the onset of erosion [41]. The pattern of release presented by these nanoformulations suggest that, although FITC is not chemically bound, as a result of the stable structure of nanoparticles, the release will be very slow and controlled, giving the information that the intensity of fluorescence observed in posterior studies corresponds to the action of nanoparticle and not of the free compound.

5.1.5. *Ex vivo* and *in vivo* uptake studies

The use of mannose to improve the efficiency of a PLGA-based drug delivery system in the treatment of leishmaniasis was based on the fact that the target receptor of this ligand, MR, is highly expressed in APCs (macrophages and DCs). Thus, it is of great importance to verify if the developed nanoformulations are effectively internalized by the target cells. For that *ex vivo* and *in vivo* studies were conducted with splenocytes isolated from Balb/c mice and the uptake of nanoparticles by different types of cells, namely T cells ($CD4^+$ and $CD8^+$), B cells, APCs and neutrophils evaluated. *Ex vivo* studies (n=2) were initially conducted, to avoid unnecessary use of laboratory animals and, then identical experiments were translate to *in vivo*, in order to validated the results obtained under physiological conditions. Analysis of the cellular composition of splenocytes, both *ex vivo* and *in vivo*, revealed a predominance of lymphocytes, with a significant high number of B cells as compared with $CD4^+$T and $CD8^+$T cells, whereas APCs and neutrophils represent only a small percentage of total cells in spleen (Fig.21A-B and Fig.22A-B), which is in accordance with what is described in the literature [151]. Then, in order to study the uptake of FITC-loaded uncoated and M-coated PLGA nanoparticles by different types of cells, for the *ex vivo* studies splenocytes were co-cultured, for 24h, with a defined volume of each of nanoformulations and, for *in vivo* studies, Balb/c mice were administered with the same amount of the nanoformulations (Material and Methods, section 3.7.). In splenocytes co-cultured with FITC-loaded PLGA nanoparticles (Fig.21C-D), as well as in the ones isolated from mice treated with the same

nanoformulations (Fig.22C-D), it was observed that although lymphocytes constitute the main population of cells in spleen, the uptake occurs preferentially by APCs and neutrophils. On the other hand, the uptake profile of M-PLGA nanoparticles in the *ex vivo* experiments (Fig.21E-F) is different from the one observed in *in vivo* experiments (Fig.22E-F). In splenocytes co-cultured with M-PLGA nanoparticles, similarly to what is observed for the ones co-cultured with uncoated nanoparticles, the uptake occurs preferentially by APCs and neutrophils. In splenocytes isolated from Balb/c mice, contrarily to what would be expected, APCs present an uptake almost similar to what is observed for lymphocytes, with neutrophils being the cells with higher uptake of M-PLGA nanoparticles. These results could be explained by the fact of mannosylated nanoparticles, after their administration, be first internalized by the APCs present in the liver, since they will pass through this organ before they reach the spleen. In that way, it would be interesting, in further studies, evaluate the uptake of nanoparticles, both *ex vivo* and *in vivo,* by the cells present in the liver. Results for both *ex vivo* and *in vivo* studies have demonstrated that neutrophils are the cells in which a higher uptake of nanoparticles was observed, since they are the most abundant population of circulating leucocytes and are rapidly recruited to the infected sites mediating the initial stages of an inflammatory response [151]. It is also important to note that the number of cells containing FITC-loaded nanoparticles is higher in *ex vivo* studies, which is expected since *in vivo* there is the influence of other cells and other mechanisms that could interfere with the uptake of these nanoparticles, leading to a lower number of particles retained by the spleen cells.

Although the development of a mannosylated nanoparticulate system aims to increase the uptake by APCs, through the targeting of MR, that is highly expressed in these cells, the *ex vivo* results demonstrate that there is no significant differences in the uptake of uncoated and M-coated PLGA nanoparticles by these cells (Fig 21C-F). PLGA nanoparticles are internalized mainly through clathrin-mediated endocytosis, although by the fact of them, in contrast with M-PLGA nanoparticles, do not have a ligand targeting MR, allows their internalization by other mechanisms such as phagocytosis or fluid-phase endocytosis [24]. M-PLGA nanoparticles, on the other hand, target specifically MR that mediates the internalization and deliver through clathrin-mediated endocytosis (Fig.7), being that this receptor doesn't seems to be able, *per se*, to mediate phagocytosis [66, 84]. Thus the similar uptake observed for uncoated and M-coated PLGA nanoparticles could be explained by the fact of while mannosylated nanoparticles are internalized only through the endocytic pathway, uncoated nanoparticles can be internalized by different mechanisms favoring an uptake by APCs similar to that observed for functionalized nanoparticles.

Ex vivo results strongly suggest that targeting APCs through the use of a ligand, such as mannose, that is specifically recognized by MR, seems to be a good strategy to improve the efficiency of PLGA-based drug delivery systems in the treatment of leishmaniasis. However, in further studies, it is necessary to repeat *in vivo* experiments to confirm the preferentially uptake of mannosylated nanoparticles by APCs using fluorescence microscopy of several tissues.

5.2. Mannosylated nanoparticles for immunotherapy

Functionalization of nanoparticles with ligands that are targeted to specific receptors on APCs (macrophages and DCs), can potentially improve their immunotherapeutic effect, through the induction of a robust immune response [6-7, 140]. Specifically, targeting of MR, a member of CLR family highly expressed on DCs and macrophages, seems to be a good strategy to improve the efficiency of PLGA-based drug delivery systems, since this receptor is involved in antigen internalization and presentation to immune response [91-92]. Recent studies, have demonstrated that functionalization of nanoparticles with ligands that are specifically recognized by MR induces the activation and maturation of DCs, which is evidenced by the enhanced expression of cell surface markers, including CD40, CD80, CD86 and MHC II and by the higher production of pro-inflammatory cytokines (IL-6, IL-12 and TNF-α) [6, 140]. Thus, since MR-targeting can be a promising approach to improve the immunotherapeutic effect of nanoformulations, the second aim of this work was using PLGA nanoparticles functionalized with three different ligands (M, MN, Ms) that have a strong binding affinity to MR, evaluate the extent in which these mannosylated nanoformulations affect the activation status of the cells and the type of response that they will modulate in APCs. These studies were performed in macrophages, since no published studies evaluating the immunotherapeutic potential of nanoformulations in these cells were found in literature and, also in DCs to validate the system with data from the literature [6, 8, 140, 152].

The expression of MR on different days of BMMϕ differentiation was assessed, in order to define the most suitable day to perform the *in vitro* uptake and activation studies. The results have shown that the expression of this receptor is time-dependent, with a maximum expression at day 8 of differentiation (77.9% cells $F4/80^+$ / MR^+) (Fig 23A-B). Interestingly, a significant decrease in the expression of the receptor was observed from day 8 to day 9 (Fig.23A), which could be explained by a down-regulation of the mechanisms involved in MR expression as result of aging of cells. Thus, based on these results the following *in vitro* studies were performed at day 8 of BMMϕ differentiation.

Then, uptake studies of fluorescently labeled uncoated and M-, MN- and Ms-coated PLGA nanoparticles were conducted to see if these nanoparticles have a differential uptake in

BMMϕ, if this is time-dependent and to define the most suitable time of incubation that should be used in subsequent *in vitro* studies. The data on Fig.24A-D shows that 30 minutes of incubation with the nanoparticles is sufficient to have a good fluorescence signal, since after that time, ≈90% of all nanoparticles had already been internalized by BMMϕ. Nevertheless, to assure that nanoparticles are co-cultured with cells enough time to induce a detectable effect, a 20h incubation period was used in the posterior activation studies (Fig 24) [8]. The analysis of differential uptake of nanoparticles after an incubation period of 20h (Fig.25) suggests that uncoated PLGA nanoparticles have a higher uptake compared to mannosylated nanoparticles. PLGA nanoparticles are internalized mainly through clathrin-mediated endocytosis, although by the fact of them, in contrast with M-PLGA nanoparticles, do not have a ligand targeting MR, allows their internalization by other mechanisms such as phagocytosis or fluid-phase endocytosis [24]. Funtionalized nanoparticles, on the other hand, target specifically MR that mediates the internalization and deliver through clathrin-mediated endocytosis (Fig.7), being that this receptor doesn't seems to be able, *per se*, to mediate phagocytosis [66, 84]. Thus these facts could explain the differential uptake observed at 20h between uncoated and M-, MN- and Ms-coated PLGA nanoparticles. Another possible explanation for the differential uptake of uncoated and mannosylated PLGA nanoparticles is related with the fact of although the E.E. of FITC is equivalent for all the nanoformulations, the presence of different sugars in the surface of nanoparticles could mask the fluorescence of the compound.

In order to confirm that all nanoparticles are efficiently internalized by BMMϕ and also to have an idea of their distribution in cells, fluorescence microscopy was used. The results (Fig.26A-D) clearly show that, similar to what is observed in the *in vitro* uptake studies, all nanoparticles are efficiently internalized. These images also show that, although all nanoparticles are located in the cytoplasm, their distribution pattern is different, whereas non-functionalized (Fig.26A) and M-functionalized (Fig.26B) PLGA nanoparticles have a more diffuse distribution pattern, MN- (Fig.26C) and Ms-functionalized (Fig.26D) nanoparticles seems to be internalized in vesicles, which is evidence by the presence of green dots in the cytoplasm, suggesting that their uptake occurs by an endocytic pathway. Future studies will detailed the different distribution patterns of each nanoformulation, namely through the use of fluorescent endocytic markers (*e.g.*Lysotrack) clarifying the intracellular trafficking of these manosylated nanoformulations.

Since macrophages, contrary to DCs, do not have a constitutive expression of migratory (MHC II) and co-stimulatory molecules (CD40, CD80 and CD86), they need to be previously activated to express these molecules [152]. Thus, through determination of the expression of specific cell surface markers is possible to assess the influence of non-functionalized and M-, MN, and Ms- functionalized PLGA nanoparticles in the activation

status of macrophages. Results show that functionalization of PLGA nanoparticles with any of the three sugars leads to a statistically significant increase in the expression of CD40, CD86, CD80, MHC II (Fig. 27A-D and Fig.28) and MR (Fig.27E), when compared to non-functionalized nanoparticles. While M-functionalization favors a moderate activation of macrophages, the functionalization with MN and Ms induces a higher surface expression of migratory (MHC II) (Fig.27D and Fig.28) and co-stimulatory molecules (CD40, CD86 and CD80) (Fig.27A-C and Fig.28) and also of MR (Fig.27E), influencing more significantly the activation and maturation of macrophages and consequently the efficient activation of T cells. Therefore, MHC II, a molecule involved in antigen presentation to $CD4^+$T cells; CD40, CD80 and CD86, co-stimulatory molecules that are specifically recognized by receptors in T cells surface and are essential for the activation and differentiation of $CD4^+$T cells; and MR, that is involved in antigen uptake and processing, have all an important role in the formation of an adaptive immune response [152].

Although the expression of MHC II, CD40, CD80 and CD86 in macrophages is essential it is not sufficient to an induction of T cell activation. Thus, it is crucial that the activation of macrophages lead to the production of different cytokines, in order to favor the development of a more effective immune response. The profile of cytokines produced by BMMϕ co-cultured with non-functionalized and functionalized nanoparticles was assessed through determination of the production of intracellular cytokines, including IL-4, IL-6, IL-12 and TNF-α (Fig.29A-D). The results reveal that, similar to what is observed for cell surface markers, MN- and Ms-PLGA nanoparticles are the nanoformulations that stimulate more efficiently the activation of macrophages, which is reflected by the higher production of intracellular cytokines, IL-4, IL-6, IL-12 and TNF-α, being that TNF-α (Fig.29D) is the one with higher production. IL-4 stimulates the maturation of näive T cells in Th2 cells and is an important autocrine growth factor for these newly formed cells [151]. Furthermore, it was described that this cytokine together with IL-13, promote an up-regulation of MR and MHC II molecules, stimulating endocytosis and antigen presentation, and thus favoring an alternative activation of macrophages [153]. Thus, despite this cytokine being produced in small amounts (<2%), the higher production induced by MN- and Ms-PLGA nanoparticles (Fig.29A) could be in part related with the higher expression of MHC II and MR observed when BMMϕ are co-cultured with these nanoformulations (Fig.27D and 27E). IL-6 has pleiotropic effects on cell growth, differentiation, survival and migration during immune responses, acting also as B cell differentiation factor [151]. On the other hand, TNF-α is also a pleiotropic cytokine whose main physiological function is the recruitment of phagocytes to the infection sites and consequent activation of these cells [151]. This cytokine act together with IFN-ɣ to promote the classical activation of

macrophages [155]. IL-12 is a stimulatory cytokine that drives Th1 responses associated with generation of cellular immunity [151]. Having said that, the higher production of IL-6, IL-12 and TNF-α (Fig.29A, C-D), as compared with the production of IL-4 (Fig.29B), observed when BMMϕ are co-cultured with MN- and Ms- functionalized nanoparticles, suggest that these nanoformulations have a pro-inflammatory profile and that macrophages might be activated by the classical pathway.

Thus, these results clearly demonstrate that functionalization of PLGA nanoparticles with MN and Ms improve their immunotherapeutic effect, through the induction of a more efficient activation of macrophages, which could lead to the development of a robust immune response.

The fact of PLGA nanoparticles functionalized with MN and Ms stimulate more efficiently the activation of macrophages, which is reflected by the higher expression of cell surface markers and by the production of intracellular cytokines, could be related to a greater internalization of these nanoparticles, as compared to non-functionalized and M-functionalized ones. However results from the uptake studies (Fig.24A-D, and Fig.25) shows that all nanoparticles are efficiently internalized by BMMϕ, being that the non-functionalized ones seems to have even a greater uptake. So, taken togheter these results suggest that although internalization is an important factor it will not be sufficient to enhance macrophages activation.

The studies evaluating the immunotherapeutic potential of nanoformulations specifically targeting MR are described in DCs [6, 8, 140, 152]. In that way and, in order to validate the system used with BMMϕ with the data from literature, the extent in which the developed nanoparticles affect the activation status of DCs was evaluated.

Since the data from the literature relative to the day of BMDCs differentiation in which the MR expression is higher are contradictory, some authors consider day 7 [8] and others consider day 9 [6], initially the MR expression was evaluated on different days of BMDCs differentiation. In this case and since at day 6 less than 22% of cells are DCs the assessment was made between day 7 and 9 of BMDCs differentiation (Fig.30A). The MHC II expression (Fig.30B) was also quantified, since this is a molecule highly expressed in mature DCs, giving information about the differentiation/maturation state of these cells. The data obtained show no significant differences on the levels of MR expression (Fig.30A) but, the expression of MHC II (Fig.30B) increased significantly with time being the maximum expression observed at day 9 (68.1% cells $CD11c^{+}$/MHC-II^{+}). Thus, BMDCs with 9 days of differentiation was chosen, to perform posterior *in vitro* studies, since the high percentage of mature DCs was observed at that day.

As already mentioned, the functionalization of nanoparticles with ligands that are specifically recognized by MR induces the activation and maturation of DCs, which is

evidenced by the enhanced expression of cell surface markers and by the higher production of pro-inflammatory cytokines [6, 140]. Thus, to verify if PLGA nanoparticles functionalized with M, MN and Ms induce the same results, the expression of cell surface markers as well as the production of intracellular cytokines in BMDCs co-cultured with those nanoformulations was evaluated. The results show that both non-functionalized and functionalized PLGA nanoparticles enhanced the expression of CD40 (Fig.31A and Fig.32), CD86 (Fig.31B and Fig.32), MHCII (Fig.31C and Fig.32) and MR (Fig.31D) when compared to non-stimulated BMDCs. Contrarily to what is observed for BMMϕ, in BMDCs the functionalization of PLGA nanoparticles with any of the three sugars influence in the same way the activation and maturation of cells. The high MFI values obtained for MHC II molecule (Fig.31C), in comparison with the values obtained for the co-stimulatory molecules are in accordance with previous studies in which were demonstrated that at day 9 DCs are completely maturated and differentiated (Fig.30B). On the other hand the lower values of MFI obtained for MR is in accordance with the results obtained for the evaluation of the expression of this receptor on different days of BMDCs differentiation (Fig.30A), in which, was observed that even at day 9 the expression of these receptor was very low. Comparing the MFI values of antigen presenting and co-stimulatory molecules obtained for BMMϕ and BMDCs co-cultured with the same type of nanoparticles is possible observe that they are higher for BMDCs, which may be related with the fact of these cells are the only APCs that constitutively express these molecules and, so the stimulation of these cells will enhance even more their expression. The results obtained are in accordance with data from the literature [6, 140], which means that the system used with BMMϕ is suitable to evaluate the extent in which mannosylated nanoformulations affect the activation status of cells

The profile of cytokines produced by BMDCs co-cultured with non-functionalized and functionalized nanoparticles was assessed through determination of the production of intracellular cytokines, including IL-4, IL-6 and IL-12. Results show that stimulation of BMDCs with PLGA nanoparticles functionalized with any of the three sugars increased statistically significant the production of IL-4 (Fig.33A) and IL-6 (Fig.33B). It was demonstrated that the exposure of DCs to certain stimulus (*e.g.*retrovirus) results in the intracellular production, but not in secretion of IL-4 [155]. Thus, based on that, the fact of functionalized nanoparticles stimulates a higher intracellular production of IL-4 (Fig.33A) by BMDCs, doesn't mean that this cytokine will be secreted and will, consequently, stimulate the maturation of näive T cells in Th2 cells. In that way, it will be important in further studies, to quantify the secreted cytokines. DCs are the major cells contributing for IL-12 production in primary immune responses, being that the production of this cytokine, in addition to the enhanced expression of co-stimulatory and antigen presenting

molecules, an important factor for the induction of efficient T cell activation [156]. In what concerns the production of this cytokine, results demonstrate that the co-culture of BMDCs with non functionalized PLGA nanoparticles, leads to the production of higher levels of IL-12 (Fig.33 C), as compared with functionalized nanoparticles, reaching values almost identical to those observed for LPS (positive control). When we are evaluating the effect of different nanoformulations in the activation status of a cell, besides the production of cytokines, it is also crucial to assess the expression of co-stimulatory and antigen presenting molecules. Thus, in that way, although it was observed that non functionalized PLGA nanoparticles induces a higher intracellular production of IL-12 (Fig.33C), an important cytokine in the development of an immune response, the fact of M-, MN- and Ms-functionalized nanoparticles induce a higher expression of CD40, CD86, MHC II (Fig.31A-C and Fig. 32) and MR (Fig.31D) as well as the production of IL-12 (Fig.33C), even at lower levels, and IL-6 (Fig.33B), make them more effective nanoformulations in the activation and maturation of BMDCs. Although the production of cytokines is important to evaluate the efficiency with which nanoformulations induces DC activation these results cannot be compared with data from the literature [6, 140] to validate the system adopted, since the methods used for evaluate the cytokines productions are different (usually the measurement is based on secreted cytokines).

To summarize, the functionalization of PLGA nanoparticles with ligands that are specifically recognized by MR in APCs, particularly with MN and Ms, improve their immunotherapeutic effect, through the induction of a more efficient activation of macrophages and DCs, which could lead to the development of a robust immune response. Therefore, in order to complement these studies it would be interesting to evaluate the ability of these nanoformulations to stimulate specific $CD4^+$ and $CD8^+$ - T cells responses.

VI. CONCLUSIONS

The novel nanoformulations developed in the present work, through the functionalization of the surface of PLGA nanoparticles with mannose residues, constitutes a promising strategy for efficient delivery of AmB and seems to have potential as immunotherapeutic agents in the treatment of VL.

It was demonstrated that mannosylation of PLGA nanoparticles can be efficiently achieved by a simple chemical reaction (CR1), once the M-PLGA nanoparticles obtained by this reaction, in comparison with the ones prepared by PA and CR2, present a small size (< 200 nm), a low PDI (<0.1), good storage stability, were spherical in shape, have higher mannose residues oriented to the exterior of the NP, and do not present toxicity against human THP-1 differentiated macrophages and intracellular *L.infantum* amastigotes.

The results from storage stability studies clearly demonstrate that the best storage temperature condition to maintain M-PLGA nanoparticles for long periods of time (8 weeks) is at 4ºC.

The mannosylated nanoparticulate system, prepared by PA and CR1, were used to encapsulate AmB and their efficiency as drug delivery system, in the treatment of VL, was evaluated *in vitro* in *Leishmania*-infected macrophages. The use of AmB-loaded M-PLGA nanoparticles, prepared by CR1, as drug delivery system, is more advantageous, when compared to the ones prepared by PA, since besides having a higher encapsulation efficiency, they also favor a slow and controlled release of the compound, especially in acidic conditions, as a result of their stable structure. In line with previous *in vitro* and *in vivo* studies [4, 129-132], this work demonstrate that incorporation of AmB in uncoated and M-coated PLGA nanoparticles effectively reduce its toxicity towards macrophages, which is of great relevance, since this allows the *in vivo* administration of higher doses of AmB, without the toxic effects normally associated with the administration of the free compound. On the other hand, the encapsulation of AmB in M-PLGA nanoparticles, prepared either by PA or CR1, also improves it antileishmanial activity, being this effect more pronounced in nanoparticles prepared by CR1, which could be explained by the slow and more controlled release observed in this case.

The results from *ex vivo* and *in vivo* studies performed in order to evaluate the M-PLGA nanoparticles uptake, demonstrate that although lymphocytes constitute the main population of cells in spleen, the uptake occurs preferentially by APCs (macrophages and DCs), the target cells in VL, and neutrophils.

In the second part of the work it was demonstrated that the functionalization of PLGA nanoparticles with ligands that specifically target MR in APCs, particularly with MN and

Ms, improve their immunotherapeutic effect, through the induction of a more efficient activation of macrophages and DCs, evidenced by the enhanced expression of cell surface markers, including CD40, CD80, CD86 and MHC II and by the higher production of pro-inflammatory cytokines (IL-4, IL-6, IL-12 and TNF-α), which could lead to the development of a robust immune response.

To summarize, the results from this work have demonstrated that mannosylated nanoformulations, in particular the ones prepared by CR1, could have a promising role in the delivery of AmB and consequently in the treatment of leishmaniasis. Furthermore, the use of nanoformulations functionalized with ligands that specifically target MR in APCs seems to promote the development of a robust immune response.

VII. FUTURE PERSPECTIVES

In the last years the research interest in the area of developing nanotechnology suffered a huge growth. In particular, the application of polymeric nanoparticles as drug delivery systems in the treatment of different diseases, including leishmaniasis, has been extensively investigated, in an attempt to reduce toxicity and side effects of drugs currently used [130-132]. Thus, this work arises from the need to create a nanoparticulate system that overcome some of the main drawbacks associated with AmB, one of the more effective drugs used in the treatment of leishmaniasis, and that allows a more efficient delivery of these drug. Besides that, it is of great importance to understand in which extent the developed nanoformulations interfere/interact with the host immune system. In my point of view the results obtained in this work, to date, could contribute, in the future, to the development of a treatment capable of complement the ones that are currently available, however much work remains to be done.

In further studies, it will be important evaluate the *in vivo* biodistribution pattern and the targeting potential for macrophage-rich organs of the developed nanoparticulate system, in comparising with free AmB, using healthy Balb/c mice. Furthermore, the *in vivo* efficacy of the nanoformulations should be evaluated against VL, using Balb/c mice previously infected with *L.infantum* as model.

Since e*x vivo* and *in vivo* studies clearly demonstrate that M-PLGA nanoparticles are preferentially taken by APCs, in further studies it would be interesting to verify, both *ex vivo* and *in vivo*, if the immunological state of the mice influence in some way the uptake of nanoparticles by APCs, through the use of splenocytes isolated from non-infected and *L.infantum*-infected Balb/c mice. To complement these studies and confirm the obtained results, we can use immunohistochemistry techniques in order to evaluate the biodistribution of nanoparticles among different organs and their differential uptake by lymphocytes, APCs and neutrophils.

In the second part of this work it was demonstrated that functionalization of PLGA nanoparticles with ligands that specifically target MR in APCs, induce a more efficient activation of macrophages and DCs. Therefore, in order to complement these studies we need to evaluate the ability of these nanoformulations to stimulate specific $CD4^+$ and $CD8^+$ - T cells responses (Th1 and Th2 responses). On the other hand, since the results obtained strongly suggest that MN and Ms are more effective than M in the induction of an immunological response, it would be interesting to do a comparative *ex vivo* and *in vivo* study of the differential uptake of those nanoformulations in lymphocytes ($CD4^+$ and $CD8^+$ and B), APCs and neutrophils. Furthermore, if we verify that in fact the nanoformulations

functionalized with MN and Ms are more effective, we can encapsulate AmB and evaluate their *in vitro* and *in vivo* efficacy in the treatment of VL.

The fluorescence studies performed to evaluate the uptake of non functionalized and M-, MN- and Ms- functionalized PLGA nanoparticles by BMMϕ lead us to hypothesize that nanoparticles functionalized with MN and Ms are internalized by an endocytic pathway. Thus, in further studies it would be interesting study in more detail the different distribution patterns of each nanoformulation, namely through the use of fluorescent endocytic markers (*e.g.*Lysotrack).

Finally in order to verify if the increased activation of macrophages and DCs, induced by functionalized nanoparticles, are directly correlated with MR-ligand interaction and occurs via receptor-mediated encodytosis or by other mechanism, such as phagocytosis, we can perform *in vitro* studies in which MR, endocytosis and/or phagocytosis are inhibited.

VIII. REFERENCES

1. Singh, S. and Sivakumar, R., *Challenges and new discoveries in the treatment of leishmaniasis.* J Infect Chemother, 2004. **10**(6): p. 307-15.
2. Tiuman, T.S., Santos, A.O., Ueda-Nakamura, T., Filho, B.P., and Nakamura, C.V., *Recent advances in leishmaniasis treatment.* Int J Infect Dis, 2011. **15**(8): p. e525-32.
3. Guerin, P.J., Olliaro, P., Sundar, S., Boelaert, M., Croft, S.L., Desjeux, P., Wasunna, M.K., and Bryceson, A.D., *Visceral leishmaniasis: current status of control, diagnosis, and treatment, and a proposed research and development agenda.* Lancet Infect Dis, 2002. **2**(8): p. 494-501.
4. Espuelas, M.S., Legrand, P., Irache, J.M., Gamazo, C., Orecchioni, A.M., Devissaguet, J.P., and Ygartua, P., *Poly(epsilon-caprolacton) nanospheres as an alternative way to reduce amphotericin B toxicity.* Int J Pharm, 1997. **158**(1): p. 19-27.
5. Fessi, H., Puisieux, F., Devissaguet, J.P., Ammoury, N., and Benita, S., *Nanocapsule Formation by Interfacial Polymer Deposition Following Solvent Displacement.* Int J Pharm, 1989. **55**(1): p. R1-R4.
6. Carrillo-Conde, B., Song, E.H., Chavez-Santoscoy, A., Phanse, Y., Ramer-Tait, A.E., Pohl, N.L., Wannemuehler, M.J., Bellaire, B.H., and Narasimhan, B., *Mannose-functionalized "pathogen-like" polyanhydride nanoparticles target C-type lectin receptors on dendritic cells.* Mol Pharm, 2011. **8**(5): p. 1877-86.
7. Hamdy, S., Haddadi, A., Shayeganpour, A., Samuel, J., and Lavasanifar, A., *Activation of antigen-specific T cell-responses by mannan-decorated PLGA nanoparticles.* Pharm Res, 2011. **28**(9): p. 2288-301.
8. Ghotbi, Z., Haddadi, A., Hamdy, S., Hung, R.W., Samuel, J., and Lavasanifar, A., *Active targeting of dendritic cells with mannan-decorated PLGA nanoparticles.* J Drug Target, 2011. **19**(4): p. 281-92.
9. Black, C.D.V. and Gregoriadis, G., *Intracellular Fate and Effect of Liposome-Entrapped Actinomycin-D Injected into Rats.* Biochem Soc T, 1974. **2**(5): p. 869-71.
10. Couvreur, P., Tulkens, P., Roland, M., Trouet, A., and Speiser, P., *Nanocapsules: a new type of lysosomotropic carrier.* FEBS Lett, 1977. **84**(2): p. 323-26.
11. Duncan, R. and Gaspar, R., *Nanomedicine(s) under the microscope.* Mol Pharm, 2011. **8**(6): p. 2101-41.
12. Lamprecht, A., *Nanotherapeutics: drug delivery concepts in nanoscience.* Pan Stanford Pub; Distributed by World Scientific Pub.:Singapore Hackensack, NJ, 2009. p xii, 279.
13. Danhier, F., Ansorena, E., Silva, J.M., Coco, R., Le Breton, A., and Preat, V., *PLGA-based nanoparticles: an overview of biomedical applications.* J Control Release, 2012. **161**(2): p. 505-22.
14. Leroux, J.C., Allemann, E., DeJaeghere, F., Doelker, E., and Gurny, R., *Biodegradable nanoparticles - From sustained release formulations to improved site specific drug delivery.* J Control Release, 1996. **39**(2-3): p. 339-50.
15. Panyam, J. and Labhasetwar, V., *Biodegradable nanoparticles for drug and gene delivery to cells and tissue.* Adv Drug Deliv Rev, 2003. **55**(3): p. 329-47.
16. Soppimath, K.S., Aminabhavi, T.M., Kulkarni, A.R., and Rudzinski, W.E., *Biodegradable polymeric nanoparticles as drug delivery devices.* J Control Release, 2001. **70**(1-2): p. 1-20.
17. Singh, M. and O'Hagan, D., *The preparation and characterization of polymeric antigen delivery systems for oral administration.* Adv Drug Deliv Rev, 1998. **34**(2-3): p. 285-304.
18. Qiu, L.Y. and Bae, Y.H., *Polymer architecture and drug delivery.* Pharm Res, 2006. **23**(1): p. 1-30.
19. Edlund, U. and Albertsson, A.C., *Polyesters based on diacid monomers.* Adv Drug Deliv Rev, 2003. **55**(4): p. 585-609.

20. Brannonpeppas, L., *Recent Advances on the Use of Biodegradable Microparticles and Nanoparticles in Controlled Drug-Delivery.* Int J Pharm, 1995. **116**(1): p. 1-9.
21. Kumari, A., Yadav, S.K., and Yadav, S.C., *Biodegradable polymeric nanoparticles based drug delivery systems.* Colloids Surf B Biointerfaces, 2010. **75**(1): p. 1-18.
22. Jain, R.A., *The manufacturing techniques of various drug loaded biodegradable poly(lactide-co-glycolide) (PLGA) devices.* Biomaterials, 2000. **21**(23): p. 2475-90.
23. Dinarvand, R., Sepehri, N., Manoochehri, S., Rouhani, H., and Atyabi, F., *Polylactide-co-glycolide nanoparticles for controlled delivery of anticancer agents.* Int J Nanomed, 2011. **6**: p. 877-95.
24. Vasir, J.K. and Labhasetwar, V., *Biodegradable nanoparticles for cytosolic delivery of therapeutics.* Adv Drug Deliv Rev, 2007. **59**(8): p. 718-28.
25. Acharya, S. and Sahoo, S.K., *PLGA nanoparticles containing various anticancer agents and tumour delivery by EPR effect.* Adv Drug Deliver Rev, 2011. **63**(3): p. 170-83.
26. Mundargi, R.C., Babu, V.R., Rangaswamy, V., Patel, P., and Aminabhavi, T.M., *Nano/micro technologies for delivering macromolecular therapeutics using poly(D,L-lactide-co-glycolide) and its derivatives.* J Control Release, 2008. **125**(3): p. 193-209.
27. Vauthier, C. and Bouchemal, K., *Methods for the preparation and manufacture of polymeric nanoparticles.* Pharm Res, 2009. **26**(5): p. 1025-58.
28. Bilati, U., Allemann, E., and Doelker, E., *Development of a nanoprecipitation method intended for the entrapment of hydrophilic drugs into nanoparticles.* Eur J Pharm Sci, 2005. **24**(1): p. 67-75.
29. Nahar, M. and Jain, N.K., *Preparation, characterization and evaluation of targeting potential of amphotericin B-loaded engineered PLGA nanoparticles.* Pharm Res, 2009. **26**(12): p. 2588-98.
30. Gaumet, M., Vargas, A., Gurny, R., and Delie, F., *Nanoparticles for drug delivery: The need for precision in reporting particle size parameters.* Eur J Pharm Biopharm, 2008. **69**(1): p. 1-9.
31. Feng, S.S., *Nanoparticles of biodegradable polymers for new-concept chemotherapy.* Expert Rev Med Devices, 2004. **1**(1): p. 115-25.
32. Instruments, M., *Zeta potential - An introduction in 30 minutes.* Available from: http://www.malvern.com/search?openagent=1&lang=unifiedeng&section=unified&count=10&query=zeta+potential (Accessed in July 2012).
33. Cheng, J., Teply, B.A., Sherifi, I., Sung, J., Luther, G., Gu, F.X., Levy-Nissenbaum, E., Radovic-Moreno, A.F., Langer, R., and Farokhzad, O.C., *Formulation of functionalized PLGA-PEG nanoparticles for in vivo targeted drug delivery.* Biomaterials, 2007. **28**(5): p. 869-76.
34. Kim, S.H., Jeong, J.H., Chun, K.W., and Park, T.G., *Target-specific cellular uptake of PLGA nanoparticles coated with poly(L-lysine)-poly(ethylene glycol)-folate conjugate.* Langmuir, 2005. **21**(19): p. 8852-57.
35. Mosqueira, V.C., Legrand, P., Gulik, A., Bourdon, O., Gref, R., Labarre, D., and Barratt, G., *Relationship between complement activation, cellular uptake and surface physicochemical aspects of novel PEG-modified nanocapsules.* Biomaterials, 2001. **22**(22): p. 2967-79.
36. Govender, T., Stolnik, S., Garnett, M.C., Illum, L., and Davis, S.S., *PLGA nanoparticles prepared by nanoprecipitation: drug loading and release studies of a water soluble drug.* J Control Release, 1999. **57**(2): p. 171-85.
37. Calvo, J., Lavandera, J.L., Agueros, M., and Irache, J.M., *Cyclodextrin/poly(anhydride) nanoparticles as drug carriers for the oral delivery of atovaquone.* Biomed Microdevices, 2011. **13**(6): p. 1015-25.
38. Kirthivasan, B., Singh, D., Bommana, M.M., Raut, S.L., Squillante, E., and Sadoqi, M., *Active brain targeting of a fluorescent P-gp substrate using polymeric magnetic nanocarrier system.* Nanotechnology, 2012. **23**(25): p. 1-9
39. Bivas-Benita, M., Romeijn, S., Junginger, H.E., and Borchard, G., *PLGA-PEI nanoparticles for gene delivery to pulmonary epithelium.* Eur J Pharm Biopharm, 2004. **58**(1): p. 1-6.

40. Lima, S.C., Rodrigues, V., Garrido, J., Borges, F., Lin, P.K.T., and da Silva, A.C., *In vitro evaluation of bisnaphthalimidopropyl derivatives loaded into pegylated nanoparticles against Leishmania infantum protozoa.* Int J Antimicrob Ag, 2012. **39**(5): p. 424-30.
41. Fredenberg, S., Wahlgren, M., Reslow, M., and Axelsson, A., *The mechanisms of drug release in poly(lactic-co-glycolic acid)-based drug delivery systems-A review.* Int J Pharm, 2011. **415**(1-2): p. 34-52.
42. D'Souza, S.S., Faraj, J.A., and DeLuca, P.P., *A model-dependent approach to correlate accelerated with real-time release from biodegradable microspheres.* Aaps PharmSciTech, 2005. **6**(4): p. E553-64.
43. Berchane, N.S., Carson, K.H., Rice-Ficht, A.C., and Andrews, M.J., *Effect of mean diameter and polydispersity of PLG microspheres on drug release: Experiment and theory.* Int J Pharm, 2007. **337**(1-2): p. 118-26.
44. Berkland, C., Kim, K., and Pack, D.W., *PLG microsphere size controls drug release rate through several competing factors.* Pharmaceut Res, 2003. **20**(7): p. 1055-62.
45. Mei, L., Song, C.X., Jin, X., Che, Y.Z., Jin, Z., and Sun, H.F., *[Surface-modified paclitaxel-loaded nanoparticles as local delivery system for the prevention of vessel restenosis].* Yao Xue Xue Bao, 2007. **42**(1): p. 81-86.
46. Storm, G., Belliot, S.O., Daemen, T., and Lasic, D.D., *Surface Modification of Nanoparticles to Oppose Uptake by the Mononuclear Phagocyte System.* Adv Drug Deliver Rev, 1995. **17**(1): p. 31-48.
47. Hans, M.L. and Lowman, A.M., *Biodegradable nanoparticles for drug delivery and targeting.* Curr Opin Solid St M, 2002. **6**(4): p. 319-27.
48. Alexis, F., Pridgen, E., Molnar, L.K., and Farokhzad, O.C., *Factors affecting the clearance and biodistribution of polymeric nanoparticles.* Mol Pharmaceut, 2008. **5**(4): p. 505-15.
49. Torchilin, V.P. and Trubetskoy, V.S., *Which Polymers Can Make Nanoparticulate Drug Carriers Long-Circulating.* Adv Drug Deliver Rev, 1995. **16**(2-3): p. 141-55.
50. Stolnik, S., Illum, L., and Davis, S.S., *Long Circulating Microparticulate Drug Carriers.* Adv Drug Deliver Rev, 1995. **16**(2-3): p. 195-214.
51. Owens, D.E. and Peppas, N.A., *Opsonization, biodistribution, and pharmacokinetics of polymeric nanoparticles.* Int J Pharm, 2006. **307**(1): p. 93-102.
52. Gref, R., Domb, A., Quellec, P., Blunk, T., Muller, R.H., Verbavatz, J.M., and Langer, R., *The Controlled Intravenous Delivery of Drugs Using Peg-Coated Sterically Stabilized Nanospheres.* Adv Drug Deliver Rev, 1995. **16**(2-3): p. 215-33.
53. Tobio, M., Sanchez, A., Vila, A., Soriano, I.I., Evora, C., Vila-Jato, J.L., and Alonso, M.J., *The role of PEG on the stability in digestive fluids and in vivo fate of PEG-PLA nanoparticles following oral administration.* Colloids Surf B Biointerfaces, 2000. **18**(3-4): p. 315-23.
54. Calvo, P., Gouritin, B., Brigger, I., Lasmezas, C., Deslys, J.P., Williams, A., Andreux, J.P., Dormont, D., and Couvreur, P., *PEGylated polycyanoacrylate nanoparticles as vector for drug delivery in prion diseases.* J Neurosci Meth, 2001. **111**(2): p. 151-55.
55. Avgoustakis, K., Beletsi, A., Panagi, Z., Klepetsanis, P., Karydas, A.G., and Ithakissios, D.S., *PLGA-mPEG nanoparticles of cisplatin: in vitro nanoparticle degradation, in vitro drug release and in vivo drug residence in blood properties.* J Control Release, 2002. **79**(1-3): p. 123-35.
56. Bender, A.R., vonBriesen, H., Kreuter, J., Duncan, I.B., and RubsamenWaigmann, H., *Efficiency of nanoparticles as a carrier system for antiviral agents in human immunodeficiency virus-infected human monocytes/macrophages in vitro.* Antimicrob Agents Ch, 1996. **40**(6): p. 1467-71.
57. Yang, J., Sun, H., and Song, C., *Preparation, characterization and in vivo evaluation of pH-sensitive oral insulin-loaded poly(lactic-co-glycolicacid) nanoparticles.* Diabetes Obes Metab, 2012. **14**(4): p. 358-64.

58. De Campos, A.M., Sanchez, A., and Alonso, M.J., *Chitosan nanoparticles: a new vehicle for the improvement of the delivery of drugs to the ocular surface. Application to cyclosporin A.* Int J Pharm, 2001. **224**(1-2): p. 159-68.
59. Petrelli, F., Borgonovo, K., and Barni, S., *Targeted delivery for breast cancer therapy: the history of nanoparticle-albumin-bound paclitaxel.* Expert Opin Pharmaco, 2010. **11**(8): p. 1413-32.
60. Sykes, R., *'Towards the magic bullet'. Hamao Umezawa memorial award lecture.* Int J Antimicrob Agents, 2000. **14**(1): p. 1-12.
61. Schlosser, E., Mueller, M., Fischer, S., Basta, S., Busch, D.H., Gander, B., and Groettrup, M., *TLR ligands and antigen need to be coencapsulated into the same biodegradable microsphere for the generation of potent cytotoxic T lymphocyte responses.* Vaccine, 2008. **26**(13): p. 1626-37.
62. Kelly, C., Jefferies, C., and Cryan, S.A., *Targeted liposomal drug delivery to monocytes and macrophages.* J Drug Deliv, 2011. **2011**: p. 1-11.
63. Wileman, T.E., Lennartz, M.R., and Stahl, P.D., *Identification of the Macrophage Mannose Receptor as a 175-Kda Membrane-Protein.* P Natl Acad Sci USA, 1986. **83**(8): p. 2501-05.
64. Shepherd, V.L., Lee, Y.C., Schlesinger, P.H., and Stahl, P.D., *L-Fucose-terminated glycoconjugates are recognized by pinocytosis receptors on macrophages.* Proc Natl Acad Sci U S A, 1981. **78**(2): p. 1019-22.
65. Largent, B.L., Walton, K.M., Hoppe, C.A., Lee, Y.C., and Schnaar, R.L., *Carbohydrate-specific adhesion of alveolar macrophages to mannose-derivatized surfaces.* J Biol Chem, 1984. **259**(3): p. 1764-69.
66. East, L. and Isacke, C.M., *The mannose receptor family.* Bba-Gen Subjects, 2002. **1572**(2-3): p. 364-86.
67. Taylor, P.R., Gordon, S., and Martinez-Pomares, L., *The mannose receptor: linking homeostasis and immunity through sugar recognition.* Trends Immunol, 2005. **26**(2): p. 104-10.
68. McKenzie, E.J., Taylor, P.R., Stillion, R.J., Lucas, A.D., Harris, J., Gordon, S., and Martinez-Pomares, L., *Mannose receptor expression and function define a new population of murine dendritic cells.* J Immunol, 2007. **178**(8): p. 4975-83.
69. Avrameas, A., McIlroy, D., Hosmalin, A., Autran, B., Debre, P., Monsigny, M., Roche, A.C., and Midoux, P., *Expression of a mannose/fucose membrane lectin on human dendritic cells.* Eur J Immunol, 1996. **26**(2): p. 394-400.
70. Sallusto, F., Cella, M., Danieli, C., and Lanzavecchia, A., *Dendritic Cells Use Macropinocytosis and the Mannose Receptor to Concentrate Macromolecules in the Major Histocompatibility Complex Class-Ii Compartment - down-Regulation by Cytokines and Bacterial Products.* J Exp Med, 1995. **182**(2): p. 389-400.
71. Linehan, S.A., Martinez-Pomares, L., Stahl, P.D., and Gordon, S., *Mannose receptor and its putative ligands in normal murine lymphoid and nonlymphoid organs: In situ expression of mannose receptor by selected macrophages, endothelial cells, perivascular microglia, and mesangial cells, but not dendritic cells.* J Exp Med, 1999. **189**(12): p. 1961-72.
72. Lew, D.B., Songumize, E., Pontow, S.E., Stahl, P.D., and Rattazzi, M.C., *A Mannose Receptor Mediates Mannosyl-Rich Glycoprotein-Induced Mitogenesis in Bovine Airway Smooth-Muscle Cells.* J Clin Invest, 1994. **94**(5): p. 1855-63.
73. Shepherd, V.L., Tarnowski, B.I., and Mclaughlin, B.J., *Isolation and Characterization of a Mannose Receptor from Human Pigment-Epithelium.* Invest Ophth Vis Sci, 1991. **32**(6): p. 1779-84.
74. Stein, M., Keshav, S., Harris, N., and Gordon, S., *Interleukin 4 potently enhances murine macrophage mannose receptor activity: a marker of alternative immunologic macrophage activation.* J Exp Med, 1992. **176**(1): p. 287-92.
75. Doyle, A.G., Herbein, G., Montaner, L.J., Minty, A.J., Caput, D., Ferrara, P., and Gordon, S., *Interleukin-13 Alters the Activation State of Murine Macrophages in-Vitro - Comparison with Interleukin-4 and Interferon-Gamma.* Eur J Immunol, 1994. **24**(6): p. 1441-45.

76. Martinez-Pomares, L., Reid, D.M., Brown, G.D., Taylor, P.R., Stillion, R.J., Linehan, S.A., Zamze, S., Gordon, S., and Wong, S.Y., *Analysis of mannose receptor regulation by IL-4, IL-10, and proteolytic processing using novel monoclonal antibodies.* J Leukoc Biol, 2003. **73**(5): p. 604-13.
77. Harris, N., Super, M., Rits, M., Chang, G., and Ezekowitz, R.A., *Characterization of the murine macrophage mannose receptor: demonstration that the downregulation of receptor expression mediated by interferon-gamma occurs at the level of transcription.* Blood, 1992. **80**(9): p. 2363-73.
78. Schreiber, S., Blum, J.S., Stenson, W.F., MacDermott, R.P., Stahl, P.D., Teitelbaum, S.L., and Perkins, S.L., *Monomeric IgG2a promotes maturation of bone-marrow macrophages and expression of the mannose receptor.* Proc Natl Acad Sci U S A, 1991. **88**(5): p. 1616-20.
79. Shepherd, V.L., Lane, K.B., and Abdolrasulnia, R., *Ingestion of Candida albicans down-regulates mannose receptor expression on rat macrophages.* Arch Biochem Biophys, 1997. **344**(2): p. 350-56.
80. Cowan, H.B., Vick, S., Conary, J.T., and Shepherd, V.L., *Dexamethasone up-regulates mannose receptor activity by increasing mRNA levels.* Arch Biochem Biophys, 1992. **296**(1): p. 314-20.
81. Schreiber, S., Blum, J.S., Chappel, J.C., Stenson, W.F., Stahl, P.D., Teitelbaum, S.L., and Perkins, S.L., *Prostaglandin E specifically upregulates the expression of the mannose-receptor on mouse bone marrow-derived macrophages.* Cell Regul, 1990. **1**(5): p. 403-13.
82. Clohisy, D.R., Bar-Shavit, Z., Chappel, J.C., and Teitelbaum, S.L., *1,25-Dihydroxyvitamin D3 modulates bone marrow macrophage precursor proliferation and differentiation. Up-regulation of the mannose receptor.* J Biol Chem, 1987. **262**(33): p. 15922-29.
83. Kruskal, B.A., Sastry, K., Warner, A.B., Mathieu, C.E., and Ezekowitz, R.A.B., *Phagocytic Chimeric Receptors Require Both Transmembrane and Cytoplasmic Domains from the Mannose Receptor.* J Exp Med, 1992. **176**(6): p. 1673-80.
84. Le Cabec, V., Emorine, L.J., Toesca, I., Cougoule, C., and Maridonneau-Parini, I., *The human macrophage mannose receptor is not a professional phagocytic receptor.* J Leukocyte Biol, 2005. **77**(6): p. 934-43.
85. Ezekowitz, R.A.B., Sastry, K., Bailly, P., and Warner, A., *Molecular Characterization of the Human Macrophage Mannose Receptor - Demonstration of Multiple Carbohydrate Recognition-Like Domains and Phagocytosis of Yeasts in Cos-1 Cells.* J Exp Med, 1990. **172**(6): p. 1785-94.
86. Chakraborty, P. and Das, P.K., *Role of Mannose N-Acetylglucosamine Receptors in Blood Clearance and Cellular Attachment of Leishmania-Donovani.* Mol Biochem Parasit, 1988. **28**(1): p. 55-62.
87. Chatterjee, D., Lowell, K., Rivoire, B., Mcneil, M.R., and Brennan, P.J., *Lipoarabinomannan of Mycobacterium-Tuberculosis - Capping with Mannosyl Residues in Some Strains.* J Biol Chem, 1992. **267**(9): p. 6234-39.
88. Zhang, J., Tachado, S.D., Patel, N., Zhu, J., Imrich, A., Manfruelli, P., Cushion, M., Kinane, T.B., and Koziel, H., *Negative regulatory role of mannose receptors on human alveolar macrophage proinflammatory cytokine release in vitro.* J Leukoc Biol, 2005. **78**(3): p. 665-74.
89. Chieppa, M., Bianchi, G., Doni, A., Del Prete, A., Sironi, M., Laskarin, G., Monti, P., Piemonti, L., Biondi, A., Mantovani, A., Introna, M., and Allavena, P., *Cross-linking of the mannose receptor on monocyte-derived dendritic cells activates an anti-inflammatory immunosuppressive program.* J Immunol, 2003. **171**(9): p. 4552-60.
90. Shibata, Y., Metzger, W.J., and Myrvik, Q.N., *Chitin particle-induced cell-mediated immunity is inhibited by soluble mannan: mannose receptor-mediated phagocytosis initiates IL-12 production.* J Immunol, 1997. **159**(5): p. 2462-67.

91. Engering, A.J., Cella, M., Fluitsma, D., Brockhaus, M., Hoefsmit, E.C., Lanzavecchia, A., and Pieters, J., *The mannose receptor functions as a high capacity and broad specificity antigen receptor in human dendritic cells.* Eur J Immunol, 1997. **27**(9): p. 2417-25.
92. Tan, M.C., Mommaas, A.M., Drijfhout, J.W., Jordens, R., Onderwater, J.J., Verwoerd, D., Mulder, A.A., van der Heiden, A.N., Scheidegger, D., Oomen, L.C., Ottenhoff, T.H., Tulp, A., Neefjes, J.J., and Koning, F., *Mannose receptor-mediated uptake of antigens strongly enhances HLA class II-restricted antigen presentation by cultured dendritic cells.* Eur J Immunol, 1997. **27**(9): p. 2426-35.
93. Awasthi, A., Mathur, R.K., and Saha, B., *Immune response to Leishmania infection.* Indian J Med Res, 2004. **119**(6): p. 238-58.
94. Herwaldt, B.L., *Leishmaniasis.* Lancet, 1999. **354**(9185): p. 1191-99.
95. Wilson, M.E., Jeronimo, S.M., and Pearson, R.D., *Immunopathogenesis of infection with the visceralizing Leishmania species.* Microb Pathog, 2005. **38**(4): p. 147-60.
96. Mauricio, I.L., Stothard, J.R., and Miles, M.A., *The strange case of Leishmania chagasi.* Parasitol Today, 2000. **16**(5): p. 188-89.
97. Kaye, P. and Scott, P., *Leishmaniasis: complexity at the host-pathogen interface.* Nat Rev Microbiol, 2011. **9**(8): p. 604-15.
98. LeishRisk, *An introduction to neglected diseases and leishmaniasis.* Available from: http://www.leishrisk.net/Default.aspx?Menu=MenuMain&MIID=34&WPID=40&L=E (Accessed in July 2012).
99. Centers for Disease Control (CDC), C.f.D.C.a.P., *Laboratory identification of parasites of public health concern - Parasite image library.* Available from: http://www.dpd.cdc.gov/dpdx/HTML/ImageLibrary/Leishmaniasis_il.html (Accessed in July 2012).
100. van Zandbergen, G., Klinger, M., Mueller, A., Dannenberg, S., Gebert, A., Solbach, W., and Laskay, T., *Cutting edge: neutrophil granulocyte serves as a vector for Leishmania entry into macrophages.* J Immunol, 2004. **173**(11): p. 6521-25.
101. Kamhawi, S., *Phlebotomine sand flies and Leishmania parasites: friends or foes?* Trends Parasitol, 2006. **22**(9): p. 439-45.
102. Naderer, T. and McConville, M.J., *The Leishmania-macrophage interaction: a metabolic perspective.* Cell Microbiol, 2008. **10**(2): p. 301-08.
103. Desjeux, P., *Leishmaniasis - Public health aspects and control.* Clin Dermatol, 1996. **14**(5): p. 417-23.
104. Kedzierski, L., *Leishmaniasis Vaccine: Where are We Today?* J Glob Infect Dis, 2010. **2**(2): p. 177-85.
105. WHO, *WHO Report on global surveillance of epidemic-prone infectious diseases*, 2000. Availablefrom:www.who.int/entity/csr/resources/publications/surveillance/WHO_Report_Infectious_Diseases.pdf (Accessed in July 2012).
106. Pearson, R.D. and Sousa, A.Q., *Clinical spectrum of Leishmaniasis.* Clin Infect Dis, 1996. **22**(1): p. 1-13.
107. Chappuis, F., Sundar, S., Hailu, A., Ghalib, H., Rijal, S., Peeling, R.W., Alvar, J., and Boelaert, M., *Visceral leishmaniasis: what are the needs for diagnosis, treatment and control?* Nat Rev Microbiol, 2007. **5**(11): p. 873-82.
108. Desjeux, P., *Leishmaniasis: current situation and new perspectives.* Comp Immunol Microb, 2004. **27**(5): p. 305-18.
109. Desjeux, P., *The increase in risk factors for leishmaniasis worldwide.* Trans R Soc Trop Med Hyg, 2001. **95**(3): p. 239-43.
110. WHO, *Leishmaniasis - Burden of disease.* Available from: http://www.who.int/leishmaniasis/burden/en/ (Acessed July 2012).
111. Singh, N., Kumar, M., and Singh, R.K., *Leishmaniasis: current status of available drugs and new potential drug targets.* Asian Pac J Trop Med, 2012. **5**(6): p. 485-97.
112. Murray, H.W., *Treatment of visceral leishmaniasis in 2004.* Am J Trop Med Hyg, 2004. **71**(6): p. 787-94.

113. Sundar, S., *Drug resistance in Indian visceral leishmaniasis.* Trop Med Int Health, 2001. **6**(11): p. 849-54.
114. Berman, J.D., *Human leishmaniasis: clinical, diagnostic, and chemotherapeutic developments in the last 10 years.* Clin Infect Dis, 1997. **24**(4): p. 684-703.
115. Yardley, V. and Croft, S.L., *A comparison of the activities of three amphotericin B lipid formulations against experimental visceral and cutaneous leishmaniasis.* Int J Antimicrob Agents, 2000. **13**(4): p. 243-48.
116. Di Giorgio, C., Faraut-Gambarelli, F., Imbert, A., Minodier, P., Gasquet, M., and Dumon, H., *Flow cytometric assessment of amphotericin B susceptibility in Leishmania infantum isolates from patients with visceral leishmaniasis.* J Antimicrob Chemother, 1999. **44**(1): p. 71-76.
117. Lachaud, L., Bourgeois, N., Plourde, M., Leprohon, P., Bastien, P., and Ouellette, M., *Parasite susceptibility to amphotericin B in failures of treatment for visceral leishmaniasis in patients coinfected with HIV type 1 and Leishmania infantum.* Clin Infect Dis, 2009. **48**(2): p. e16-22.
118. Sundar, S., Jha, T.K., Thakur, C.P., Bhattacharya, S.K., and Rai, M., *Oral miltefosine for the treatment of Indian visceral leishmaniasis.* Trans R Soc Trop Med Hyg, 2006. **100 Suppl 1**: p. S26-33.
119. Croft, S.L., Yardley, V., and Kendrick, H., *Drug sensitivity of Leishmania species: some unresolved problems.* Trans R Soc Trop Med Hyg, 2002. **96 Suppl 1**: p. S127-29.
120. Sundar, S., Jha, T.K., Thakur, C.P., Sinha, P.K., and Bhattacharya, S.K., *Injectable paromomycin for Visceral leishmaniasis in India.* N Engl J Med, 2007. **356**(25): p. 2571-81.
121. Bryceson, A., *A policy for leishmaniasis with respect to the prevention and control of drug resistance.* Trop Med Int Health, 2001. **6**(11): p. 928-34.
122. Seaman, J., Pryce, D., Sondorp, H.E., Moody, A., Bryceson, A.D., and Davidson, R.N., *Epidemic visceral leishmaniasis in Sudan: a randomized trial of aminosidine plus sodium stibogluconate versus sodium stibogluconate alone.* J Infect Dis, 1993. **168**(3): p. 715-20.
123. Romero, E.L. and Morilla, M.J., *Drug delivery systems against leishmaniasis? Still an open question.* Expert Opin Drug Deliv, 2008. **5**(7): p. 805-23.
124. Owais, M. and Gupta, C.M., *Targeted drug delivery to macrophages in parasitic infections.* Curr Drug Deliv, 2005. **2**(4): p. 311-18.
125. Alving, C.R., Steck, E.A., Chapman, W.L., Jr., Waits, V.B., Hendricks, L.D., Swartz, G.M., Jr., and Hanson, W.L., *Therapy of leishmaniasis: superior efficacies of liposome-encapsulated drugs.* Proc Natl Acad Sci U S A, 1978. **75**(6): p. 2959-63.
126. New, R.R. and Chance, M.L., *Treatment of experimental cutaneous leishmaniasis by liposome-entrapped Pentostam.* Acta Trop, 1980. **37**(3): p. 253-6.
127. Papagiannaros, A., Bories, C., Demetzos, C., and Loiseau, P.M., *Antileishmanial and trypanocidal activities of new miltefosine liposomal formulations.* Biomed Pharmacother, 2005. **59**(10): p. 545-50.
128. Couvreur, P. and Vauthier, C., *Nanotechnology: intelligent design to treat complex disease.* Pharm Res, 2006. **23**(7): p. 1417-50.
129. Gaspar, R., Preat, V., Opperdoes, F.R., and Roland, M., *Macrophage activation by polymeric nanoparticles of polyalkylcyanoacrylates: activity against intracellular Leishmania donovani associated with hydrogen peroxide production.* Pharm Res, 1992. **9**(6): p. 782-87.
130. Rodrigues, J.M., Jr., Croft, S.L., Fessi, H., Bories, C., and Devissaguet, J.P., *The activity and ultrastructural localization of primaquine-loaded poly (d,l-lactide) nanoparticles in Leishmania donovani infected mice.* Trop Med Parasitol, 1994. **45**(3): p. 223-28.
131. Espuelas, M.S., Legrand, P., Loiseau, P.M., Bories, C., Barratt, G., and Irache, J.M., *In vitro antileishmanial activity of amphotericin B loaded in poly(epsilon-caprolactone) nanospheres.* J Drug Target, 2002. **10**(8): p. 593-99.

132. Durand, R., Paul, M., Rivollet, D., Houin, R., Astier, A., and Deniau, M., *Activity of pentamidine-loaded methacrylate nanoparticles against Leishmania infantum in a mouse model.* Int J Parasitol, 1997. **27**(11): p. 1361-67.
133. Torres-Santos, E.C., Rodrigues, J.M., Jr., Moreira, D.L., Kaplan, M.A., and Rossi-Bergmann, B., *Improvement of in vitro and in vivo antileishmanial activities of 2', 6'-dihydroxy-4'-methoxychalcone by entrapment in poly(D,L-lactide) nanoparticles.* Antimicrob Agents Chemother, 1999. **43**(7): p. 1776-78.
134. Rathore, A., Jain, A., Gulbake, A., Shilpi, S., Khare, P., and Jain, S.K., *Mannosylated liposomes bearing Amphotericin B for effective management of visceral Leishmaniasis.* J Liposome Res, 2011. **21**(4): p. 333-40.
135. Copland, M.J., Baird, M.A., Rades, T., McKenzie, J.L., Becker, B., Reck, F., Tyler, P.C., and Davies, N.M., *Liposomal delivery of antigen to human dendritic cells.* Vaccine, 2003. **21**(9-10): p. 883-90.
136. Masuko, T., Minami, A., Iwasaki, N., Majima, T., Nishimura, S., and Lee, Y.C., *Carbohydrate analysis by a phenol-sulfuric acid method in microplate format.* Anal Biochem, 2005. **339**(1): p. 69-72.
137. Moreira, D., Santarem, N., Loureiro, I., Tavares, J., Silva, A.M., Amorim, A.M., Ouaissi, A., Cordeiro-da-Silva, A., and Silvestre, R., *Impact of continuous axenic cultivation in Leishmania infantum virulence.* PLoS Negl Trop Dis, 2012. **6**(1): p. e1469.
138. Mosmann, T., *Rapid colorimetric assay for cellular growth and survival: application to proliferation and cytotoxicity assays.* J Immunol Methods, 1983. **65**(1-2): p. 55-63.
139. Roy, G., Dumas, C., Sereno, D., Wu, Y., Singh, A.K., Tremblay, M.J., Ouellette, M., Olivier, M., and Papadopoulou, B., *Episomal and stable expression of the luciferase reporter gene for quantifying Leishmania spp. infections in macrophages and in animal models.* Mol Biochem Parasitol, 2000. **110**(2): p. 195-206.
140. Presicce, P., Taddeo, A., Conti, A., Villa, M.L., and Della Bella, S., *Keyhole limpet hemocyanin induces the activation and maturation of human dendritic cells through the involvement of mannose receptor.* Mol Immunol, 2008. **45**(4): p. 1136-45.
141. Wasan, K.M., Wasan, E.K., Gershkovich, P., Zhu, X., Tidwell, R.R., Werbovetz, K.A., Clement, J.G., and Thornton, S.J., *Highly effective oral amphotericin B formulation against murine visceral leishmaniasis.* J Infect Dis, 2009. **200**(3): p. 357-60.
142. Monsigny, M., Petit, C., and Roche, A.C., *Colorimetric determination of neutral sugars by a resorcinol sulfuric acid micromethod.* Anal Biochem, 1988. **175**(2): p. 525-30.
143. Venier-Julienne, M.C., Vouldoukis, I., Monjour, L., and Benoit, J.P., *In vitro study of the anti-leishmanial activity of biodegradable nanoparticles.* J Drug Target, 1995. **3**(1): p. 23-29.
144. Lemoine, D., Francois, C., Kedzierewicz, F., Preat, W., Hoffman, M., and Maincent, P., *Stability study of nanoparticles of poly(epsilon-caprolactone), poly(D,L-lactide) and poly(D,L-lactide-co-glycolide).* Biomaterials, 1996. **17**(22): p. 2191-97.
145. Venier-Julienne, M.C. and Benoît, J.P., *Preparation, purification and morphology of polymeric nanoparticles as drug carriers.* Pharmaceutica Acta Helvetiae, 1996. **71**(2): p. 121-28.
146. Italia, J.L., Yahya, M.M., Singh, D., and Ravi Kumar, M.N., *Biodegradable nanoparticles improve oral bioavailability of amphotericin B and show reduced nephrotoxicity compared to intravenous Fungizone.* Pharm Res, 2009. **26**(6): p. 1324-31.
147. Zolnik, B.S. and Burgess, D.J., *Evaluation of in vivo-in vitro release of dexamethasone from PLGA microspheres.* J Control Release, 2008. **127**(2): p. 137-45.
148. Paila, Y.D., Saha, B., and Chattopadhyay, A., *Amphotericin B inhibits entry of Leishmania donovani into primary macrophages.* Biochem Biophys Res Commun, 2010. **399**(3): p. 429-33.
149. Da Costa Martins, R., Gamazo, C., and Irache, J.M., *Design and influence of gamma-irradiation on the biopharmaceutical properties of nanoparticles containing an antigenic complex from Brucella ovis.* Eur J Pharm Sci, 2009. **37**(5): p. 563-72.

150. Barichello, J.M., Morishita, M., Takayama, K., and Nagai, T., *Encapsulation of hydrophilic and lipophilic drugs in PLGA nanoparticles by the nanoprecipitation method.* Drug Dev Ind Pharm, 1999. **25**(4): p. 471-76.
151. Abbas, A.K., Lichtman, A.H., and Pillai, S., *Cellular and Molecular Immunology*. 6th ed. 2009: Saunders. p.576.
152. Hamdy, S., Haddadi, A., Hung, R.W., and Lavasanifar, A., *Targeting dendritic cells with nano-particulate PLGA cancer vaccine formulations.* Adv Drug Deliv Rev, 2011. **63**(10-11): p. 943-55.
153. Gordon, S., *Alternative activation of macrophages.* Nat Rev Immunol, 2003. **3**(1): p. 23-35.
154. Mosser, D.M., *The many faces of macrophage activation.* J Leukoc Biol, 2003. **73**(2): p. 209-12.
155. Maroof, A., Penny, M., Kingston, R., Murray, C., Islam, S., Bedford, P.A., and Knight, S.C., *Interleukin-4 can induce interleukin-4 production in dendritic cells.* Immunology, 2006. **117**(2): p. 271-79.
156. Kalinski, P., Hilkens, C.M.U., Wierenga, E.A., and Kapsenberg, M.L., *T-cell priming by type-1 and type-2 polarized dendritic cells: the concept of a third signal.* Immunol Today, 1999. **20**(12): p. 561-67.